NATIONAL ADVISORY COMMITTEE FOR AERONAUTICS

TECHNICAL MEMORANDUM 1439

APPLICATION OF THE METHOD OF COORDINATE PERTURBATION TO UNSTEADY DUCT FLOW

By Seymour C. Himmel

Case Institute of Technology

Washington
September 1958

TABLE OF CONTENTS

NATIONAL ADVISORY COMMITTEE FOR AERONAUTICS

TECHNICAL MEMORANDUM 1439

APPLICATION OF THE METHOD OF COORDINATE PERTURBATION TO UNSTEADY DUCT FLOW[1]

By Seymour C. Himmel

SUMMARY

The method of coordinate perturbation is applied to the unsteady flow of a compressible fluid in ducts of variable cross section. Solutions, in the form of perturbation series, are obtained for unsteady flows in ducts for which the logarithmic derivative of area variation with respect to the space coordinate is a function of the "smallness" parameter of the perturbation series.

This technique is applied to the problem of the interaction of a disturbance and a shock wave in a diffuser flow. It is found that, for a special choice of the function describing the disturbance, the path of the shock wave can be expressed in closed form to first order. The method is then applied to the determination of the flow field behind a shock wave moving on a prescribed path in the x,t-plane. Perturbation-series solutions for quite general shock paths are developed.

The perturbation-series solutions are compared with the more exact solutions obtained by the application of the method of characteristics. The approximate solutions are shown to be in reasonably accurate agreement with the solutions obtained by the method of characteristics.

I. INTRODUCTION

Problems involving the unsteady flow of a compressible fluid in ducts of variable cross section are frequently encountered in the study of nonsteady-state operation of air-breathing propulsion systems. At supersonic flight speeds such problems are often complicated by the presence of

[1]The information presented herein constitutes the major part of a thesis that was offered in partial fulfillment of the requirements for the degree of doctor of philosophy, Case Institute of Technology, Cleveland, Ohio, June 1958.

shock waves in the flow. A typical example of a situation involving both an unsteady duct flow and a shock wave is that which arises when the throttle setting of a turbojet or a ramjet engine operating at supersonic flight speed is changed. As a result of the change of throttle setting, a disturbance is generated in the subsonic flow region of the diffuser that propagates upstream in the diffuser and interacts with the shock wave. The interaction of the disturbance and the shock wave causes the latter to change its position in the diffuser and its strength. A knowledge of the history of the shock motion and of the flow variables within the diffuser during such transient operation is of great value in the study of engine dynamics and the design of engine control systems.

The difficulties encountered in attempting the solution of the partial differential equations describing the flow of a compressible fluid are well known. The usual procedure in solving problems governed by these equations is to reduce them to a more manageable form by omitting terms whose effects are of small magnitude for the problem under investigation. In the case of ducts of variable cross section, such simplifications lead to the concept of quasi-one-dimensional flow commonly employed in steady-flow theory. In the quasi-one-dimensional approximation, it is assumed that the cross-sectional area of the duct varies slowly with distance measured along the axis of the duct. Under these conditions the velocity of the fluid is assumed to have the direction of the duct axis and all flow variables are assumed to be uniform over any duct cross section. For unsteady quasi-one-dimensional flows one has to deal, therefore, with a single space coordinate and the time as the independent variables of the problem. Even with these simplifications the equations cannot, in general, be solved analytically.

In the main, unsteady quasi-one-dimensional flow problems have been treated by the method of characteristics (cf. ref. 1 and the extensive bibliography therein). Solutions are obtained by numerical methods or by a combination of graphical and numerical methods. In either case much labor is involved and only the answer to an individual problem is obtained. A reasonably accurate approximate analytical method for treating unsteady quasi-one-dimensional flow problems is therefore desirable.

Among those who have studied unsteady duct flow by analytical methods are Kantrowitz (ref. 2) and R. E. Meyer (ref. 3). Kantrowitz studied the formation and the stability of shock waves in duct flows by linearizing the equations of motion. He was able to demonstrate the instability of shock-free diffuser flows by this method. For diffuser flows in which a shock wave is a part of the equilibrium flow, he was able to demonstrate the stability of the position of the shock. Because he was primarily concerned with stability considerations, Kantrowitz considered disturbances in the form of pulses, and his discussion of the interaction of a shock wave and a disturbance centers about conditions in the immediate vicinity of the shock.

Meyer treated waves of finite amplitude in ducts by considering the relations among the derivatives of the Riemann invariants along the characteristics. In this manner he developed a first-order theory for advancing and receding wave fronts in shock-free duct flows. By means of this theory, he demonstrated the inherent instability of shock-free diffuser flows and was able to give a partial solution for the interaction of two wave fronts.

In what follows, an approximate analytic method for treating the unsteady quasi-one-dimensional flow of a perfect fluid is developed. This method differs from those previously considered in that it is based on the method of coordinate perturbations (ref. 4). Solutions, in the form of perturbation series, are obtained for unsteady flows in ducts for which the logarithmic derivative of area variation with respect to the space coordinate is a function of the "smallness" parameter of the perturbation series. These perturbation series have as independent variables the characteristic parameters of the hyperbolic differential equations governing the flow. This technique is applied to the problem of the interaction of a disturbance and a shock wave in a diffuser flow. It is found that, for a special choice of the function describing the disturbance, the path of the shock wave can be expressed in closed form to first order. The method is then applied to the determination of the flow field behind a shock wave moving on a prescribed path in the x,t-plane. Perturbation-series solutions for quite general shock paths are developed.

The solutions obtained by the approximate analytic method are compared with the more exact solutions obtained by the application of the method of characteristics using a finite-difference technique. The perturbation series solutions are shown to be in reasonably accurate agreement with the solutions obtained by the method of characteristics.

The author is very pleased to be able to take this opportunity of acknowledging his indebtedness to Professor G. Kuerti for his guidance, encouragement, and many valuable suggestions and criticisms throughout the preparation of this thesis.

II. APPLICATION OF THE METHOD OF COORDINATE PERTURBATION TO QUASI-ONE-DIMENSIONAL FLOW

In the usual perturbation theories for supersonic flow and wave propagation, the solutions are represented by perturbation series in which the flow variables are given as functions of the physical coordinates of the problem. For example, for a small deviation from a uniform two-dimensional steady flow, the velocity components u and v are

given by expressions such as

$$u = U + \epsilon u^{(1)}(x,y) + \epsilon^2 u^{(2)}(x,y) + \cdots,$$
$$v = \epsilon v^{(1)}(x,y) + \epsilon^2 v^{(2)}(x,y) + \cdots \tag{2.1}$$

(All symbols are defined in the appendix.) In these equations, U is the undisturbed flow velocity and $u^{(1)}(x,y)$ is a deviation (in the x direction) from the uniform flow. The magnitude of the deviation is governed by a "smallness" parameter ϵ. For many problems this method is adequate. In some cases, however, such solutions prove to be inadequate; for example, in the Prandtl-Meyer expansion in two-dimensional steady flow (cf. section 2 of ref. 4).

For hyperbolic differential equations the characteristic parameters are the natural independent variables. In a perturbation theory based on the characteristic form of the differential equations, it may be expected that the difficulties encountered in the more usual perturbation method may be avoided. Such a theory was developed by C. C. Lin (ref. 4) for quasi-linear systems in two independent variables; it is based on ideas implied in the work of R. E. Meyer (ref. 3) and suggested by K. O. Friedrichs (refs. 5 and 6). It is referred to as the method of "coordinate perturbation."

In this method characteristic parameters α and β are introduced, and the physical coordinates (say, x and y in two-dimensional steady supersonic flow) as well as the flow variables u, v are expressed in terms of the parameters. The perturbation solution thus appears in the form

$$\left.\begin{aligned} u &= u^{(0)}(\alpha,\beta) + \epsilon u^{(1)}(\alpha,\beta) + \epsilon^2 u^{(2)}(\alpha,\beta) + \cdots, \\ v &= v^{(0)}(\alpha,\beta) + \epsilon v^{(1)}(\alpha,\beta) + \epsilon^2 v^{(2)}(\alpha,\beta) + \cdots, \\ x &= x^{(0)}(\alpha,\beta) + \epsilon x^{(1)}(\alpha,\beta) + \epsilon^2 x^{(2)}(\alpha,\beta) + \cdots, \\ y &= y^{(0)}(\alpha,\beta) + \epsilon y^{(1)}(\alpha,\beta) + \epsilon^2 y^{(2)}(\alpha,\beta) + \cdots \end{aligned}\right\} \tag{2.2}$$

Parametric representations, such as that given above, have disadvantages associated with the mapping onto the characteristic plane. First, boundary conditions are normally specified in the physical plane, and it is usually difficult to impose the boundary conditions in the plane of characteristic parameters. Second, a single-valued solution in the plane

of characteristics could become multiple-valued in the physical plane. However, if, as in the case considered, the flow is a perturbation from a uniform state, the freedom in the choice of the characteristic parameters makes it possible to avoid multiple-valued mappings and to specify the boundary conditions easily.

In the paper in which the perturbation theory was developed, Lin treated problems of two-dimensional steady supersonic flow and emphasized the proper choice of the mapping, that is, of the parameters α and β. He was able to give a convergence proof for this case. In her thesis (ref. 7), P. Fox applied the method to the propagation of plane ("strictly" one-dimensional), cylindrical, and spherical waves. She was able to give a convergence proof for the case of plane waves. In what follows, the method of coordinate perturbation is applied to quasi-one-dimensional flow.

A. Equations of Motion

The equations governing the homentropic, quasi-one-dimensional flow of a compressible fluid are (ref. 8):

$$\left.\begin{aligned} u'u'_{x'} + u'_{t'} + \frac{2}{\gamma - 1} c'c'_{x'} &= 0, \\ c'u'_{x'} + \frac{2}{\gamma - 1} u'c'_{x'} + \frac{2}{\gamma - 1} c'_{t'} + c'u' \frac{A'_{x'}}{A'} &= 0 \end{aligned}\right\} \tag{2.3}$$

where $A' = A'(x')$ is the cross-sectional area of the duct at the station x'. These equations are in terms of dimensional quantities. In what follows, it will be convenient to use dimensionless quantities for the variables given by:

$$u = \frac{u'}{c'_*}; \quad c = \frac{c'}{c'_*}; \quad t = \frac{t'c'_*}{\sqrt{A'_*}}; \quad x = \frac{x'}{\sqrt{A'_*}}; \quad A = \frac{A'}{A'_*} \tag{2.4}$$

where the asterisk refers to the critical condition of the basic steady-flow problem; that is, where the local particle speed equals the local speed of sound. Transformation of equations (2.3) to equations involving the dimensionless quantities does not change the form of the equations but merely affects the boundary conditions.

When the dimensionless equations (2.3) are written in canonical form, they become:

$$\left.\begin{aligned} x_\alpha &= (u + c)t_\alpha, \\ x_\beta &= (u - c)t_\beta, \\ u_\alpha + \sigma c_\alpha &= - uc \frac{A_x}{A} t_\alpha, \\ u_\beta - \sigma c_\beta &= uc \frac{A_x}{A} t_\beta, \end{aligned}\right\} \tag{2.5}$$

where

$$\sigma \equiv \frac{2}{\gamma - 1} \tag{2.6}$$

and α and β are the characteristic parameters. Thus, (2.3) is replaced by four differential equations for four unknowns in such a way that each equation involves only differentiation with respect to one characteristic parameter.

While the pair (2.3) is irreducible in the sense of reference 6 and thus Riemann's method of integration can no longer be applied, equations (2.3) or the equivalent system (2.5) can, of course, be solved by the application of the method of characteristics, and many solutions for particular problems have been calculated in this manner (cf. for example, ref. 1). It is advantageous, however, to develop an approximate analytical solution for perturbation problems governed by these equations. Such a solution is obtained by the application of the method of coordinate perturbation.

B. Perturbation Solution

A solution of equations (2.5) is sought in the form of perturbation series given by

$$\left.\begin{aligned} x &= x^{(0)}(\alpha,\beta) + \epsilon x^{(1)}(\alpha,\beta) + \epsilon^2 x^{(2)}(\alpha,\beta) + \cdots, \\ t &= t^{(0)}(\alpha,\beta) + \epsilon t^{(1)}(\alpha,\beta) + \epsilon^2 t^{(2)}(\alpha,\beta) + \cdots, \\ u &= u^{(0)}(\alpha,\beta) + \epsilon u^{(1)}(\alpha,\beta) + \epsilon^2 u^{(2)}(\alpha,\beta) + \cdots, \\ c &= c^{(0)}(\alpha,\beta) + \epsilon c^{(1)}(\alpha,\beta) + \epsilon^2 c^{(2)}(\alpha,\beta) + \cdots \end{aligned}\right\} \tag{2.7}$$

The solution is, of course, a function of the duct area variation $A(x)$. In order to render the initial investigation as simple as possible, the duct area was assumed to vary according to the relation

$$A = e^{-b(x-L)} \tag{2.8}$$

where b is a dimensionless constant and L is the dimensionless location of the duct throat (cf. (2.4)). For this choice of area distribution, equations (2.5) become

$$\left.\begin{aligned} x_\alpha &= (u + c)t_\alpha, \\ x_\beta &= (u - c)t_\beta, \\ u_\alpha + \sigma c_\alpha &= ucbt_\alpha, \\ u_\beta - \sigma c_\beta &= -ucbt_\beta. \end{aligned}\right\} \tag{2.9}$$

Substitution of equations (2.7) into equations (2.9) yields

$$\left.\begin{aligned}
\sum_{n=0}^{\infty} \epsilon^n x_\alpha^{(n)} &= \left[\sum_{n=0}^{\infty} \epsilon^n (u^{(n)} + c^{(n)})\right]\left[\sum_{n=0}^{\infty} \epsilon^n t_\alpha^{(n)}\right], \\
\sum_{n=0}^{\infty} \epsilon^n x_\beta^{(n)} &= \left[\sum_{n=0}^{\infty} \epsilon^n (u^{(n)} - c^{(n)})\right]\left[\sum_{n=0}^{\infty} \epsilon^n t_\beta^{(n)}\right], \\
\sum_{n=0}^{\infty} \epsilon^n (u_\alpha^{(n)} + \sigma c_\alpha^{(n)}) &= b\left[\sum_{n=0}^{\infty} \epsilon^n c^{(n)}\right]\left[\sum_{n=0}^{\infty} \epsilon^n u^{(n)}\right]\left[\sum_{n=0}^{\infty} \epsilon^n t_\alpha^{(n)}\right], \\
\sum_{n=0}^{\infty} \epsilon^n (u_\beta^{(n)} - \sigma c_\beta^{(n)}) &= -b\left[\sum_{n=0}^{\infty} \epsilon^n c^{(n)}\right]\left[\sum_{n=0}^{\infty} \epsilon^n u^{(n)}\right]\left[\sum_{n=0}^{\infty} \epsilon^n t_\beta^{(n)}\right]
\end{aligned}\right\} \tag{2.10}$$

Upon expansion of these equations and equating the coefficients of like powers of ϵ, there is obtained

$$\left.\begin{aligned}
x_\alpha^{(k)} &= \sum_{\lambda=0}^{k} (u^{(\lambda)} + c^{(\lambda)}) t_\alpha^{(k-\lambda)}, \\
x_\beta^{(k)} &= \sum_{\lambda=0}^{k} (u^{(\lambda)} - c^{(\lambda)}) t_\beta^{(k-\lambda)}, \\
u_\alpha^{(k)} + \sigma c_\alpha^{(k)} &= b \sum_{j=0}^{k} \left[\sum_{\lambda=0}^{j} c^{(\lambda)} u^{(j-\lambda)}\right] t_\alpha^{(k-j)}, \\
u_\beta^{(k)} - \sigma c_\beta^{(k)} &= -b \sum_{j=0}^{k} \left[\sum_{\lambda=0}^{j} c^{(\lambda)} u^{(j-\lambda)}\right] t_\beta^{(k-j)}; \quad k=0,1,2\cdots
\end{aligned}\right\} \tag{2.11}$$

Typical sets of these equations are:

Zeroth order:

$$\left.\begin{aligned} x_\alpha^{(0)} &= (u^{(0)} + c^{(0)})t_\alpha^{(0)}, \\ x_\beta^{(0)} &= (u^{(0)} - c^{(0)})t_\beta^{(0)}, \\ u_\alpha^{(0)} + \sigma c_\alpha^{(0)} &= bu^{(0)}c^{(0)}t_\alpha^{(0)}, \\ u_\beta^{(0)} - \sigma c_\beta^{(0)} &= -bu^{(0)}c^{(0)}t_\beta^{(0)}. \end{aligned}\right\} \tag{2.12}$$

First order:

$$\left.\begin{aligned} x_\alpha^{(1)} &= (u^{(0)} + c^{(0)})t_\alpha^{(1)} + (u^{(1)} + c^{(1)})t_\alpha^{(0)}, \\ x_\beta^{(1)} &= (u^{(0)} - c^{(0)})t_\beta^{(1)} + (u^{(1)} - c^{(1)})t_\beta^{(0)}, \\ u_\alpha^{(1)} + \sigma c_\alpha^{(1)} &= b\left[u^{(0)}c^{(0)}t_\alpha^{(1)} + (u^{(0)}c^{(1)} + u^{(1)}c^{(0)})t_\alpha^{(0)}\right], \\ u_\beta^{(1)} - \sigma c_\beta^{(1)} &= -b\left[u^{(0)}c^{(0)}t_\beta^{(1)} + (u^{(0)}c^{(1)} + u^{(1)}c^{(0)})t_\beta^{(0)}\right]. \end{aligned}\right\} \tag{2.13}$$

It is of interest to note that, whereas the zeroth-order equations are quasi-linear (they are identical in structure with (2.9)), the higher order equations are linear and homogeneous in the unknowns of the same order; that is, the coefficients of the unknowns are functions of the solutions of the lower order equations.

We wish to consider small unsteady perturbations of a steady flow in a duct; thus, the unperturbed flow should be a steady duct flow. This unperturbed flow is represented by the zeroth-order solution. The steady flow in a quasi-one-dimensional duct is completely determined by the continuity and Bernoulli equations in dimensionless form:

$$A^{-1} = \left(\frac{\sigma + 1}{\sigma}\right)^{\sigma/2} u\left[1 - \frac{u^2}{\sigma + 1}\right]^{\sigma/2}, \tag{2.14}$$

$$u^2 + \sigma c^2 = \sigma + 1. \tag{2.15}$$

These equations must be considered as time-independent integrals of the nondimensional form of equations (2.3) and, since equations (2.5) are equivalent to equations (2.3), they are solutions of these also. The zeroth-order equations (2.12) are the same as equations (2.5) with the area variation given by equation (2.8) used to evaluate the term A_x/A. Thus, the solution of the zeroth-order equations is given by

$$e^{b(x^{(0)}-L)} = \left(\frac{\sigma+1}{\sigma}\right)^{\sigma/2} u^{(0)} \left[1 - \frac{(u^{(0)})^2}{\sigma+1}\right]^{\sigma/2}, \tag{2.16}$$

$$u^{(0)2} + \sigma c^{(0)2} = \sigma + 1. \tag{2.17}$$

In order to proceed to the solution of the higher order equations, the zeroth-order solutions must be expressed as functions of α and β. To determine the form taken by these functions, an example was chosen with $\sigma = 1$ ($\gamma = 3$). This choice of γ permits a simple algebraic form of the solution of equations (2.16) and (2.17) for $u^{(0)}$ and $c^{(0)}$ as functions of $x^{(0)}$. For subsonic flow downstream of the throat, these solutions are:

$$u^{(0)} = -\left[1 - \sqrt{1 - e^{2b(x^{(0)}-L)}}\right]^{1/2}, \tag{2.18}$$

$$c^{(0)} = \left[1 + \sqrt{1 - e^{2b(x^{(0)}-L)}}\right]^{1/2}, \tag{2.19}$$

from which it can be shown that

$$u^{(0)} + c^{(0)} = \sqrt{2}\left[1 - e^{b(x^{(0)}-L)}\right]^{1/2}, \tag{2.20}$$

$$u^{(0)} - c^{(0)} = -\sqrt{2}\left[1 + e^{b(x^{(0)}-L)}\right]^{1/2}. \tag{2.21}$$

The zeroth-order characteristics are determined from the first two of equations (2.12). On a characteristic β = constant, we have therefore:

$$\frac{dx^{(0)}}{\left[1 - e^{b(x^{(0)}-L)}\right]^{1/2}} = \sqrt{2}\, dt^{(0)}. \tag{2.22}$$

Setting

$$\zeta(x^{(0)}) = e^{b(x^{(0)}-L)} \tag{2.23}$$

whence

$$d\zeta = \zeta b\, dx^{(0)}, \tag{2.24}$$

equation (2.22) becomes

$$\frac{d\zeta}{\zeta(1-\zeta)^{1/2}} = \sqrt{2}\, b\, dt^{(0)}. \tag{2.25}$$

Integrating this along the β = constant characteristic, we obtain

$$\ln\left[\frac{\sqrt{1-\zeta}-1}{\sqrt{1-\zeta}+1}\right] = \sqrt{2}\, bt^{(0)} + \mathcal{F}(\beta). \tag{2.26}$$

At this stage the freedom of selection of the characteristic parameters mentioned previously enters. This means that the equations are invariant if one replaces α and β by $\alpha' = f(\alpha)$ and $\beta' = g(\beta)$. It can be easily demonstrated that under these circumstances we may stipulate that a given curve of the flow plane (i.e., the x,t-plane) should be the image of a given curve of the α,β-plane. Now it is desired to have the zeroth-order solution represent the initial steady flow in the channel; that is, along the line $t = 0$, for example. Therefore, we select the characteristic parameters such that on $t = 0$, $x = \alpha = \beta$ (i.e., the x-axis is the image of $\alpha - \beta = 0$). For this choice of the parameters, equation (2.26) becomes

$$\ln\left[\frac{\sqrt{1-\zeta}-1}{\sqrt{1-\zeta}+1}\right] - \ln\left[\frac{\sqrt{1-\zeta(\beta)}-1}{\sqrt{1-\zeta(\beta)}+1}\right] = \sqrt{2}\, bt^{(0)}. \tag{2.27}$$

Similarly, on an α = constant characteristic we have

$$\ln\left[\frac{\sqrt{1+\zeta(\alpha)}-1}{\sqrt{1+\zeta(\alpha)}+1}\right] - \ln\left[\frac{\sqrt{1+\zeta}-1}{\sqrt{1+\zeta}+1}\right] = \sqrt{2}\, bt^{(0)}. \tag{2.28}$$

Eliminating $t^{(0)}$ from the last two equations and solving for ζ, we obtain

$$\zeta = e^{b(x^{(0)}-L)} = 4\frac{\eta+\xi}{(\eta-\xi)^2}\sqrt{-\xi\eta}, \tag{2.29}$$

where

$$\xi = \frac{\sqrt{1-e^{b(\beta-L)}}-1}{\sqrt{1-e^{b(\beta-L)}}+1} \tag{2.30}$$

and

$$\eta = \frac{\sqrt{1+e^{b(\alpha-L)}}+1}{\sqrt{1+e^{b(\alpha-L)}}-1}. \tag{2.31}$$

From these equations we obtain for the physical coordinates:

$$x^{(0)} = L + \frac{1}{b}\ln\left[4\frac{\eta+\xi}{(\eta-\xi)^2}\sqrt{-\xi\eta}\right], \tag{2.32}$$

$$\sqrt{2}\,bt^{(0)} = \ln\left[\frac{1}{\xi}\cdot\frac{\sqrt{(\eta-\xi)^2-4(\eta+\xi)\sqrt{-\xi\eta}}-(\eta-\xi)}{\sqrt{(\eta-\xi)^2-4(\eta+\xi)\sqrt{-\xi\eta}}+(\eta-\xi)}\right]. \tag{2.33}$$

By substituting equation (2.29) into equations (2.18) and (2.19), the particle velocity and speed of sound are given by

$$u^{(0)} = -\frac{1}{(\eta-\xi)}\left[(\eta-\xi)^2-\sqrt{(\eta-\xi)^4+16(\eta+\xi)^2\,\xi\eta}\right]^{1/2}, \tag{2.34}$$

$$c^{(0)} = \frac{1}{(\eta-\xi)}\left[(\eta-\xi)^2+\sqrt{(\eta-\xi)^4+16(\eta+\xi)^2\,\xi\eta}\right]^{1/2}. \tag{2.35}$$

These rather formidable equations give the parameters of a steady duct flow (i.e., the zeroth-order solution) in terms of the characteristic parameters α and β. The higher order approximations are given by linear equations where the coefficients are functions of the lower order solutions. For example, the first-order equations (2.13) have coefficients derivable from equations (2.32) to (2.35). The higher order equations are, however, complicated and must be solved simultaneously. No simple analytical technique seems applicable - perhaps a numerical technique would be feasible.

To illustrate the nature of the zeroth-order solution for the area variation selected, an example was computed. The flow situation is illustrated in the sketch.

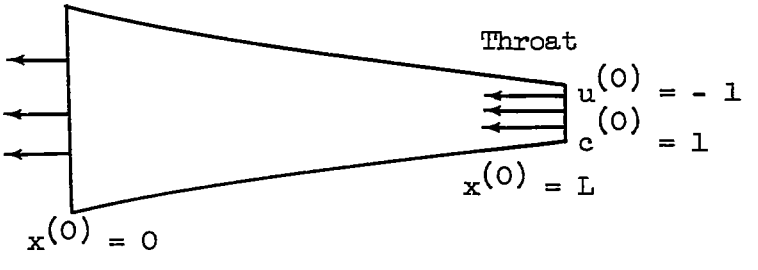

We have a duct with area increasing to the left. The throat of the duct is located at $x^{(0)} = L$, and the flow is from right to left. The coefficient b was chosen as 1, and L was taken as 2. Typical characteristics of the zeroth-order solution for subsonic flow downstream of the throat are shown in figure (2.1). The characteristics β = constant are essentially straight at the left, that is, the region of large areas, and have increasing curvature as they approach the throat, where they have a vertical tangent. The characteristics α = constant are essentially straight throughout the duct. The variations of particle and sonic speed and Mach number along the duct are shown in figure (2.2).

At this point it is of value to digress from the particular problem at hand and to note an important feature of the method of coordinate perturbation that is implicit in the preceding development. In the case under consideration, we find that α and β may, at the same time, be considered as the characteristic parameters of a zeroth-order solution and of an "exact" solution (in the example, the steady duct flow). That is, the perturbation-series solution begins with the exact characteristics of the underlying flow. The lines α = constant and β = constant are mapped by $x^{(0)}(\alpha,\beta)$ and $t^{(0)}(\alpha,\beta)$ onto the characteristics in the $x^{(0)},t^{(0)}$-plane and by $x(\alpha,\beta)$ and $t(\alpha,\beta)$ onto the characteristics in the x,t-plane. Had it been possible to determine the solutions of the equations of higher order, these higher-order terms would not only have

changed the distribution of the flow variables along the zeroth-order characteristics in the physical plane but would also have changed the characteristics themselves. That is, the lines α = constant and β = constant would no longer be mapped by $x(\alpha,\beta)$ and $t(\alpha,\beta)$ onto the characteristics of the underlying flow in the x,t-plane but instead would be mapped onto the approximate characteristics of the perturbed flow. In other words, the significance and the properties of the characteristics are retained in the method of coordinate perturbation. This is in marked contrast to the more usual perturbation theories in the physical plane, in which the characteristics of the perturbed flow do not appear explicitly.

C. The "Epsilon Duct"

A way of avoiding the difficulties involved in obtaining the higher order solutions for the preceding example presents itself when the duct area variation itself is considered as being of the same order as the "smallness" parameter ϵ. In particular, the case $A_x/A = -\epsilon$ was studied; such a duct shall be referred to as an "epsilon duct." Such a choice amounts to requiring that the duct area vary slowly, but places no restriction on the over-all area variation (i.e., over a long stretch of the duct). For this choice of area variation, equations (2.9) become

$$\left.\begin{aligned} x_\alpha &= (u + c)t_\alpha, \\ x_\beta &= (u - c)t_\beta, \\ u_\alpha + \sigma c_\alpha &= \epsilon u c t_\alpha, \\ u_\beta - \sigma c_\beta &= -\epsilon u c t_\beta. \end{aligned}\right\} \tag{2.36}$$

Substituting equations (2.7) into equations (2.36) and equating the coefficients of like powers of ϵ yields

$$\left.\begin{aligned}
x_\alpha^{(k)} &= \sum_{\lambda=0}^{k} (u^{(\lambda)} + c^{(\lambda)})t_\alpha^{(k-\lambda)}, \\
x_\beta^{(k)} &= \sum_{\lambda=0}^{k} (u^{(\lambda)} - c^{(\lambda)})t_\beta^{(k-\lambda)}; \qquad k=0,1,2 \cdots \\
u_\alpha^{(0)} + \sigma c_\alpha^{(0)} &= 0; \quad u_\beta^{(0)} - \sigma c_\beta^{(0)} = 0; \\
u_\alpha^{(k)} + \sigma c_\alpha^{(k)} &= \sum_{j=0}^{k-1} \left[\sum_{\lambda=0}^{j} c^{(\lambda)}u^{(j-\lambda)}\right] t_\alpha^{(k-1-j)}, \\
u_\beta^{(k)} - \sigma c_\beta^{(k)} &= -\sum_{j=0}^{k-1} \left[\sum_{\lambda=0}^{j} c^{(\lambda)}u^{(j-\lambda)}\right] t_\beta^{(k-1-j)}; \qquad k=1,2,3 \cdots
\end{aligned}\right\} \quad (2.37)$$

Typical sets of the approximate equations are:

Zeroth order:

$$\left.\begin{aligned}
x_\alpha^{(0)} &= (u^{(0)} + c^{(0)})t_\alpha^{(0)}, \\
x_\beta^{(0)} &= (u^{(0)} - c^{(0)})t_\beta^{(0)}, \\
u_\alpha^{(0)} + \sigma c_\alpha^{(0)} &= 0, \\
u_\beta^{(0)} - \sigma c_\beta^{(0)} &= 0.
\end{aligned}\right\} \quad (2.38)$$

First order:

$$\left.\begin{aligned} x_\alpha^{(1)} &= (u^{(0)} + c^{(0)})t_\alpha^{(1)} + (u^{(1)} + c^{(1)})t_\alpha^{(0)}, \\ x_\beta^{(1)} &= (u^{(0)} - c^{(0)})t_\beta^{(1)} + (u^{(1)} - c^{(1)})t_\beta^{(0)}, \\ u_\alpha^{(1)} + \sigma c_\alpha^{(1)} &= c^{(0)}u^{(0)}t_\alpha^{(0)}, \\ u_\beta^{(1)} - \sigma c_\beta^{(1)} &= -c^{(0)}u^{(0)}t_\beta^{(0)}. \end{aligned}\right\} \quad (2.39)$$

Second order:

$$\left.\begin{aligned} x_\alpha^{(2)} &= (u^{(0)} + c^{(0)})t_\alpha^{(2)} + (u^{(1)} + c^{(1)})t_\alpha^{(1)} + (u^{(2)} + c^{(2)})t_\alpha^{(0)}, \\ x_\beta^{(2)} &= (u^{(0)} - c^{(0)})t_\beta^{(2)} + (u^{(1)} - c^{(1)})t_\beta^{(1)} + (u^{(2)} - c^{(2)})t_\beta^{(0)}, \\ u_\alpha^{(2)} + \sigma c_\alpha^{(2)} &= c^{(0)}u^{(0)}t_\alpha^{(1)} + (c^{(0)}u^{(1)} + c^{(1)}u^{(0)})t_\alpha^{(0)}, \\ u_\beta^{(2)} - \sigma c_\beta^{(2)} &= -c^{(0)}u^{(0)}t_\beta^{(1)} - (c^{(0)}u^{(1)} + c^{(1)}u^{(0)})t_\beta^{(0)}. \end{aligned}\right\} \quad (2.40)$$

Third order:

$$\left.\begin{aligned} x_\alpha^{(3)} &= (u^{(0)} + c^{(0)})t_\alpha^{(3)} + (u^{(1)} + c^{(1)})t_\alpha^{(2)} + (u^{(2)} + c^{(2)})t_\alpha^{(1)} + (u^{(3)} + c^{(3)})t_\alpha^{(0)}, \\ x_\beta^{(3)} &= (u^{(0)} - c^{(0)})t_\beta^{(3)} + (u^{(1)} - c^{(1)})t_\beta^{(2)} + (u^{(2)} - c^{(2)})t_\beta^{(1)} + (u^{(3)} - c^{(3)})t_\beta^{(0)}, \\ u_\alpha^{(3)} + \sigma c_\alpha^{(3)} &= c^{(0)}u^{(0)}t_\alpha^{(2)} + (c^{(0)}u^{(1)} + c^{(1)}u^{(0)})t_\alpha^{(1)} + (c^{(0)}u^{(2)} + c^{(1)}u^{(1)} + c^{(2)}u^{(0)})t_\alpha^{(0)}, \\ u_\beta^{(3)} - \sigma c_\beta^{(3)} &= -c^{(0)}u^{(0)}t_\beta^{(2)} - (c^{(0)}u^{(1)} + c^{(1)}u^{(0)})t_\beta^{(1)} - (c^{(0)}u^{(2)} + c^{(1)}u^{(1)} + c^{(2)}u^{(0)})t_\beta^{(0)}. \end{aligned}\right\} \quad (2.41)$$

The interesting thing about these equations is that the right hand sides of the equations resulting from the compatability conditions (i.e., the third and fourth equations of each set) involve functions of the lower order solutions only; that is, if the latter are known, of the independent variables. Thus, in principle, these equations can always be solved by quadratures. The equations resulting from the characteristic conditions (i.e., the first two equations of each set) are also always linear, and the coefficient of the derivative of the k-th order approximation of t is always the sum or difference of the zeroth-order solution for u and c.

The form of the equations suggests that it would be particularly simple to obtain solutions for problems where the initial conditions are specified on a line x = constant; for in such cases the zeroth-order solutions for u and c would be constants. This renders the solutions for the physical coordinates relatively simple for all orders.

To demonstrate such a solution, and in order to be able to check the values obtained against a known exact solution, it was decided to solve the problem wherein it is specified that on the section $x = 0$ the values of the particle and sonic speed are given by the constants U and C, respectively (i.e., a time-independent flow). The constants U and C are subject to the condition

$$U^2 + \sigma C^2 = \sigma + 1, \tag{2.42}$$

that is, the Bernoulli equation. The solution generated under these conditions should be the steady-state duct flow.

Equations (2.38) to (2.41) are to be solved, therefore, under the boundary conditions given above. The boundary conditions are to be satisfied in the following manner: Contrary to the choice in the previous section, now the line $x = 0$ is to be mapped on $\alpha = \beta$ such that $\alpha = \beta = t$. Thus, we choose

$$\left.\begin{aligned} x^{(n)}(\alpha,\alpha) &= x^{(n)}(\beta,\beta) = 0 \quad \text{for} \quad n \geq 0; \\ t^{(0)}(\alpha,\alpha) &= \alpha,\ t^{(0)}(\beta,\beta) = \beta, \\ t^{(n)}(\alpha,\alpha) &= t^{(n)}(\beta,\beta) = 0 \quad \text{for} \quad n > 0; \end{aligned}\right\} \tag{2.43}$$

and

$$\left.\begin{aligned} u^{(0)}(\alpha,\alpha) &= u^{(0)}(\beta,\beta) = U, \\ c^{(0)}(\alpha,\alpha) &= c^{(0)}(\beta,\beta) = C, \\ u^{(n)}(\alpha,\alpha) = u^{(n)}(\beta,\beta) &= c^{(n)}(\alpha,\alpha) = c^{(n)}(\beta,\beta) = 0 \quad \text{for} \quad n > 0. \end{aligned}\right\} \tag{2.44}$$

The second pair of the zeroth-order set (eqs. (2.38)) gives for the particle and sonic velocities simply

$$u^{(0)} = U;\ c^{(0)} = C.$$

Inserting these in the equations for the characteristics and integrating yields

$$x^{(0)} - (U + C)t^{(0)} = \mathcal{F}(\beta),$$

$$x^{(0)} - (U - C)t^{(0)} = \mathcal{G}(\alpha).$$

Applying the boundary conditions, we obtain

$$\mathcal{F}(\beta) = - (U + C)\beta,$$

$$\mathcal{G}(\alpha) = - (U - C)\alpha.$$

Therefore,

$$x^{(0)} = - (\alpha - \beta) \frac{U^2 - C^2}{2C},$$

$$t^{(0)} = \beta \frac{U + C}{2C} - \alpha \frac{U - C}{2C}.$$

The solutions of the higher order sets are obtained in a similar manner. The solutions up to the third order are

$$\left.\begin{aligned} u^{(0)} &= U, \\ u^{(1)} &= (\alpha - \beta) \frac{UC}{2}, \\ u^{(2)} &= (\alpha - \beta)^2 \frac{U}{8\sigma} (\sigma C^2 - U^2), \\ u^{(3)} &= (\alpha - \beta)^3 \frac{UC}{48\sigma} (\sigma C^2 - 5U^2); \end{aligned}\right\} \qquad (2.45a)$$

$$\left.\begin{aligned} c^{(0)} &= C, \\ c^{(1)} &= - (\alpha - \beta) \frac{U^2}{2\sigma}, \\ c^{(2)} &= - (\alpha - \beta)^2 \frac{U^2 C}{4\sigma}, \\ c^{(3)} &= - (\alpha - \beta)^3 \frac{U^2}{24\sigma^2} (2\sigma C^2 - U^2); \end{aligned}\right\} \qquad (2.45b)$$

$$\left.\begin{aligned} x^{(0)} &= -(\alpha-\beta)\frac{U^2-C^2}{2C}, \\ x^{(1)} &= -(\alpha-\beta)^2\frac{U^2}{8\sigma C^2}\left[C^2(2\sigma+1)+U^2\right], \\ x^{(2)} &= -(\alpha-\beta)^3\frac{U^2}{24\sigma C}\left[\frac{(\sigma C^2+U^2)^2}{\sigma C^2}+(\sigma+1)C^2\right], \\ x^{(3)} &= -(\alpha-\beta)^4\frac{1}{8}\left[(K-N)\frac{U}{C}+(K+N)\right]; \end{aligned}\right\} \tag{2.45c}$$

$$\left.\begin{aligned} t^{(0)} &= \beta\frac{U+C}{2C}-\alpha\frac{U-C}{2C}, \\ t^{(1)} &= -(\alpha-\beta)^2\frac{U}{8\sigma C^2}(\sigma C^2+U^2), \\ t^{(2)} &= -(\alpha-\beta)^3\frac{U}{48\sigma^2C^3}(\sigma C^2+U^2)(\sigma C^2+2U^2), \\ t^{(3)} &= -(\alpha-\beta)^4\frac{1}{8C}(K-N) \end{aligned}\right\} \tag{2.45d}$$

where,

$$K-N=\frac{U}{48\sigma^3C^3}(\sigma C^2+U^2)(\sigma C^2+6U^2), \tag{2.46}$$

$$K+N=\frac{U^2}{16\sigma^2C^2}(\sigma C^2+U^2)(2\sigma^2C^2+U^2)+\frac{U^2}{48\sigma^2}\left[\sigma(\sigma+4)C^2-(5\sigma+2)U^2\right]. \tag{2.47}$$

As anticipated, the solutions for the flow variables are independent of the time as is seen from the fact that u, c, and x are functions of $(\alpha - \beta)$ alone, and the possibility of the elimination of $(\alpha - \beta)$ from these equations makes u and c functions of x alone.

Although attempts were made, it was not possible to prove analytically the convergence of the perturbation series. In any case, however, it would have been necessary to resort to numerical examples in order to investigate the accuracy of the representation in the various regions of x.

As an example, the duct $\epsilon = 0.1$, $L = 6$ was chosen; that is, the duct area variation is given by $A = \exp\left[-0.1(x - 6)\right]$. A plot of the duct area variation is given in figure (2.3). The cross-sectional area varies in the ratio of approximately 1.81:1 from initial line ($x = 0$) to throat.

This duct was first investigated for the case of subsonic flow downstream of the throat with $\sigma = 1$ ($\gamma = 3$). With the flow coming from the right, we have, from the steady-flow equations (2.14) and (2.15), on $x = 0$

$$U = -0.40504; \quad C = 1.35497.$$

Inserting these values in equations (2.45), we obtain the series solution

$$\left.\begin{aligned}
-u &= 0.40504 + 0.02744(\alpha - \beta) + 0.00085(\alpha - \beta)^2 + 0.00001(\alpha - \beta)^3, \\
c &= 1.35497 - 0.00820(\alpha - \beta) - 0.00056(\alpha - \beta)^2 - 0.00002(\alpha - \beta)^3, \\
x &= 0.61695(\alpha - \beta) - 0.00633(\alpha - \beta)^2 - 0.00029(\alpha - \beta)^3 - \\
&\quad 0.00001(\alpha - \beta)^4, \\
t &= 0.35053\beta + 0.64946\alpha + 0.00552(\alpha - \beta)^2 + 0.00015(\alpha - \beta)^3 + \\
&\quad 0.000003(\alpha - \beta)^4.
\end{aligned}\right\} \quad (2.48)$$

The second- and third-order solutions are shown in figures (2.4) and (2.5) by the data symbols. The exact steady duct flow is given by the solid curves. As can be seen in figure (2.4), the flow velocity is very well represented by the second-order solution up to about $x = 4$. The third-order solution extends the accurate representation up to $x = 5.5$. Only in the immediate vicinity of the throat ($x = 6$) does the departure from the exact solution become relatively large. The sonic speed is also well represented by the approximate solutions, as seen in figure (2.5). Again, large departures from the exact solution occur only near the throat.

The variation of the space coordinate x with the quantity $(\alpha - \beta)$ is shown in figure (2.6). Proceeding from the second- to the third-order solution decreases the variation of x with $(\alpha - \beta)$ for the larger values of this quantity. That is, the higher degree terms of $(\alpha - \beta)$ cause the $x,(\alpha - \beta)$-relation to become more horizontal for values of the argument above 7. For values of $(\alpha - \beta)$ less than 7, the second- and third-order solutions give the same value for x. It may be recalled that values of $(\alpha - \beta)$ which yield values of x greater than 6 are not pertinent to the solution.

A typical β = constant curve in the x,t-plane of the third-order solution is shown in figure (2.7) along with the exact characteristic. The case shown in that of $\beta = 0$, and the points indicated by the data symbols are obtained by setting $\beta = 0$ in the last two of equations (2.48) and eliminating α. The exact characteristic is obtained by setting $b = \epsilon$ in equation (2.27) and using the appropriate value of L. It is evident that the approximation to the actual characteristic is very good up to the vicinity of the throat, in which region the departures become large.

D. Factors Affecting Convergence and Accuracy

From the preceding example, it appears that the approximate solution does converge to the duct flow solution. There are a number of factors that may affect the nature and rapidity of the convergence. Among these are the magnitude of ϵ, the over-all area ratio of the duct, the location of the initial line on which U and C are specified, and whether the flow is subsonic or supersonic.

1. Effect of ϵ. - The first step in this investigation was to determine the effect of the magnitude of ϵ on the solutions. For this purpose a set of approximate duct flow solutions were computed for different values of ϵ. The values of duct length were so chosen that the product ϵL was constant. For the type of duct considered, that is, $A = \exp\left[-\epsilon(x - L)\right]$, this results in a set of ducts of the same over-all area ratio between $x = 0$ and $x = L$ but with different rates of change of area. These examples were computed for the case of subsonic flow downstream of the throat with $\sigma = 5$ ($\gamma = 7/5$). The values of the parameters ϵ and L used are:

ϵ	L
0.1	6.0
0.2	3.0
0.4	1.5

For these cases we have, from the steady-flow equations, the boundary conditions on $x = 0$:

$$U = -0.36841; \quad C = 1.08298.$$

For these values the approximate solution is given by

$$\left.\begin{aligned} -u &= 0.36841 + \epsilon(0.19949)(\alpha - \beta) + \epsilon^2(0.05276)(\alpha - \beta)^2 + \\ &\quad \epsilon^3(0.00862)(\alpha - \beta)^3, \\ c &= 1.08298 - \epsilon(0.01357)(\alpha - \beta) - \epsilon^2(0.00735)(\alpha - \beta)^2 - \\ &\quad \epsilon^3(0.00262)(\alpha - \beta)^3, \\ x &= 0.47883(\alpha - \beta) - \epsilon(0.03772)(\alpha - \beta)^2 - \epsilon^2(0.01376)(\alpha - \beta)^3 - \\ &\quad \epsilon^3(0.00038)(\alpha - \beta)^4. \end{aligned}\right\} \quad (2.49)$$

The results of the computations for these examples are shown in figures (2.8) to (2.10) as plots of u and c as functions of x. For all the values of ϵ, the approximate solutions converge on the exact solution. The accuracy of the representation is quite good, the third-order solution being quite accurate for about 80 percent of the duct length. Moreover, comparison of the three figures shows that the accuracy of the representation at corresponding points (i.e., equal area ratios) in the ducts is the same for all values of ϵ. This leads to the conclusion that the accuracy of the approximate solution is not a function of ϵ alone.

2. Effect of over-all area ratio. - The over-all area ratio of an "epsilon duct" is a function of the product ϵL. To investigate the effect of the over-all area ratio on the solutions, two additional examples were computed for an ϵ of 0.2. For subsonic flow the values of L selected and the corresponding initial values of the flow variables on $x = 0$ are:

L	U	C
5.0	-0.23889	1.09022
7.5	-0.14270	1.09365

The solution for $L = 5$ is given by

$$\left.\begin{aligned} -u &= 0.23889 + \epsilon(0.13022)(\alpha - \beta) + \epsilon^2(0.03515)(\alpha - \beta)^2 + \\ &\quad \epsilon^3(0.00614)(\alpha - \beta)^3, \\ c &= 1.09022 - \epsilon(0.00571)(\alpha - \beta) - \epsilon^2(0.00311)(\alpha - \beta)^2 - \\ &\quad \epsilon^3(0.00113)(\alpha - \beta)^3, \\ x &= 0.51894(\alpha - \beta) - \epsilon(0.01576)(\alpha - \beta)^2 - \epsilon^2(0.00575)(\alpha - \beta)^3 - \\ &\quad \epsilon^3(0.00157)(\alpha - \beta)^4. \end{aligned}\right\} (2.50)$$

For $L = 7.5$ the solution is

$$\left.\begin{aligned} -u &= 0.14270 + \epsilon(0.07803)(\alpha - \beta) + \epsilon^2(0.02126)(\alpha - \beta)^2 + \\ &\quad \epsilon^3(0.00382)(\alpha - \beta)^3, \\ c &= 1.09365 - \epsilon(0.00204)(\alpha - \beta) - \epsilon^2(0.00111)(\alpha - \beta)^2 - \\ &\quad \epsilon^3(0.00041)(\alpha - \beta)^3, \\ x &= 0.53752(\alpha - \beta) - \epsilon(0.00561)(\alpha - \beta)^2 - \epsilon^2(0.00205)(\alpha - \beta)^3 - \\ &\quad \epsilon^3(0.00056)(\alpha - \beta)^4. \end{aligned}\right\} (2.51)$$

The results of these computations are shown in figures (2.11) and (2.12), where the particle and sonic velocities are plotted as functions of x. Again, the approximate solutions converge on the exact solution. Comparison of these solutions as well as that shown in figure (2.9), which is for $L = 3$ and $\epsilon = 0.2$, indicates that the greater the length of the duct (i.e., the over-all area ratio from $x = 0$ to $x = L$), the smaller is the value of x/L at which a given departure from the exact solution occurs. For example, the coordinate $\bar{x}$ at which the third-order solution for u has an error of 0.01 is given in the following table for the three ducts considered:

L	$\bar{x}$	$\bar{x}/L$	$A_0/A_{\bar{x}}$	$(u_{\bar{x}})_{exact}$
3.0	2.64	0.88	1.70	0.760
5.0	3.80	0.76	2.14	0.573
7.5	4.90	0.65	2.66	0.405

Although a given error in u occurs at smaller values of x/L as the duct length increases, it should be noted that the ratio of the area at $x = 0$ to that at $\bar{x}$ increases as the duct length increases. A similar statement holds when the comparison is made on the basis of a given percentage error in u.

For a given value of ϵ, the value of L determines not only the over-all area ratio of the duct but also the values of the flow variables at $x = 0$, since the steady flow is sonic at $x = L$. The larger the value of L, the smaller is the value of U on $x = 0$. A concomitant of small values of U is a decreased rate of change of the flow variables with x (or area ratio) in the vicinity of $x = 0$ (cf. figs. (2.9) and (2.12)). It is this latter property of subsonic flow that results in the accurate representation of the flow over larger area ratios for the "epsilon ducts" with larger L.

3. Effect of the location of the initial line. - To this point, only the case wherein the initial conditions have been specified at the largest area of the duct, that is, at $x = 0$, has been considered. If the initial conditions are specified at the throat, that is, at $x = L$, where the rates of change of the flow variables with distance are greatest, the effect of this factor can be observed. For this purpose, equations (2.36) were solved with the conditions specified at $x = L$. The solutions for this case are the same as those given by equations (2.45) with the exception of the zeroth-order term for x. This is replaced by

$$x^{(0)} = L - (\alpha - \beta)\frac{U^2 - C^2}{2C}. \tag{2.52}$$

For this case we have at the boundary $x = L$ the initial values of $U = -1$, $C = 1$. The steady-flow solution for $\sigma = 5$ is represented by the following equations:

$$\left.\begin{aligned} -u &= 1 + \epsilon(0.5)(\alpha - \beta) + \epsilon^2(0.1)(\alpha - \beta)^2, \\ c &= 1 - \epsilon(0.1)(\alpha - \beta) - \epsilon^2(0.05)(\alpha - \beta)^2 - \epsilon^3(0.015)(\alpha - \beta)^3, \\ x &= L - \epsilon(0.3)(\alpha - \beta)^2 - \epsilon^2(0.11)(\alpha - \beta)^3 - \\ &\quad \epsilon^3(0.03075)(\alpha - \beta)^4. \end{aligned}\right\} \tag{2.53}$$

These equations represent the supersonic branch as well as the subsonic branch. To obtain the subsonic branch, the argument of the series $(\alpha - \beta)$ must be taken as negative to make $\left|\frac{u}{c}\right| < 1$. An example of the subsonic case was computed with $\epsilon = 0.1$ and $L = 6$, and the results are shown in figure (2.13). The representations of the particle and sonic

velocities given by the approximate solutions are seen to alternate above and below the exact values. The approximate solution does, however, appear to be converging to the exact solution as higher order terms are used. In the neighborhood of the throat the approximate solutions are good representations of the flow, despite the rapid variation of the flow parameters with x. Although the solutions do appear to converge to the exact solution, the convergence is not as rapid as that obtained for the corresponding case with conditions specified at $x = 0$ (fig. 2.8). This is especially noticeable for the sonic speed (fig. 2.13b), where the second-order solution reaches a maximum at about $x = 4$ and then decreases with increasing x.

Some insight into the reasons for this behavior can be obtained from figure (2.14), which shows the variation of x as a function of $(\alpha - \beta)$ for this example. The second-order representation of x has a minimum in the vicinity of $(\alpha - \beta) = -17$, whereas the third-order representation exhibits no such behavior up to this value of the argument. This change in the nature of the relationship between x and $(\alpha - \beta)$ is a result of the fact that, for negative values of the argument, the expression for x is in effect an alternating series. The coefficients of the series are of sufficient magnitude to have large effects on the representation of x for the larger values of the argument. It should be noted that for negative values of the argument the series for u and c also have alternating signs.

Thus, for subsonic flow, it can be concluded that specifying the initial conditions at $x = L$, where the rates of change of the flow variables with x are high, results in less rapid convergence of the solutions than for the corresponding case where the initial conditions are given on $x = 0$.

4. Supersonic flow. - Thus far, only subsonic flows have been considered. We now examine the character of the perturbation solutions for supersonic flow. First, consider the case with initial conditions given at the throat. For positive values of $(\alpha - \beta)$, equations (2.53) yield the supersonic branch of the duct flow. In this case the series do not have alternating signs. The results for $\epsilon = 0.1$ and $L = 6$ are shown in figure (2.15). In this case the approximations converge quite rapidly to the exact solution, and the accuracy of the third-order solution is quite good for the entire length of the duct. Whereas in the subsonic case specified on $x = L$ convergence of the representation of c was poorer than that of u, in the supersonic case the opposite is true. In fact, the third-order representation of c is excellent for the entire length considered. One possible reason for the fact that the representation of u does not appear to be as accurate as that for c is that the coefficient of the term of third degree in $(\alpha - \beta)$ in the equation for u is zero in this case.

There remains one further case to examine. This is supersonic flow with conditions specified at $x = 0$. For this case we have, for the same duct as in the last two examples, on $x = 0$, $U = -1.67289$ and $C = 0.80019$. For these values the flow is represented by

$$\left.\begin{aligned} -u &= 1.67289 + \epsilon(0.66931)(\alpha - \beta) + \epsilon^2(0.01685)(\alpha - \beta)^2 - \\ &\quad \epsilon^3(0.06018)(\alpha - \beta)^3, \\ c &= 0.80019 - \epsilon(0.27986)(\alpha - \beta) - \epsilon^2(0.11197)(\alpha - \beta)^2 - \\ &\quad \epsilon^3(0.01681)(\alpha - \beta)^3, \\ x &= -1.34859(\alpha - \beta) - \epsilon(1.07539)(\alpha - \beta)^2 - \epsilon^2(0.43969)(\alpha - \beta)^3 - \\ &\quad \epsilon^3(0.16413)(\alpha - \beta)^4. \end{aligned}\right\} \quad (2.54)$$

For values of x greater than zero, $(\alpha - \beta)$ must be taken as negative. This again leads to a series with alternating signs for the representation of x. The results of the evaluation of equations (2.54) are shown in figure (2.16). For this case, as for subsonic flow specified at $x = L$, the approximate solutions of increasing order alternate above and below the exact solution. Again, the third-order solution is a good representation of the flow variables over most of the duct length. Departures of appreciable magnitude for the third-order solution occur in the vicinity of $x = 5.3$. It is to be noted that both the first- and third-order solutions for the flow variables fold back on themselves, the former at about $x = 4.2$ and the latter at about $x = 5.5$. This is again the result of the nature of the x, $(\alpha - \beta)$-relation shown in figure (2.17). The first-order representation reaches a maximum of 4.2 at $(\alpha - \beta) = -6.25$, and the third-order representation has a maximum of $5.\overline{55}$ at $(\alpha - \beta) = -9.0$. These maxima result from the strong influence of the term of highest degree of $(\alpha - \beta)$ in each case. These are the even-powered terms that, for negative values of the argument, serve to reduce the rate of change of x with $(\alpha - \beta)$ and thus produce the maxima.

5. Recapitulation. - From the preceding examination of the factors affecting the convergence and accuracy of the perturbation-series solution for steady duct flow, it was established that for both supersonic and subsonic flows the series converge to the exact solution. The extent of accurate representation of the flow depends on the over-all area ratio of the channel and thus on the values of the flow variables on the initial line. For subsonic flow the extent of accurate representation was greatest when the initial values were given at the large end of the duct, that is, at $x = 0$. For supersonic flow the opposite was true; that is, the extent of accurate representation was greatest when the initial conditions were given at the throat. However, the differences caused by the change of the data carrier in the supersonic case are not as great as for subsonic flow.

In both supersonic and subsonic flow the poorer representations occur when negative values of the argument of the series must be employed.

It should be noted that the particular area function chosen, that is, the "epsilon duct," is not the only one for which such solutions are possible. The particular case used should be viewed as but one of a family of area functions that should be amenable to the method used. This family can be represented by $A = e^{\pm\epsilon P(x)}$ where $P(x)$ is a polynomial in x. For such area functions similar results should be obtainable.

E. Unsteady Flow

To this point, the perturbation-series solution has been investigated only for the case of constant conditions on the initial line. Such initial conditions were chosen so that the solutions obtained could be easily compared with a known exact solution, the steady duct flow. We now turn to the case of unsteady quasi-one-dimensional flow. For perturbation-series solutions for unsteady flows in a duct, the specification of boundary conditions becomes complex, and more detailed consideration must be given to the nature of the initial data than was the case for steady flow.

1. Boundary conditions. - In the usual perturbation problems, such as those for steady two-dimensional flow and one-dimensional unsteady flow, there is an underlying uniform state or flow that is constant both in space and time. For example, in two-dimensional steady flow the underlying uniform flow is frequently chosen as a constant value of u, as indicated in equation (2.1). For one-dimensional wave propagation problems, the underlying flow is either a constant steady flow or a state of rest. In such cases the physical interpretation of a given set of boundary data is quite straightforward and no great difficulties arise.

In contrast to these cases, the underlying flow in a quasi-one-dimensional problem is uniform, in the true sense of the word, only for one particular circumstance, that is, a state of rest. For all other cases the underlying "uniform" state is a steady duct flow in which, of course, the flow variables are not constant in space. For such problems an implicit boundary condition is then: Along some line t = constant in the x,t-plane, a steady duct flow must exist. Alternatively, one could specify that, along a certain characteristic which separates the regions of steady and unsteady flow (corresponding to the "rest" characteristic of a disturbance advancing into a gas at rest), the steady duct flow relation holds. This requirement introduces some difficulties in the specification of initial data for the solution of problems by the perturbation method under consideration.

Consider two intersecting noncharacteristic arcs J and K in the x,t-plane enclosing a region R (see sketch).

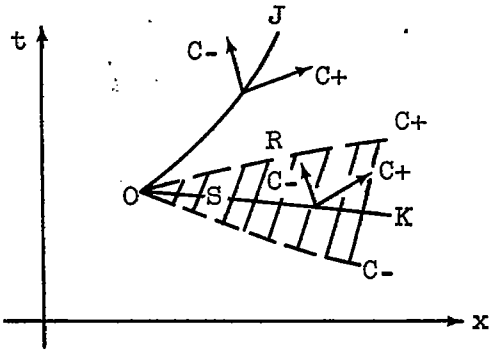

As developed in section 28 of reference 6, if a direction is assigned to each of the two families of characteristics (in the sketch the direction of increasing time is chosen), it can happen that the two characteristics issuing from any point on K enter R, whereas only one characteristic from any point on J enters R. An arc such as K is called space-like, and the arc J is called time-like. In the reference cited above, it is established that, for problems in which the boundary conditions are specified on both time-like and space-like arcs, two data on the space-like arc and one datum on the time-like arc determine an unique solution in the region between the arcs. In such problems, a relation exists between the two dependent variables on the time-like arc.

The form taken by the differential equations for the perturbation problem (eqs. (2.37)) is such that it is most convenient to specify the initial data on a time-like arc. This was the case for the steady-flow examples presented earlier in this section. In that case it was reasonable to specify both dependent variables on the time-like arc, $x = 0$ or $x = L$, because the relation between the dependent variables was known and, further, they were constant. In the more general case of an unsteady disturbance of a steady flow, one cannot arbitrarily specify two data on a time-like arc as noted above. If such a specification were made, the region S, bounded by the characteristics issuing from point O, would contain an unsteady flow. This would imply that a disturbance originating at point O would influence the flow field to the right of O at an earlier time, a physically untenable condition. On the other hand, if it were attempted to specify a steady flow on the bounding C+ characteristic (the "rest" characteristic) issuing from point O and a single datum on the time-like arc, the problem would become almost hopelessly complex because the initial data along the "rest" characteristic would have to be given by equations such as (2.30) to (2.33).

There are, however, two ways of avoiding the difficulties noted above. The first is to consider the problem wherein two data are arbitrarily

specified on a time-like arc from a different viewpoint. The second is to seek the relation between the dependent variables on the time-like arc that will not produce an unsteady flow below the "rest" characteristic.

2. The "inverse" problem. - We consider first the case of an arbitrary disturbance of one or both of the dependent variables specified on a time-like arc. Such a problem can be viewed in the following manner: We give on a time-like arc, say on the line $x = x_0$, a certain distribution of u and c, one or both functions of time. We then ask what occurred at another station at a previous time to cause the flow at $x = x_0$ to vary in the manner prescribed. For the flow to have been a steady duct flow prior to some time t_0 on the boundary, it is necessary merely to specify that for all $t \leq t_0$ the values of u and c on the boundary are to be constant and satisfy the Bernoulli equation. This situation is shown in the sketch.

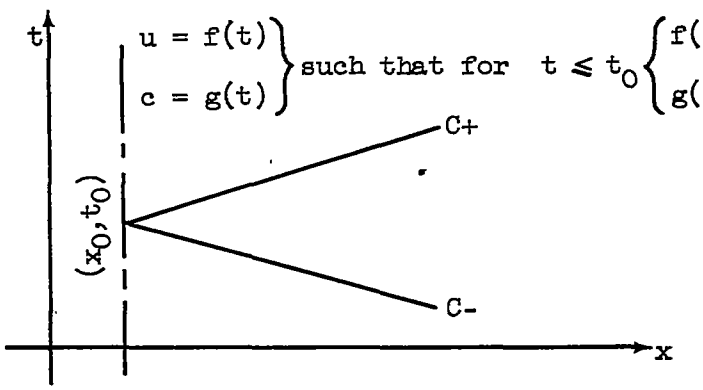

Under these conditions there will be a steady duct flow below the C- characteristic through (x_0, t_0). A physical example of such a problem would be that of inquiring how to vary the entrance conditions into a duct so that a given flow variation at the exit might result.

Such problems are referred to as "inverse" problems in the sequel. It was found that the solution of such problems could be written in a quite general fashion. An example of such a solution follows.

Consider the case of an "epsilon duct" originally containing a steady flow. Let a disturbance in sonic speed of order of magnitude ϵ start at a specified time at a given cross section of the duct. For convenience let the cross section be that at $x = 0$ and let the disturbance begin at $t = 0$ at this cross section. The boundary conditions under which equations (2.37) are to be solved are, therefore, on $x = 0$,

$$\left.\begin{aligned} u &= U, \\ c &= C + \epsilon f(t), \end{aligned}\right\} \tag{2.55}$$

where

$$\left.\begin{aligned} f(t) &= 0, \qquad \text{for} \qquad t \leqslant 0; \\ U^2 + \sigma C^2 &= \sigma + 1. \end{aligned}\right\} \tag{2.56}$$

These boundary conditions are to be satisfied in the following manner: The line $x = 0$ is to be mapped on $\alpha = \beta$ such that $\alpha = \beta = t$, that is, according to equations (2.43) and

$$\left.\begin{aligned} u^{(0)}(\alpha,\alpha) &= u^{(0)}(\beta,\beta) = U, \\ u^{(n)}(\alpha,\alpha) &= u^{(n)}(\beta,\beta) = 0, \qquad n > 0; \\ c^{(0)}(\alpha,\alpha) &= c^{(0)}(\beta,\beta) = C, \\ c^{(1)}(\alpha,\alpha) &= f(\alpha), \; c^{(1)}(\beta,\beta) = f(\beta), \\ c^{(n)}(\alpha,\alpha) &= c^{(n)}(\beta,\beta) = 0, \qquad n > 1. \end{aligned}\right\} \tag{2.57}$$

(Note the peculiar way in which the boundary conditions for this problem can be accommodated in the ϵ-scheme.)

The solutions, under these conditions, up to second order are:

$$\left.\begin{aligned} u^{(0)} &= U, \\ u^{(1)} &= U_1^{(1)}(\alpha - \beta) + U_2^{(1)} f(\beta) - U_3^{(1)} f(\alpha), \\ u^{(2)} &= U_1^{(2)}(\alpha - \beta)^2 + U_2^{(2)}(\alpha - \beta) f(\alpha) - U_3^{(2)}(\alpha - \beta) f(\beta) - \\ &\qquad U_4^{(2)} \int_\alpha^\beta f(\tau)\,d\tau; \end{aligned}\right\} \tag{2.58a}$$

$$\left.\begin{aligned} c^{(0)} &= C, \\ c^{(1)} &= -C_1^{(1)}(\alpha - \beta) + C_2^{(1)} f(\beta) + C_3^{(1)} f(\alpha), \\ c^{(2)} &= -C_1^{(2)}(\alpha - \beta)^2 + C_2^{(2)} (\alpha - \beta) f(\beta) + C_3^{(2)}(\alpha - \beta) f(\alpha) + \\ &\qquad C_4^{(2)} \int_\alpha^\beta f(\tau)\,d\tau; \end{aligned}\right\} \tag{2.58b}$$

$$
\begin{aligned}
x^{(0)} &= -X_1^{(0)}(\alpha - \beta), \\
x^{(1)} &= -X_1^{(1)}(\alpha - \beta)^2 + X_2^{(1)}(\alpha - \beta)f(\beta) + X_3^{(1)}(\alpha - \beta)f(\alpha) + \\
&\quad X_4^{(1)} \int_\alpha^\beta f(\tau)d\tau, \\
x^{(2)} &= -X_1^{(2)}(\alpha - \beta)^3 + X_2^{(2)}(\alpha - \beta)^2 f(\beta) + X_3^{(2)}(\alpha - \beta)^2 f(\alpha) + \\
&\quad X_4^{(2)} \int_\alpha^\beta (\tau - \beta)f(\tau)d\tau + X_5^{(2)} \int_\alpha^\beta (\alpha - \tau)f(\tau)dt + \\
&\quad X_6^{(2)} f(\beta) \int_\alpha^\beta f(\tau)d\tau + X_7^{(2)} f(\alpha) \int_\alpha^\beta f(\tau)d\tau + \\
&\quad X_8^{(2)} \int_\alpha^\beta \left[f(\tau)\right]^2 d\tau + X_9^{(2)}(\alpha - \beta)\left[f(\beta)\right]^2 + \\
&\quad X_{10}^{(2)}(\alpha - \beta)\left[f(\alpha)\right]^2 + X_{11}^{(2)}(\alpha - \beta)f(\alpha)f(\beta);
\end{aligned}
\tag{2.58c}
$$

$$
\begin{aligned}
t^{(0)} &= T_1^{(0)}\beta - T_2^{(0)}\alpha, \\
t^{(1)} &= -T_1^{(1)}(\alpha - \beta)^2 + T_2^{(1)}(\alpha - \beta)f(\beta) + T_3^{(1)}(\alpha - \beta)f(\alpha) + \\
&\quad T_4^{(1)} \int_\alpha^\beta f(\tau)d\tau, \\
t^{(2)} &= -T_1^{(2)}(\alpha - \beta)^3 + T_2^{(2)}(\alpha - \beta)^2 f(\beta) + T_3^{(2)}(\alpha - \beta)^2 f(\alpha) + \\
&\quad T_4^{(2)} \int_\alpha^\beta (\tau - \beta)f(\tau)d\tau + T_5^{(2)} \int_\alpha^\beta (\alpha - \tau)f(\tau)d\tau + \\
&\quad T_6^{(2)} f(\beta) \int_\alpha^\beta f(\tau)d\tau + T_7^{(2)} f(\alpha) \int_\alpha^\beta f(\tau)d\tau + \\
&\quad T_8^{(2)} \int_\alpha^\beta \left[f(\tau)\right]^2 d\tau + T_9^{(2)}(\alpha - \beta)\left[f(\beta)\right]^2 + \\
&\quad T_{10}^{(2)}(\alpha - \beta)\left[f(\alpha)\right]^2 + T_{11}^{(2)}(\alpha - \beta)f(\alpha)f(\beta).
\end{aligned}
\tag{2.58d}
$$

In obtaining these solutions, the following identity has been used:

$$\underbrace{\int_a^y \cdots \int_a^y}_{n} f(y)\underbrace{dy \cdots dy}_{n} = \frac{1}{(n-1)!}\int_a^y (y-\xi)^{(n-1)} f(\xi)\,d\xi. \qquad (2.59)$$

The coefficients appearing in equations (2.58) are functions of U, C, and σ and are listed below:

$$\left.\begin{aligned} U_1^{(1)} &= \frac{UC}{2} & U_1^{(2)} &= \frac{U}{8\sigma}(\sigma C^2 - U^2) \\ U_2^{(1)} &= \frac{\sigma}{2} & U_2^{(2)} &= \frac{(U+C)(U-\sigma C)}{8C} \\ U_3^{(1)} &= \frac{\sigma}{2} & U_3^{(2)} &= \frac{(U-C)(U+\sigma C)}{8C} \\ & & U_4^{(2)} &= \frac{\sigma+1}{4}U \end{aligned}\right\} \qquad (2.60a)$$

$$\left.\begin{aligned} C_1^{(1)} &= \frac{U^2}{2\sigma} & C_1^{(2)} &= \frac{CU^2}{4\sigma} \\ C_2^{(1)} &= \frac{1}{2} & C_2^{(2)} &= \frac{1}{8}(U-C)^2 \\ C_3^{(1)} &= \frac{1}{2} & C_3^{(2)} &= \frac{1}{8}(U+C)^2 \\ & & C_4^{(2)} &= \frac{U^2+C^2}{4C} \end{aligned}\right\} \qquad (2.60b)$$

$$
\left.
\begin{aligned}
X_1^{(0)} &= \frac{U^2 - C^2}{2C} \\
X_1^{(1)} &= \frac{U^2}{8\sigma C^2}\left[(2\sigma + 1)C^2 + U^2\right] \\
X_2^{(1)} &= \frac{\sigma + 1}{8C^2}(U - C)^2 \\
X_3^{(1)} &= \frac{\sigma + 1}{8C^2}(U + C)^2 \\
X_4^{(1)} &= \frac{\sigma - 1}{4C^2}(U^2 + C^2) \\
X_1^{(2)} &= \frac{U^2}{24\sigma C}\left[\frac{(U^2 + \sigma C^2)^2}{\sigma C^2} + (\sigma + 1)C^2\right] \\
X_2^{(2)} &= \frac{(\sigma + 1)}{64\sigma C^3}(U - C)\left[U^2(5U + C) + \sigma C^2(7U - C)\right] \\
X_3^{(2)} &= \frac{(\sigma + 1)}{64\sigma C^3}\left\{(U + C)\left[U^2(5U - C) + \sigma C^2(7U + C)\right]\right\} \\
X_4^{(2)} &= \frac{1}{32\sigma C^3}\left\{\sigma(\sigma+1)C^2(U+C)^2 + U^2\left[C^2(4\sigma-3)(\sigma+1) + 6UC(\sigma+1) + U^2(5\sigma-3)\right]\right\} \\
X_5^{(2)} &= \frac{1}{32\sigma C^3}\left\{\sigma C^2\left[(\sigma+1)C^2 - 8UC + 7(\sigma+1)U^2\right] + \right. \\
&\qquad \left. U^2\left[(5\sigma-3)U^2 + 4(\sigma+1)UC - (\sigma+1)C^2\right]\right\} \\
X_6^{(2)} &= -\frac{\sigma + 1}{32C^3}(U - C)\left[3(\sigma - 1)U + (\sigma + 3)C\right] \\
X_7^{(2)} &= -\frac{\sigma^2 - 1}{32C^3}(U + C)(3U + C) \\
X_8^{(2)} &= -\frac{\sigma - 1}{32C^3}\left[(\sigma + 1)C^2 + (\sigma - 7)U^2 + 2(\sigma + 1)UC\right] \\
X_9^{(2)} &= \frac{\sigma + 1}{64C^3}(U - C)\left[(3\sigma + 1)C - (\sigma + 3)U\right] \\
X_{10}^{(2)} &= -\frac{\sigma + 1}{64C^3}(U + C)\left[(3\sigma + 1)C + (\sigma + 3)U\right] \\
X_{11}^{(2)} &= \frac{(\sigma + 1)^2}{16C^3}(C^2 - U^2)
\end{aligned}
\right\} \qquad (2.60c)
$$

$$T_1^{(0)} = \frac{U + C}{2C}$$

$$T_2^{(0)} = \frac{U - C}{2C}$$

$$T_1^{(1)} = \frac{U}{8\sigma C^2}\,(U^2 + \sigma C^2)$$

$$T_2^{(1)} = \frac{\sigma + 1}{8C^2}\,(U - C)$$

$$T_3^{(1)} = \frac{\sigma + 1}{8C^2}\,(U + C)$$

$$T_4^{(1)} = \frac{\sigma - 1}{4}\,\frac{U}{C^2}$$

$$T_1^{(2)} = \frac{U}{48\sigma^2 C^3}\,(U^2 + \sigma C^2)(2U^2 + \sigma C^2)$$

$$T_2^{(2)} = -\frac{\sigma + 1}{64\sigma C^3}\left[\sigma C^2(C - 3U) + U^2(3C - 5U)\right]$$

$$T_3^{(2)} = \frac{\sigma + 1}{64\sigma C^3}\left[\sigma C^2(C + 3U) + U^2(3C + 5U)\right]$$

$$T_4^{(2)} = -\frac{1}{32\sigma C^3}\left\{\sigma C^2\left[C(\sigma-3) - U(\sigma+1)\right] - U^2\left[(7\sigma+3)C + (5\sigma-3)U\right]\right\}$$

$$T_5^{(2)} = \frac{1}{32\sigma C^3}\left\{\sigma C^2\left[(\sigma-3)C + 3(\sigma+1)U\right] + U^2\left[(5\sigma-3)U - (5\sigma+1)C\right]\right\}$$

$$T_6^{(2)} = -\frac{\sigma + 1}{32C^3}\left[3(\sigma - 1)U + (\sigma + 3)C\right]$$

$$T_7^{(2)} = -\frac{\sigma^2 - 1}{32C^3}\,(3U + C)$$

$$T_8^{(2)} = -\frac{\sigma - 1}{32C^3}\left[(\sigma - 7)U + 2(\sigma + 1)C\right]$$

$$T_9^{(2)} = -\frac{(\sigma + 1)(\sigma + 3)}{64C^3}\,(U - C)$$

$$T_{10}^{(2)} = -\frac{(\sigma + 1)(\sigma + 3)}{64C^3}\,(U + C)$$

$$T_{11}^{(2)} = -\frac{(\sigma + 1)^2}{16C^3}\,U\,.$$

(2.60d)

It is to be noted that in equations (2.58) the terms independent of the disturbance function are exactly those given by equations (2.45) for the steady-flow solution. Thus, the solution for the unsteady flow also generates the underlying steady duct flow below the "rest" characteristic.

To illustrate the character of the solution, an example was computed for a duct with an initial exit Mach number of 0.35 (i.e., on $x = 0$). For this Mach number and for $\sigma = 5$ ($\gamma = 7/5$) with the flow coming from the right, we have $U = -0.37879$ and $C = 1.08226$. For the disturbance, a "finite ramp" function

$$f(t) = \begin{cases} Bt & \text{for} \quad 0 \leq t \leq \delta \\ B\delta & \quad\quad t > \delta \\ 0 & \quad\quad t < 0 \end{cases} \tag{2.61}$$

was chosen with $B = 0.0086905$ and $\delta = 4.0$. For an ϵ of 0.1, this represents about a 1/3 percent disturbance in sonic speed on the boundary $x = 0$ at the conclusion of the "ramp." Equations (2.58) were programmed for computation by an IBM type-650 digital computer by using the Bell Interpretive System (ref. 9). The program was set up so that the variations of the flow variables on lines of constant x could be calculated. The values of the coefficients of equations (2.58) (cf. eqs. (2.60)) for the initial values given above are listed in table (2.1). The results of the computations are shown in figures (2.18) and (2.19) for $x = 0.5$ and 1.0, respectively. In both figures the region between $\alpha = 0$ and $\beta = 0$ is seen to be an unsteady flow field, as expected from the nature of the initial conditions. In this region both u and c vary. In the region bounded by $\alpha = 4$ and $\beta = 0$, the particle velocity is essentially constant; this reflects the constant value of u between these characteristics on $x = 0$. In this region the rate of change of sonic speed with time increases above that below $\beta = 0$. In the region bounded by $\alpha = 4$ and $\beta = 4$, the magnitude of the particle velocity decreases, and the sonic speed continues to increase until the $\beta = 4$ characteristic is reached, at which time a new steady state is achieved.

In both figures the first- and second-order solutions are quite similar in shape. The principal difference is in the level of the solution which, however, reflects principally the accuracy of the representation of the underlying steady flow. The changes in level in going from the first- to the second-order solution is greater at $x = 1$ than at $x = 0.5$, as expected. It is obvious also that the time interval during which the particle velocity is almost constant is shorter at $x = 1$ than at $x = 0.5$, which is to be expected from the triangular nature of the region between $\beta = 0$ and $\alpha = 4$ (shown in the inset in fig. (2.18)).

In order to compare the perturbation-series solution with an exact solution, this problem was solved by the method of characteristics with a finite difference technique. Consider a noncharacteristic arc i and two points on this arc, j and (j+1) (see sketch). At these

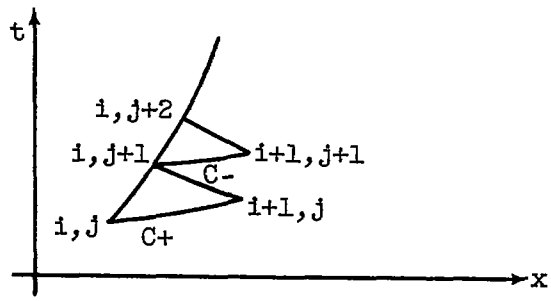

points the dependent variables u and c are known. To determine the location of point (i+1,j) and the values of flow variables at this point, equations (2.36) are written as difference equations. The resulting equations are:

$$\left.\begin{aligned}
&x_{i+1,j} - x_{i,j} = (u_{i,j} + c_{i,j})(t_{i+1,j} - t_{i,j}),\\
&x_{i+1,j} - x_{i,j+1} = (u_{i,j+1} - c_{i,j+1})(t_{i+1,j} - t_{i,j+1}),\\
&(u_{i+1,j} - u_{i,j}) + \sigma(c_{i+1,j} - c_{i,j}) = \epsilon \frac{u_{i,j}c_{i,j}}{u_{i,j} + c_{i,j}} (x_{i+1,j} - x_{i,j}),\\
&(u_{i+1,j} - u_{i,j+1}) - \sigma(c_{i+1,j} - c_{i,j+1}) =\\
&\qquad - \epsilon \frac{u_{i,j+1}c_{i,j+1}}{u_{i,j+1} - c_{i,j+1}} (x_{i+1,j} - x_{i,j+1}).
\end{aligned}\right\} \tag{2.62}$$

The equations for x and t are solved first; this yields the coordinates of the point (i+1,j). Using these values, the last two equations yield the values of flow variables at this point. This is a first approximation to the result. Improved accuracy results when average values, rather than initial values, are used for the slopes of the characteristics appearing in the difference equations. For this purpose, average values of the flow parameters that appear in the expressions for these slopes are computed by using the values of $u_{i+1,j}$ and $c_{i+1,j}$ obtained from the preceding

approximation. These average values are designated by barred symbols and are given by:

$$\left.\begin{aligned} \bar{u}_{i,j} &= \frac{1}{2}\left[u_{i,j} + u_{i+1,j}\right], \\ \bar{c}_{i,j} &= \frac{1}{2}\left[c_{i,j} + c_{i+1,j}\right], \end{aligned}\right\} \tag{2.63a}$$

$$\left.\begin{aligned} \bar{u}_{i,j+1} &= \frac{1}{2}\left[u_{i,j+1} + u_{i+1,j}\right], \\ \bar{c}_{i,j+1} &= \frac{1}{2}\left[c_{i,j+1} + c_{i+1,j}\right]. \end{aligned}\right\} \tag{2.63b}$$

Substituting these values into their proper positions in equations (2.62) yields the following equations for the second approximation of the location of point (i+1,j) and the values of the flow variables at this point:

$$\left.\begin{aligned} x'_{i+1,j} - x_{i,j} &= (\bar{u}_{i,j} + \bar{c}_{i,j})(t'_{i+1,j} - t_{i,j}), \\ x'_{i+1,j} - x_{i,j+1} &= (\bar{u}_{i,j+1} - \bar{c}_{i,j+1})(t'_{i+1,j} - t_{i,j+1}), \\ (u'_{i+1,j} - u_{i,j}) + \sigma(c'_{i+1,j} - c_{i,j}) &= \epsilon \frac{\bar{u}_{i,j}\bar{c}_{i,j}}{(\bar{u}_{i,j} + \bar{c}_{i,j})}(x'_{i+1,j} - x_{i,j}) \\ (u'_{i+1,j} - u_{i,j+1}) - \sigma(c'_{i+1,j} - c_{i,j+1}) &= \\ - \epsilon \frac{(\bar{u}_{i,j+1}\bar{c}_{i,j+1})}{(\bar{u}_{i,j+1} - \bar{c}_{i,j+1})}&(x'_{i+1,j} - x_{i,j+1}). \end{aligned}\right\} \tag{2.64}$$

This iteration procedure is repeated until the desired accuracy is obtained; that is, until the difference between the values of the flow variables for successive iterations is sufficiently small.

These equations were also programmed for solution on the digital computer. The characteristic net for the problem is shown in figure (2.20). The variations of the flow variables at constant values of x were obtained by linear interpolation between the values at the net points and are shown as the data symbols on figures (2.18) and (2.19). In both the figures the method-of-characteristics solution is in excellent agreement with the second-order perturbation-series solution. The differences are quite small and are slightly greater at $x = 1$ than at $x = 0.5$. From this, the perturbation-series solution is concluded to give an accurate representation of the unsteady flow.

To compute the series solution (both first- and second-order) at a given value of x required about 2.5 minutes of machine time. The solution of this same problem by the method of characteristics, using the same computing machine, took 12 times as long in machine time alone. The ratio of machine times will increase as the magnitude of x increases, because of the nature of the method-of-characteristics solution. To the machine time must be added that required to plot the characteristic net and to perform the necessary interpolations. The advantage of the perturbation solution from the computational point of view is quite marked. Further comparisons of this nature will be made in section IV.

3. The "simple-wave-type" disturbance. - In the preceding paragraphs the solution for an unsteady flow was obtained with both dependent variables arbitrarily specified on a time-like arc. As expected, this led to a solution with an unsteady flow below what normally might be called the "rest" characteristic. As noted earlier in this section, in order to obtain solutions with steady flow below the "rest" characteristic, only one datum can be arbitrarily specified on a time-like arc. That is, there is a relation between the dependent variables on such a boundary. It was attempted to determine whether a general u,c-relation on such time-like arcs could be derived which would permit specification of these variables on the boundary and still produce solutions with a steady duct flow below the "rest" characteristic. Unfortunately no such relation could be established analytically. It was therefore decided to investigate some simple u,c-relations to see whether the desired result could be approximated. Taking a clue from the nature of the zeroth-order equations, which are the same as those for one-dimensional flow, it was decided to investigate a disturbance in which the Riemann variable $Q = u - \sigma c$ remained constant on the boundary. One-dimensional flows in which a Riemann variable is constant throughout the flow field are called simple waves. Such flows are characterized by the fact that they exist adjacent to a region of constant state. Because of the nature of the u,c-relation, such disturbances shall herein be called "simple-wave-type" disturbances.

For such "simple-wave-type" disturbances in an "epsilon duct" the problem may be stated as follows: Given a steady duct flow with flow variables U and C at a given cross section. Let there be a disturbance

in the flow at this section, commencing at a specified time, of such nature that the parameter $Q = u - \sigma c$ is constant on the boundary. Determine the ensuing flow in the duct.

The boundary conditions for the problem are then (choosing $x = 0$ as the cross section and $t = 0$ as the beginning of the disturbance for convenience), on $x = 0$,

$$\left.\begin{aligned} u &= U + \epsilon\sigma\, f(t), \\ c &= C + \epsilon\, f(t), \end{aligned}\right\} \tag{2.65}$$

where

$$\left.\begin{aligned} f(t) &= 0 \qquad \text{for} \qquad t \leqslant 0, \\ U^2 &+ \sigma C^2 = \sigma + 1. \end{aligned}\right\} \tag{2.66}$$

The boundary conditions are to be satisfied as follows: The line $x = 0$ is to be mapped on $\alpha = \beta$ such that $\alpha = \beta = t$, that is, according to equations (2.43) and

$$\left.\begin{aligned} u^{(0)}(\alpha,\alpha) &= u^{(0)}(\beta,\beta) = U, \\ u^{(1)}(\alpha,\alpha) &= \sigma\, f(\alpha),\ u^{(1)}(\beta,\beta) = \sigma\, f(\beta), \\ u^{(n)}(\alpha,\alpha) &= u^{(n)}(\beta,\beta) = 0, \qquad n > 1; \\ c^{(0)}(\alpha,\alpha) &= c^{(0)}(\beta,\beta) = C, \\ c^{(1)}(\alpha,\alpha) &= f(\alpha),\ c^{(1)}(\beta,\beta) = f(\beta), \\ c^{(n)}(\alpha,\alpha) &= c^{(n)}(\beta,\beta) = 0, \qquad n > 1. \end{aligned}\right\} \tag{2.67}$$

For these boundary conditions we see that on $x = 0$ we always have

$$Q = u - \sigma c = U - \sigma C, \tag{2.68}$$

that is, a constant value of one of the Riemann variables on the boundary. For these boundary conditions the solutions up to second order are:

$$\left.\begin{aligned} u^{(0)} &= U, \\ u^{(1)} &= U_1^{(1)}(\alpha - \beta) + U_2^{(1)} f(\beta), \\ u^{(2)} &= U_1^{(2)}(\alpha - \beta)^2 + U_2^{(2)}(\alpha - \beta) f(\beta) + U_3^{(2)} \int_\alpha^\beta f(\tau)\,d\tau; \end{aligned}\right\} \quad (2.69a)$$

$$\left.\begin{aligned} c^{(0)} &= C, \\ c^{(1)} &= C_1^{(1)}(\alpha - \beta) + C_2^{(1)} f(\beta), \\ c^{(2)} &= C_1^{(2)}(\alpha - \beta)^2 + C_2^{(2)}(\alpha - \beta) f(\beta) + C_3^{(2)} \int_\alpha^\beta f(\tau)\,d\tau; \end{aligned}\right\} \quad (2.69b)$$

$$\left.\begin{aligned} x^{(0)} &= X_1^{(0)}(\alpha - \beta), \\ x^{(1)} &= X_1^{(1)}(\alpha - \beta)^2 + X_2^{(1)}(\alpha - \beta) f(\beta) + X_3^{(1)} \int_\alpha^\beta f(\tau)\,d\tau, \\ x^{(2)} &= X_1^{(2)}(\alpha - \beta)^3 + X_2^{(2)}(\alpha - \beta)^2 f(\beta) + X_3^{(2)}(\alpha - \beta)\left[f(\beta)\right]^2 + \\ &\quad X_4^{(2)} \int_\alpha^\beta (\tau - \beta) f(\tau)\,d\tau + X_5^{(2)} f(\beta) \int_\alpha^\beta f(\tau)\,d\tau + \\ &\quad X_6^{(2)} \int_\alpha^\beta \left[f(\tau)\right]^2 d\tau + X_7^{(2)} \int_\alpha^\beta (\alpha - \tau) f(\tau)\,d\tau; \end{aligned}\right\} \quad (2.69c)$$

$$
\left.
\begin{aligned}
t^{(0)} &= T_1^{(0)}\beta + T_2^{(0)}\alpha, \\
t^{(1)} &= T_1^{(1)}(\alpha - \beta)^2 + T_2^{(1)}(\alpha - \beta)f(\beta) + T_3^{(1)} \int_\alpha^\beta f(\tau)d\tau, \\
t^{(2)} &= T_1^{(2)}(\alpha - \beta)^3 + T_2^{(2)}(\alpha - \beta)^2 f(\beta) + T_3^{(2)}(\alpha - \beta)\left[f(\beta)\right]^2 + \\
&\quad T_4^{(2)} \int_\alpha^\beta (\tau - \beta)f(\tau)d\tau + T_5^{(2)} f(\beta) \int_\alpha^\beta f(\tau)d\tau + \\
&\quad T_6^{(2)} \int_\alpha^\beta \left[f(\tau)\right]^2 d\tau + T_7^{(2)} \int_\alpha^\beta (\alpha - \tau)f(\tau)d\tau.
\end{aligned}
\right\} \quad (2.69d)
$$

The coefficients appearing in equations (2.69) are functions of U, C, and σ and are listed below:

$$
\left.
\begin{aligned}
U_1^{(1)} &= \frac{UC}{2} & U_1^{(2)} &= \frac{U}{8\sigma}(\sigma C^2 - U^2) \\
U_2^{(1)} &= \sigma & U_2^{(2)} &= -\frac{(U - C)(U + \sigma C)}{4C} \\
& & U_3^{(2)} &= -\frac{(U + C)(U + \sigma C)}{4C}
\end{aligned}
\right\} \quad (2.70a)
$$

$$
\left.
\begin{aligned}
C_1^{(1)} &= -\frac{U^2}{2\sigma} & C_1^{(2)} &= -\frac{U^2 C}{4\sigma} \\
C_2^{(1)} &= 1 & C_2^{(2)} &= \frac{(U - C)^2}{4C} \\
& & C_3^{(2)} &= \frac{(U + C)^2}{4C}
\end{aligned}
\right\} \quad (2.70b)
$$

$$
\left.
\begin{aligned}
X_1^{(0)} &= \frac{C^2 - U^2}{2C} \\
X_1^{(1)} &= -\frac{1}{8\sigma}\left(\frac{U}{C}\right)^2\left[(2\sigma + 1)C^2 + U^2\right] \\
X_2^{(1)} &= \frac{\sigma + 1}{4C^2}(U - C)^2 \\
X_3^{(1)} &= \frac{\sigma - 1}{4C^2}(U + C)^2 \\
X_1^{(2)} &= -\frac{U^2}{48\sigma C}\left[(3\sigma + 2)C^2 + U^2\right] + UT_1^{(2)} \\
X_2^{(2)} &= \frac{\sigma + 1}{32\sigma C^2}\left\{\sigma C^2(C - 7U) + U^2\left[(4\sigma - 1)C - U\right]\right\} + UT_2^{(2)} \\
X_3^{(2)} &= \frac{(\sigma + 1)(3\sigma + 1)}{16C^2}(U - C) + UT_3^{(2)} \\
X_4^{(2)} &= \frac{\sigma + 1}{16\sigma}\cdot\frac{(U + C)}{C^2}(U^2 + 2\sigma UC + \sigma C^2) + UT_4^{(2)} \\
X_5^{(2)} &= \frac{\sigma^2 - 1}{8C^2}(U + C) + UT_5^{(2)} \\
X_6^{(2)} &= \frac{\sigma - 1}{16C^2}\left[(\sigma - 3)U + (3\sigma - 1)C\right] + UT_6^{(2)} \\
X_7^{(2)} &= \frac{1}{8\sigma C^2}\left\{\sigma C^2\left[C + (\sigma-1)U\right] + U^2\left[(\sigma-1)U + (\sigma^2-\sigma-1)C\right]\right\} + UT_7^{(2)}
\end{aligned}
\right\} \quad (2.70c)
$$

$$
\left.
\begin{aligned}
T_1^{(0)} &= \frac{U + C}{2C} \\
T_2^{(0)} &\quad \frac{C - U}{2C} \\
T_1^{(1)} &= -\frac{1}{8\sigma} \cdot \frac{U}{C^2} (U^2 + \sigma C^2) \\
T_2^{(1)} &= \frac{\sigma + 1}{4C^2} (U - C) \\
T_3^{(1)} &= \frac{\sigma - 1}{4C^2} (U + C) \\
T_1^{(2)} &= -\frac{U}{48\sigma^2 C^3} (U^2 + \sigma C^2)(2U^2 + \sigma C^2) \\
T_2^{(2)} &= -\frac{\sigma + 1}{32\sigma C^3} \left[\sigma C^2 (C - 3U) + U^2 (3C - 5U)\right] \\
T_3^{(2)} &= -\frac{(\sigma + 1)(\sigma + 3)}{16C^3} (U - C) \\
T_4^{(2)} &= \frac{U + C}{16\sigma C^3} \left[\sigma(\sigma + 1)C^2 + 4\sigma UC + U^2(3\sigma - 1)\right] \\
T_5^{(2)} &= -\frac{\sigma^2 - 1}{8C^3} (U + C) \\
T_6^{(2)} &= \frac{\sigma - 1}{16C^3} \left[(\sigma - 3)U + (3\sigma - 1)C\right] \\
T_7^{(2)} &= \frac{\sigma - 1}{8\sigma} \cdot \frac{(U + C)}{C^3} (U^2 + \sigma C^2).
\end{aligned}
\right\} \qquad (2.70d)
$$

To illustrate the nature of the solution for the "simple-wave-type" disturbance, an example was computed for the same values of U, C, ϵ, and σ used in the preceding example. The disturbance function f(t) is again defined by equations (2.61) with B = 0.0086905 and δ = 4.0. The values of the coefficients (eqs. (2.70)) for these values of the parameters are given in table (2.2).

The results of the IBM computations are shown in figures (2.21) to (2.23) for x values of 0.5, 1.0, and 2.0, respectively. At all values of x the character of the variations of both u and c are similar, consisting of almost linear changes in the variables between their initial

and final values. The most interesting aspect of the results is the fact that in the region between $\alpha = 0$ and $\beta = 0$ the variables are essentially constant at their original values. This indicates that the "simple-wave-type" disturbance yields a flow in which the $\beta = 0$ characteristic approximates a "rest" characteristic. The principal difference between the first- and second-order solutions is again in the level of the variables; this reflects the convergence of the terms representing the steady flow to the exact solution. It is also seen that the slopes of the second-order solution during the period in which the flow quantities are changing are greater than those of the corresponding first-order solution. The maximum departure from constant conditions in the region between $\alpha = 0$ and $\beta = 0$ occurred in the second-order solution for c at $x = 2.0$. The error in c in this region is, however, only 2 percent of the total change in the variable during the transient, a quite reasonable approximation to steady conditions. Thus, even the second-order solution yields an essentially steady duct flow below $\beta = 0$.

Two other points should be noted about the nature of the transient. First, as the compressive disturbance is propagated upstream, its magnitude increases. For example, at $x = 0.5$ the total change in u is 0.0186 or 4.6 percent of its initial value. At $x = 2.0$ the change in u is 0.0235 or about 4.8 percent of its initial value. Corresponding changes in c are 0.00366 (0.34 percent) at $x = 0.5$ and 0.00426 (0.38 percent) at $x = 2.0$. The second point of interest is that at each cross section the value of Q remains essentially constant at its original value during the transient. At $x = 0.5$ the initial value of Q is -5.8042, and its terminal value is -5.8039. At $x = 2$ the corresponding values are -5.8513 and -5.8493. This fact will play an important role in the next section.

To check the accuracy of the perturbation-series solution, this problem was also solved by the method of characteristics. The characteristic net is shown in figure (2.24). Again, the values of the flow variables at fixed cross sections were obtained by linear interpolations between the net points and are shown as the data symbols on figures (2.21) to (2.23). At $x = 0.5$ and 1.0, the method-of-characteristics solution is in excellent agreement with the second-order perturbation-series solution. At $x = 2$, the agreement is not as good but is still quite acceptable; the maximum deviation occurs in the variable c, being about 6 percent of the change in c at this station. It is of interest to note that at $x = 2.0$ the method-of-characteristics solution exhibits a slight decrease in c in the region between $\alpha = 0$ and $\beta = 0$, as does the series solution. Thus, over an area ratio of 1.22 the series solution is seen to be quite accurate for the unsteady flows investigated.

F. Summary

In this section the method of coordinate perturbation was applied to the solution of quasi-one-dimensional flow problems. It was demonstrated that, for ducts for which the logarithmic derivative of area variation with respect to the space coordinate is a function of the smallness parameter ϵ, perturbation-series-type solutions for both steady and unsteady flows can be obtained.

By means of numerical examples it was demonstrated that the solutions for the steady flow converge to the exact duct flow solution. The principal factors affecting the rapidity of the convergence were shown to be the area ratio and the magnitudes of the initial data. In general, good representation of the flow was obtained over area ratios as large as 1.8:1.

For unsteady flow it was shown that solutions could be written for arbitrary disturbance functions in both flow variables specified on time-like arcs. For such initial data the problems were termed "inverse" problems because, from a physical viewpoint, the solutions give the unsteady flow in other regions of the duct (at earlier times) which would produce the specified variation of the flow quantities on the boundary. It was also shown that a reasonable approximation to the "direct" problem (i.e., one in which a region of steady flow bounded by a "rest" characteristic exists) is obtained by specifying that one of the Riemann variables is constant on the time-like boundary arc. This disturbance has been termed a "simple-wave-type" disturbance. A numerical example indicated that, even for the second-order solution, the maximum change of the dependent variables below the "rest" characteristic was of the order of 2 percent of the magnitude of the excursion of the variable during the transient. For unsteady flow the solutions obtained contained terms involving the independent variables α and β, the disturbance function and definite integrals thereof. Therefore, solutions for integrable disturbance functions are easily obtained.

Comparison of the unsteady-flow solutions with those obtained by the method of characteristics indicated that the second-order series solution accurately represents the flow. As was the case for steady flow, the accuracy of the series solution decreases with increasing distance (i.e., area ratio) from the boundary. The series solutions offer an advantage in computational effort over the method of characteristics calculations.

III. INTERACTION OF A SHOCK WAVE AND A DISTURBANCE IN A DUCT FLOW

In section II, perturbation-series solutions for unsteady quasi-one-dimensional flow were developed. These solutions are now applied to the determination of the motion of a shock wave in a diffuser flow under the influence of a disturbance originating downstream of the shock. An approximate relation is used for the shock transition. It is shown that, for a linear variation of the flow variables in a "simple-wave-type" disturbance, an analytical solution for the shock path can be obtained to first order in ϵ. This solution is compared with both first- and second-order solutions obtained by numerical integration of the differential equation of the shock path.

A. The Equation of the Shock Path

For weak and moderately strong shock waves, the shock velocity can be approximated by

$$V = (\bar{u}_s+\bar{c}_s) + \frac{1}{2}\left[(u_s+c_s) - (\bar{u}_s+\bar{c}_s)\right] + \frac{1}{8\bar{c}_s}\left[(u_s+c_s) - (\bar{u}_s+\bar{c}_s)\right]^2. \quad (3.1)$$

where $V = v/c_*$ (cf. ref. 6, eq. (72.06). In this equation the subscript s refers to the immediate shock location, the barred quantities represent conditions upstream of the shock, and the unbarred terms represent conditions downstream of the shock. This equation is correct to second order in the shock strength. Within the same degree of accuracy, the shock transition is homentropic; and, for a "forward-facing" shock wave (when the fluid particles enter the shock from the side of larger x-values), the Riemann variable Q is constant across the shock; that is,

$$u_s - \sigma c_s = \bar{u}_s - \sigma\bar{c}_s. \quad (3.2)$$

These equations are applicable for weak and moderately strong shocks, and the development that follows is valid only for such shocks.

Consider a diffuser flow in an "epsilon duct" with a stationary shock wave at the cross section $x = \overline{X}$ (see sketch).

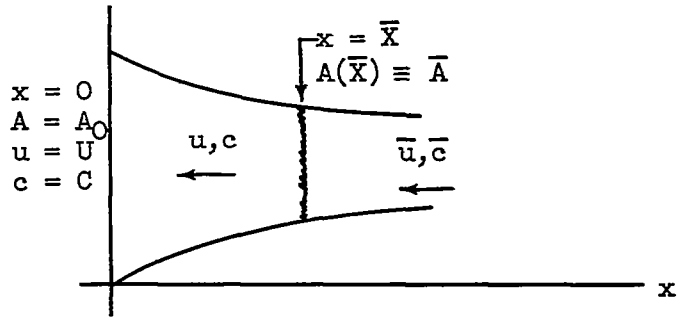

For a diffuser flow with an initially stationary shock, the conditions upstream of the shock (i.e., $\bar{u}$ and $\bar{c}$) are functions of x alone and are not influenced by any subsequent shock motion (unless, of course, the shock is regurgitated). This, and the approximate shock relations (eqs. (3.1) and (3.2)), imply that, regardless of the shock velocity (within the limits of accuracy of eq. (3.1), of course), the value of Q remains constant at a given duct cross section as the shock passes the section; although Q changes from section to section. As noted in section II-E, a "simple-wave-type" disturbance has the property that the value of Q at a given section remains approximately constant at its initial value during the transient. Thus, if the disturbance downstream of the shock is of this type, it will approximately fulfill the boundary condition at the shock, that is, equation (3.2). This is equivalent to neglecting the "back reaction" of the shock on the flow field behind the shock. In other words, the flow field behind the shock is completely specified by the solution for the "simple-wave-type" unsteady duct flow. The subsequent development is, therefore, based on the "simple-wave-type" disturbance.

The velocity of the shock wave is given by

$$dx/dt = V. \tag{3.3}$$

If the flow field behind the shock is described in terms of the characteristic parameters α and β, we have

$$\left.\begin{aligned} dx &= x_\alpha\, d\alpha + x_\beta\, d\beta, \\ dt &= t_\alpha\, d\alpha + t_\beta\, d\beta. \end{aligned}\right\} \tag{3.4}$$

Thus equation (3.3) can be written

$$\frac{x_\alpha\, d\alpha + x_\beta\, d\beta}{t_\alpha\, d\alpha + t_\beta\, d\beta} = V. \tag{3.5}$$

The partial derivatives of x and t are related by the equations of the characteristics; that is,

$$\left.\begin{aligned} x_\alpha &= (u + c)t_\alpha, \\ x_\beta &= (u - c)t_\beta. \end{aligned}\right\} \tag{3.6}$$

Substituting equations (3.6) into equation (3.5) and solving for $d\alpha/d\beta$, we obtain:

$$\frac{d\alpha}{d\beta} = \frac{[V - (u_s - c_s)]t_\beta}{[(u_s + c_s) - V]t_\alpha}, \tag{3.7}$$

where the subscript s again indicates that u and c are to be evaluated immediately downstream of the shock. Substitution of the expression for V (eq. (3.1)) then yields

$$\frac{d\alpha}{d\beta} = \frac{\left\{\frac{1}{2}(3c_s - u_s) + \frac{1}{2}(\bar{u}_s + \bar{c}_s) + \frac{1}{8\bar{c}_s}\left[(u_s + c_s) - (\bar{u}_s + \bar{c}_s)\right]^2\right\}t_\beta}{\left\{\frac{1}{2}(u_s + c_s) - \frac{1}{2}(\bar{u}_s + \bar{c}_s) - \frac{1}{8\bar{c}_s}\left[(u_s + c_s) - (\bar{u}_s + \bar{c}_s)\right]^2\right\}t_\alpha}. \tag{3.8}$$

In this equation, t and the "immediately downstream" quantities u_s, c_s are known functions of α and β given by equations (2.69) for the "simple-wave-type" disturbance. In the flow field behind the shock, up to and including the instantaneous position of the shock, x is also a known function of α and β. Therefore, in principle at least, the "immediately upstream" values $\bar{u}_s$ and $\bar{c}_s$ can be considered as functions of the characteristic variables as $\bar{u}$ and $\bar{c}$ are functions of x alone. Thus equation (3.8) may be written as

$$\frac{d\alpha}{d\beta} = G(\alpha,\beta). \tag{3.9}$$

This is an ordinary differential equation for the relation between α and β on the shock path. Substituting the solution of this equation in the equations for x and t (eqs. (2.69c) and (2.69d)) yields a parametric representation of the shock motion resulting from the disturbance specified at the boundary.

Equation (3.8) can, of course, be integrated numerically for specific cases. It is of interest to see if an analytical solution can be obtained, and such a development follows.

B. Approximate Solution for the Shock Path

The first-order solution for the unsteady flow field behind the shock for a "simple-wave-type" disturbance is repeated below for convenience:

$$\left.\begin{aligned} u &= U + \epsilon\left[U_1^{(1)}(\alpha - \beta) + U_2^{(1)}f(\beta)\right], \\ c &= C + \epsilon\left[C_1^{(1)}(\alpha - \beta) + C_2^{(1)}f(\beta)\right], \\ x &= X_1^{(0)}(\alpha - \beta) + \epsilon\left[X_1^{(1)}(\alpha - \beta)^2 + X_2^{(1)}(\alpha - \beta)f(\beta) + X_3^{(1)}\int_\alpha^\beta f(\tau)d\tau\right], \\ t &= T_1^{(0)}\beta + T_2^{(0)}\alpha + \epsilon\left[T_1^{(1)}(\alpha - \beta)^2 + T_2^{(1)}(\alpha - \beta)f(\beta) + T_3^{(1)}\int_\alpha^\beta f(\tau)d\tau\right]. \end{aligned}\right\} \quad (3.10)$$

From the last relation it is easily shown that

$$\left.\begin{aligned} t_\alpha &= T_2^{(0)} + \epsilon\left[2T_1^{(1)}(\alpha - \beta) + T_2^{(1)}f(\beta) - T_3^{(1)}f(\alpha)\right], \\ t_\beta &= T_1^{(0)} + \epsilon\left[-2T_1^{(1)}(\alpha - \beta) + (T_3^{(1)} - T_2^{(1)})f(\beta) + T_2^{(1)}(\alpha - \beta)f'(\beta)\right]. \end{aligned}\right\} \quad (3.11)$$

The first step in the development is to express $\bar{u}$ and $\bar{c}$ in terms of the characteristic parameters. For a steady duct flow with conditions U and C specified at some area A_0, the following relations hold:

$$\frac{A}{A_0} = \frac{UC^\sigma \cdot \sigma^{\sigma/2}}{u\left[(\sigma + 1) - u^2\right]^{\sigma/2}}, \quad (3.12)$$

$$u^2 + \sigma c^2 = (\sigma + 1). \quad (3.13)$$

Assume that at some area $A(\bar{X}) = \bar{A}$, upstream of and smaller than A_0, but still greater than that at which sonic flow would exist, a shock occurs (see sketch on p. 47). At this station we thus have on the downstream side of the shock

$$\frac{\bar{A}}{A_0} = \frac{\sigma^{\sigma/2} U C^{\sigma}}{u(\bar{X})\left\{(\sigma + 1) - \left[u(\bar{X})\right]^2\right\}^{\sigma/2}}.$$

For a stationary shock the conditions on its upstream side can be determined from equations (3.1) and (3.2) with $V = 0$, or more exactly from

$$u_s \bar{u}_s = 1, \qquad \text{Prandtl equation;} \tag{3.14}$$

$$u_s^2 + \sigma c_s^2 = \bar{u}_s^2 + \sigma \bar{c}_s^2, \qquad \text{energy equation.} \tag{3.15}$$

The steady supersonic flow ahead of the shock is now given by

$$\frac{A}{\bar{A}} = \frac{\sigma^{\sigma/2} \cdot \bar{u}\,(\bar{X})\left[\bar{c}(\bar{X})\right]^{\sigma}}{\bar{u}\left[(\sigma + 1) - \bar{u}^2\right]^{\sigma/2}}, \tag{3.16}$$

$$\bar{u}^2 + \sigma \bar{c}^2 = (\sigma + 1). \tag{3.17}$$

Thus, specifying an initial steady shock location by $x = \bar{X}$ and the conditions U and C at the end of the diffuser, A_0, completely determines the variables $\bar{u}$ and $\bar{c}$ ahead of the shock.

In the problem being considered, the duct-area variation is again written

$$A/\bar{A} = e^{-\epsilon(x-\bar{X})}. \tag{3.18}$$

Equation (3.16) therefore may be written

$$\bar{u}^{2/\sigma}\left[(\sigma + 1) - \bar{u}^2\right] = \sigma \bar{U}^{2/\sigma} \cdot \bar{C}^2 \, e^{\frac{\epsilon 2}{\sigma}(x-\bar{X})} \tag{3.19}$$

where, for simplicity of notation, $\bar{u}(\bar{X})$ and $\bar{c}(\bar{X})$ immediately on the upstream side of the shock at its initial location have been replaced by $\bar{U}$ and $\bar{C}$, respectively.

In order to develop the upstream flow variables as functions of α and β, it is assumed that these quantities can be represented to first order by

$$\left.\begin{aligned} \bar{u} &= \bar{U}(1 + \epsilon\bar{u}^{(1)}), \\ \bar{c} &= \bar{C}(1 + \epsilon\bar{c}^{(1)}), \end{aligned}\right\} \tag{3.20}$$

where $\bar{u}^{(1)}$ and $\bar{c}^{(1)}$ are functions of x. Expanding equation (3.19) to the first power in ϵ after substituting equations (3.20) yields:

$$\sigma\bar{C}^2 + \epsilon\frac{2(\sigma + 1)}{\sigma}(1 - \bar{U}^2)\bar{u}^{(1)} = \sigma\bar{C}^2\left[1 + \epsilon\frac{2}{\sigma}(x - \bar{X})\right].$$

Upon substituting for x from equation (3.10), the right hand side becomes

$$\sigma\bar{C}^2\left\{1 + \epsilon\frac{2}{\sigma}\left[(\alpha - \beta)\frac{C^2 - U^2}{2C} + O(\epsilon) - \bar{X}\right]\right\},$$

whence

$$\bar{u}^{(1)} = -\frac{\sigma}{\sigma + 1}\frac{\bar{C}^2}{(1 - \bar{U}^2)}\left[(\alpha - \beta)\frac{U^2 - C^2}{2C} + \bar{X}\right]. \tag{3.21}$$

Substituting equations (3.20) into (3.17), expanding to first order, and using (3.21) gives

$$\bar{c}^{(1)} = \frac{1}{\sigma + 1}\frac{\bar{U}^2}{(1 - \bar{U}^2)}\left[(\alpha - \beta)\frac{U^2 - C^2}{2C} + \bar{X}\right]. \tag{3.22}$$

A term that appears in the shock velocity relation is $(\bar{u} + \bar{c})$. This can now be written in terms of α and β as

$$\bar{u} + \bar{c} = (\bar{U} + \bar{C}) + \epsilon\frac{\bar{U}\bar{C}(\bar{U} - \sigma\bar{C})}{(\sigma + 1)(1 - \bar{U}^2)}\left[(\alpha - \beta)\frac{U^2 - C^2}{2C} + \bar{X}\right]. \tag{3.23}$$

Thus the flow variables ahead of the shock are given to first order as functions of the characteristic variables.

We now turn to the evaluation of the right hand side of equation (3.8) to first order. Consider the bracketed factor in the numerator; that is,

$$R \equiv \frac{1}{2}(3c_s - u_s) + \frac{1}{2}(\bar{u}_s + \bar{c}_s) + \frac{1}{8\bar{c}_s}\left[(u_s + c_s) - (\bar{u}_s + \bar{c}_s)\right]^2. \quad (3.24)$$

Substituting the expression for the flow variables from equations (3.10) and (3.23) and expanding equation (3.24) to first order in ϵ gives

$$R = R_0 + \epsilon\left[R_1(\alpha - \beta) + R_2 f(\beta) + R_3 \bar{X}\right], \quad (3.25)$$

where

$$\left.\begin{aligned}
R_0 &= \frac{3C - U}{2} + \frac{\bar{U} + \bar{C}}{2} + \frac{1}{8\bar{C}}\left[(U + C) - (\bar{U} + \bar{C})\right]^2, \\
R_1 &= -\frac{U(3U+\sigma C)}{4\sigma} + \frac{\bar{U}\bar{C}(\bar{U}-\sigma\bar{C})(U^2-C^2)}{4(\sigma+1)(1-\bar{U}^2)C} + \frac{[(U+C) - (\bar{U} + \bar{C})]U(\sigma C-U)}{8\sigma\bar{C}} - \\
&\quad \frac{[(U+C) - (\bar{U}+\bar{C})]\bar{U}(\bar{U}-\sigma\bar{C})(U^2-C^2)}{8(\sigma+1)(1-\bar{U}^2)C} - \frac{[(U+C) - (\bar{U}+\bar{C})]^2\,\bar{U}^2(U^2-C^2)}{16(\sigma+1)\bar{C}C(1-\bar{U}^2)}, \\
R_2 &= \frac{3 - \sigma}{2} + \frac{(\sigma + 1)[(U + C) - (\bar{U} + \bar{C})]}{4\bar{C}}, \\
R_3 &= \frac{\bar{U}\bar{C}(\bar{U}-\sigma\bar{C})}{2(\sigma+1)(1-\bar{U}^2)} - \frac{[(U+C) - (\bar{U}+\bar{C})]\bar{U}(\bar{U}-\sigma\bar{C})}{4(\sigma+1)(1-\bar{U}^2)} - \frac{[(U+C) - (\bar{U}+\bar{C})]^2\bar{U}^2}{8(\sigma+1)(1-\bar{U}^2)\bar{C}}.
\end{aligned}\right\} \quad (3.26)$$

Similarly, the bracketed factor in the denominator of equation (3.8),

$$S \equiv \frac{1}{2}(u_s + c_s) - \frac{1}{2}(\bar{u}_s + \bar{c}_s) - \frac{1}{8\bar{c}_s}\left[(u_s + c_s) - (\bar{u}_s + \bar{c}_s)\right]^2, \quad (3.27)$$

reduces to

$$S = S_0 + \epsilon\left[S_1(\alpha - \beta) + S_2 f(\beta) + S_3 \bar{X}\right], \quad (3.28)$$

where

$$\left.\begin{aligned}
S_0 &= \frac{U+C}{2} - \frac{\overline{U}+\overline{C}}{2} - \frac{[(U+C)-(\overline{U}+\overline{C})]^2}{8\overline{C}},\\
S_1 &= \frac{U(\sigma C-U)}{4\sigma} - \frac{\overline{U}\overline{C}(\overline{U}-\sigma\overline{C})(U^2-C^2)}{4(\sigma+1)(1-\overline{U}^2)C} - \frac{[(U+C)-(\overline{U}+\overline{C})]U(\sigma C-U)}{8\sigma\overline{C}} +\\
&\qquad \frac{[(U+C)-(\overline{U}+\overline{C})]\overline{U}(\overline{U}-\sigma\overline{C})(U^2-C^2)}{8(\sigma+1)(1-\overline{U}^2)C} + \frac{[(U+C)-(\overline{U}+\overline{C})]^2\overline{U}^2(U^2-C^2)}{16(\sigma+1)\overline{C}(1-\overline{U}^2)C},\\
S_2 &= \frac{\sigma+1}{2} - \frac{(\sigma+1)[(U+C)-(\overline{U}+\overline{C})]}{4\overline{C}},\\
S_3 &= -\frac{\overline{U}\overline{C}(\overline{U}-\sigma\overline{C})}{2(\sigma+1)(1-\overline{U}^2)} + \frac{[(U+C)-(\overline{U}+\overline{C})]\overline{U}(\overline{U}-\sigma\overline{C})}{4(\sigma+1)(1-\overline{U}^2)} + \frac{[(U+C)-(\overline{U}+\overline{C})]^2\overline{U}^2}{8(\sigma+1)\overline{C}(1-\overline{U}^2)}.
\end{aligned}\right\} \tag{3.29}$$

Substituting these expressions and those for the partial derivatives of t into equation (3.8) yields

$$\frac{d\alpha}{d\beta} = \frac{\{R_0 + \epsilon[R_1(\alpha-\beta) + R_2 f(\beta) + R_3\overline{X}]\}\{T_1^{(0)} + \epsilon[-2T_1^{(1)}(\alpha-\beta) + (T_3^{(1)}-T_2^{(1)})f(\beta) + T_2^{(1)}(\alpha-\beta)f'(\beta)]\}}{\{S_0 + \epsilon[S_1(\alpha-\beta) + S_2 f(\beta) + S_3\overline{X}]\}\{T_2^{(0)} + \epsilon[2T_1^{(1)}(\alpha-\beta) + T_2^{(1)}f(\beta) - T_3^{(1)}f(\alpha)]\}} \tag{3.30}$$

which, when expanded to first order, becomes

$$\frac{d\alpha}{d\beta} = B_0 + \epsilon\left[(\alpha-\beta)B_1 + f(\beta)B_2 + (\alpha-\beta)f'(\beta)B_3 + f(\alpha)B_4 + \overline{X}B_5\right]; \tag{3.31}$$

where

$$\left.\begin{aligned}
B_0 &= R_0T_1^{(0)} \Big/ S_0T_2^{(0)},\\
B_1 &= \frac{1}{S_0T_2^{(0)}}\left[-2T_1^{(1)}R_0 + T_1^{(0)}R_1 - B_0(T_2^{(0)}S_1 + 2T_1^{(1)}S_0)\right],\\
B_2 &= \frac{1}{S_0T_2^{(0)}}\left[(T_3^{(1)} - T_2^{(1)})R_0 + T_1^{(0)}R_2 - B_0(T_2^{(1)}S_0 + T_2^{(0)}S_2)\right],\\
B_3 &= R_0T_2^{(1)} \Big/ S_0T_2^{(0)},\\
B_4 &= B_0T_3^{(1)} \Big/ T_2^{(0)},\\
B_5 &= \frac{T_1^{(0)}R_3}{S_0T_2^{(0)}} - B_0\frac{S_3}{S_0}.
\end{aligned}\right\} \tag{3.32}$$

Equation (3.31) cannot be formally integrated unless the disturbance function $f(\tau)$ is known. If $f(\tau)$ is a linear function of its argument, equation (3.31) becomes a linear differential equation and can be easily integrated. Making use of this possibility, we introduce for the disturbance, the function

$$f(\tau) = \begin{cases} K\tau, & 0 \leqslant \tau \lesseqgtr \delta; \\ K\delta, & \tau > \delta; \\ 0, & \tau < 0. \end{cases} \qquad (3.33)$$

Because of the nature of this function there are three zones in the x,t-plane in which different versions of the right hand side of equation (3.31) hold. These zones are bounded by the characteristics shown in the following sketch:

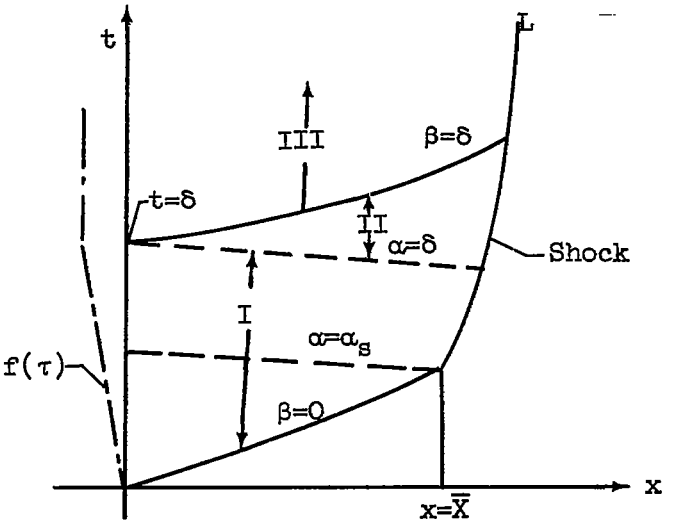

In the three zones, the function, its derivative, and integral assume the following values:

Zone	$f(\alpha)$	$f(\beta)$	$f'(\beta)$	$\int_{\alpha}^{\beta} f(\tau)d\tau$
I	$K\alpha$	$K\beta$	K	$\frac{1}{2}K(\beta^2 - \alpha^2)$
II	$K\delta$	$K\beta$	K	$K\left[\frac{1}{2}\beta^2 + \frac{1}{2}\delta^2 - \delta\alpha\right]$
III	$K\delta$	$K\delta$	0	$K\delta(\beta - \alpha)$

In zone I, equation (3.31) becomes

$$\frac{d\alpha}{d\beta} - \alpha\epsilon\left[B_1 + K(B_3 + B_4)\right] = B_0 + \epsilon\bar{X}B_5 + \epsilon\left[K(B_2 - B_3) - B_1\right]\beta. \quad (3.34)$$

The solution of this equation is

$$\alpha = D_0 + D_1\beta + (\alpha_s - D_0)e^{\epsilon D_2 \beta}, \quad (3.35)$$

where

$$\left.\begin{aligned} D_0 &= -\frac{(B_0 + \epsilon\bar{X}B_5)\left[B_1 + K(B_3 + B_4)\right] + \left[K(B_2 - B_3) - B_1\right]}{\epsilon\left[B_1 + K(B_3 + B_4)\right]^2}, \\ D_1 &= -\frac{K(B_2 - B_3) - B_1}{B_1 + K(B_3 + B_4)}, \\ D_2 &= B_1 + K(B_3 + B_4); \end{aligned}\right\} \quad (3.36)$$

and use has been made of the initial condition that, when $\beta = 0$, $\alpha = \alpha_s$. The value of α_s is determined from the initial shock location. Relations of form similar to equation (3.35) hold for the other zones; that is, α is the sum of a linear function of β and an exponential function of β. Substitution of equation (3.35) into the expressions for x and t in equation (3.10) yields, to first order in ϵ, a parametric representation of the shock path under the action of a "simple-wave-type" disturbance of the form given by equation (3.33). The shock path cannot be given explicitly in x and t because the nature of the α,β-relationship along the path does not permit the elimination of α and β algebraically.

C. Examples

The solution for the shock path presented above is correct to first order in ϵ. As noted previously, the expressions for the shock transition used in deriving this result are correct only for weak or moderately strong shock waves. Because of this fact, shocks occurring at an upstream Mach number of about 1.5 (for $\gamma = 7/5$) are about as strong a shock as can be accurately represented by the approximate equations. Therefore, the examples chosen will have an initial upstream Mach number of 1.5.

Another fact that enters into the determination of the region of applicability of the approximate solution for the shock path is the

accuracy of the representation of the initial steady flow offered by the approximate relations used. The flow conditions upstream of the shock wave have been represented by equations (3.20). For a shock at Mach 1.5 we have $\overline{U} = -1.36458$ and $\overline{C} = 0.90972$. Using equations (3.21) and (3.22) to evaluate $\overline{u}^{(1)}$ and $\overline{c}^{(1)}$, the variation of $\overline{u}$ and $\overline{c}$ with $(x - \overline{X})$ has been computed for $\epsilon = 0.1$ and is shown in figure (3.1), along with the exact values of these parameters. For values of $(x - \overline{X})$ up to 0.4, the first-order representation of the flow variables is quite good. At $(x - \overline{X}) = 0.408$, the Mach number of the flow is 1.425. Therefore, if the disturbance magnitude is limited to that which would result in a final steady-state shock location at an upstream Mach number of about 1.4, the representation of the upstream conditions should be adequate.

The disturbance function is specified on an $x =$ constant line downstream of the initial shock location. From the examples given in section II for the steady-flow solution, it was evident that the first-order representations of the flow variables are accurate only for relatively short distances upstream from the boundary. Because of this, the farther from the initial shock location the place $x =$ constant is selected, the greater will be the error in the shock path computed by the first-order solution. To illustrate the accuracy afforded by the first-order solution for the downstream flow variables, two examples have been computed. For an upstream Mach number of 1.5 the Mach number on the downstream side of the shock is 0.7011. If the boundary on which the disturbance is specified is located at the section at which the initial Mach number is 0.7, we have $\overline{X} = 0.007$, $U = -0.73179$, and $C = 1.04541$. For these conditions the downstream flow variables are shown in figure (3.2). (It will be noted that $\overline{X}$ does not enter this calculation except by determining U and C at $x = 0$.) For values of x up to 0.4 the first-order representation is quite good. If we choose the boundary at the section where the initial Mach number is 0.6, we have $\overline{X} = 0.830$, $U = -0.63481$, and $C = 1.05801$. This case is shown in figure (3.3). At the initial shock location, the first-order values of the flow variables are still reasonably accurate. Upstream of this station the departures become quite large, especially for c. It should be noted that the values of the downstream flow variables upstream of the initial shock location (which do not exist prior to movement of the shock) serve as the basis for the new downstream flow as the shock moves upstream. Hence, errors in final shock location will be larger when the boundary conditions are given farther from the initial shock position.

The first shock path calculated is for a shock initially occurring at a Mach number of 1.5 in a duct with $\epsilon = 0.1$. The disturbance function is specified at the downstream section at which the initial Mach number is 0.7 ($\overline{X} = 0.007$) as in figure (3.2). The values of U, C, $\overline{U}$, and $\overline{C}$ have been given above. The magnitude of the disturbance was selected so that the final shock position would be that corresponding to an upstream

Mach number of 1.43. For a δ of 4, the corresponding value of K (cf. eqs. (3.33)) is 0.010025. For this disturbance the shock should come to rest at $x = 0.388$ (cf. the sketch on p. 54, point L). The coefficients of equation (3.31) are:

$$B_0 = 1.04087, \qquad B_3 = -16.92621,$$

$$B_1 = -0.78888, \qquad B_4 = 0.35140,$$

$$B_2 = 16.10895, \qquad B_5 = -1.52893,$$

$$\text{and} \quad \alpha_s = 0.02629.$$

The equations relating the characteristic variables on the shock path are:

Zone I: $\alpha = -1.39236 + 1.17277\beta + 1.41865e^{-0.09550\beta}$,

Zone II: $\alpha = -1.32790 + 1.16849\beta + 1.35689e^{-0.09585\beta}$,

Zone III: $\alpha = 1.34140 + \beta - 1.46778e^{-0.07888\beta}$.

Substitution of these values into the expressions for x and t in equation (3.10) yields the shock path shown by the dash-dot line in figure (3.4). The shock asymptotically approaches a final position of $x = 0.349$, which is about 90 percent of the excursion it should have undergone. The greater part of the shock motion occurs in zone III, which starts at $x = 0.076$ on the shock path. The value of the final shock location can be obtained directly from the α,β-relation in zone III. From this equation, $(\alpha - \beta)$ is seen to have a limit of 1.34140 as $\beta \to \infty$. In zone III, the integral appearing in the expression for x is a function of $(\alpha - \beta)$, and therefore x is a function of this quantity alone in this zone.

To check the accuracy of the analytical expression for the shock path, equation (3.8) was integrated numerically by using both first- and second-order representations of the flow field behind the shock (i.e., eqs. (2.69)). The coefficients for these equations are listed in table (3.1). The numerical integration was programmed for the digital computer by using the Runge-Kutta method of integration and an increment in β of 2. (Halving the increment of β did not change the results.) The results of the numerical integration are shown as the solid and dashed lines in figure (3.4) and are tabulated in table (3.2). For this case the analytical approximation compares very well with that obtained by numerical integration.

The shock path was then calculated for the same initial shock conditions with the disturbance specified at the section at which the Mach number was 0.6 ($\bar{X} = 0.830$ as in fig. (3.3)). For a δ of 4, the value of K for a final shock Mach number of 1.43 is 0.006225. For this case the coefficients of equation (3.31) are:

$$B_0 = 1.33816, \qquad B_2 = 15.60186, \qquad B_4 = 0.63237,$$

$$B_1 = -0.48838, \qquad B_3 = -15.17776, \qquad B_5 = -1.56876,$$

$$\text{and} \quad \alpha_s = 2.69885.$$

The α,β-relations on the shock path are now:

Zone I: $\alpha = 0.57893 + 1.17443\beta + 2.11992e^{-0.05790\beta}$,

Zone II: $\alpha = 0.73649 + 1.16658\beta + 1.95260e^{-0.05829\beta}$,

Zone III: $\alpha = 5.08497 + \beta - 2.59647e^{-0.04884\beta}$.

The shock path calculated from these equations is shown in figure (3.5) as the dash-dot curve. The curve is similar in shape to that of the preceding figure and has an asymptote of $x = 1.473$. The final shock position should be $x = 1.211$. Thus, specifying the disturbance farther from the initial shock location has increased the error and caused the error to change sign. Numerical integrations of equation (3.8) for this case yielded the other curves on this figure. (The coefficients are listed in table (3.3) and the results of the integration in table (3.4).) For this case it is seen that there is an appreciable difference between the analytical approximation and the corresponding first-order numerical integration. This difference results from the higher order terms that were neglected in obtaining equation (3.31). In the first example, these terms were of small import because the disturbance was specified so close to the shock. The second-order numerical integration yields a final shock position of $x = 1.162$, which represents a shock movement of 0.332 units. The second-order integration in the first example gave a shock movement of 0.343 units, which is quite close to the result of the present example. This reflects the improvement of the representation of the downstream flow afforded by the use of the second-order representation of the disturbance function.

In these examples the shock displacement obtained from the second-order numerical integration (the most accurate result) was always less than that which should have been obtained. This error in shock displacement results from the fact that the values of $\bar{U}$ and $\bar{C}$ used in the calculations were obtained from the exact shock transition relations (eqs.

(3.14) and (3.15)) rather than the approximate relations used in deriving the equations for the shock path. In figure (3.6) the Mach number downstream of the shock is shown as a function of the Mach number ahead of the shock for both the exact and approximate transition relations. For the same downstream Mach number, the approximate transition requires a greater upstream Mach number than the exact transition relation. Because the solution for the shock path employs the approximate shock relations, the shock should come to rest at a higher upstream Mach number, that is, after a smaller excursion, than would be indicated from the exact relations. If a lower initial shock Mach number were chosen, the error in final shock location would be smaller.

D. Discussion

The solution obtained for the interaction of a shock wave and a "simple-wave-type" disturbance in a duct flow yields a shock path that may be described as an "exponential decay" approach to a final position. This result is quite similar to that obtained by Kantrowitz in reference 2, wherein he obtained a first-order linear differential equation relating x and t on the shock path by linearizing the equations of motion and the shock transition relations.

In the examples given above, it was noted that the majority of the shock motion occurred in zone III; that is, where $\beta \geq \delta$. In this region, as was required by the boundary conditions, the flow variables downstream of the shock have reached their terminal values. Thus, the effect of neglecting the "back reaction" of the shock motion on the downstream flow conditions is quite pronounced in zone III. This assumption, which is inherent in the development presented, is not as restrictive as might appear at first glance. In the next section, it will be shown that the conditions specified on the downstream boundary are reasonable approximations for the actual process.

From the examples presented, it can be concluded that the first-order analytical solution for the shock path offers a reasonably accurate representation of the path, provided that the choice of the initial conditions are such that the first-order representations of the initial steady flow (both upstream and downstream of the shock) are accurate. That is, the boundary on which the disturbance is specified should be fairly close to the initial location of the shock. Also, the disturbance magnitude should be selected so as to result in a shock displacement that is within the region of accuracy of the first-order representation of the upstream conditions. If the boundary conditions are required to be specified at fairly large distances downstream of the shock, numerical integration of the differential equation should be employed.

IV. THE FLOW FIELD BEHIND A MOVING SHOCK WAVE

In the preceding section a solution for the interaction of a shock wave with a "simple-wave-type" disturbance in a duct flow was presented. This solution was developed on the basis of two assumptions: First, that the simple-wave relation $(u - \sigma c)$ = constant held on the downstream boundary. Second, that the "back reaction" of the shock motion on the flow could be neglected. The solution obtained indicated that under these assumptions the greater part of the shock motion occurred after the downstream flow had reached its terminal state. This leads one to inquire how well the results obtained under these assumptions represent the actual process. That is, in the flow field behind a moving shock wave, does the u,c-relation at a given cross section approximate $\underline{Q}$ = constant, and is the back reaction of the shock sufficiently small in magnitude that it may be neglected?

The problem at hand is, then, to find the flow field behind a shock wave moving in a duct flow. This falls into the category of an "inverse" problem as defined in section II and is termed the "inverse-shock" problem. The solution to this problem can be viewed as yielding the nature of the disturbance that would result in a prescribed shock path.

A. Derivation of the Solution

Consider a shock path in the x,t-plane given by

$$x = \epsilon f(t). \tag{4.1}$$

The shock velocity is then given by

$$V = \frac{dx}{dt} = \epsilon f'(t). \tag{4.2}$$

Because an initially steady flow in the duct is desired, the initial velocity of the shock wave must be zero. Therefore, it is prescribed that

$$f'(0+) = 0 \tag{4.3}$$

and, for convenience,

$$f(t) = 0, \qquad t \leq 0. \tag{4.4}$$

Ahead of the shock there is a steady supersonic flow which, for the "epsilon duct," can be represented to first order by (cf. section III, eq. (3.20))

$$\left.\begin{aligned} \bar{u} &= \bar{U}(1 + \epsilon \bar{u}_s^{(1)}), \\ \bar{c} &= \bar{C}(1 + \epsilon \bar{c}_s^{(1)}), \end{aligned}\right\} \tag{4.5}$$

where $\bar{U}$ and $\bar{C}$ are the flow conditions immediately upstream of the shock at its initial location, $x = 0$ in this case, and

$$\left.\begin{aligned} \bar{u}_s^{(1)} &= \frac{\sigma}{\sigma + 1} \frac{\bar{C}^2}{(1 - \bar{U}^2)} x, \\ \bar{c}_s^{(1)} &= -\frac{1}{\sigma + 1} \frac{\bar{U}^2}{(1 - \bar{U}^2)} x. \end{aligned}\right\} \tag{4.6}$$

As shown in section III, these relations yield quite accurate representations of the upstream flow conditions for the magnitude of shock displacement considered.

After specifying the shock path and the upstream flow field, the next step is to determine the conditions on the downstream side of the shock. From the approximate shock transition relations (eqs. (3.1) and (3.2)), the conditions on the downstream side of the shock can be determined as follows:

It is assumed that on the downstream side of the shock the flow variables can be represented to first order by

$$\left.\begin{aligned} u_s &= U(1 + \epsilon u_s^{(1)}), \\ c_s &= C(1 + \epsilon c_s^{(1)}), \end{aligned}\right\} \tag{4.7}$$

where U and C are now the flow conditions immediately downstream of the shock at its initial location. Substituting equations (4.7) and (4.5) into equations (3.1) and (3.2) and expanding the resulting

expression to first order in ϵ gives, from equation (3.1),

$$\left.\begin{aligned} V = {} & \tfrac{1}{2}(U + C) + \tfrac{1}{2}(\overline{U} + \overline{C}) + \frac{1}{8\overline{C}}\left[(U + C) - (\overline{U} + \overline{C})\right]^2 + \\ & \epsilon\left\{\frac{1}{4\overline{C}}(\overline{U}u_s^{(1)} + \overline{C}c_s^{(1)})(3\overline{C} + \overline{U} - U - C) - \right. \\ & \frac{1}{8\overline{C}}(U + C - \overline{U} - \overline{C})^2\,\overline{c}_s^{(1)} + \\ & \left.\frac{1}{4\overline{C}}(Uu_s^{(1)} + Cc_s^{(1)})(\overline{C} - \overline{U} + C + U)\right\}, \end{aligned}\right\} \tag{4.8}$$

and, from equation (3.2),

$$\overline{U} - \sigma\overline{C} + \epsilon(\overline{U}u_s^{(1)} - \sigma\overline{C}c_s^{(1)}) = U - \sigma C + \epsilon(Uu_s^{(1)} - \sigma Cc_s^{(1)}). \tag{4.9}$$

Substituting equation (4.2) into equation (4.8) and equating the coefficients of like powers of ϵ in equations (4.8) and (4.9) gives

$$\left.\begin{aligned} U + C + \overline{U} + \overline{C} &= -\frac{1}{4\overline{C}}(U + C - \overline{U} - \overline{C})^2, \\ U - \sigma C &= \overline{U} - \sigma\overline{C}, \end{aligned}\right\} \tag{4.10}$$

and

$$\left.\begin{aligned} f'(t) = {} & \frac{1}{4\overline{C}}(\overline{U}u_s^{(1)} + \overline{C}c_s^{(1)})(3\overline{C} + \overline{U} - U - C) - \\ & \frac{1}{8\overline{C}}(U + C - \overline{U} - \overline{C})^2\,\overline{c}_s^{(1)} + \\ & \frac{1}{4\overline{C}}(Uu_s^{(1)} + Cc_s^{(1)})(\overline{C} - \overline{U} + U + C), \\ \overline{U}u_s^{(1)} - \sigma\overline{C}c_s^{(1)} &= Uu_s^{(1)} - \sigma Cc_s^{(1)}. \end{aligned}\right\} \tag{4.11}$$

These equations determine U, C, and the functions $u_s^{(1)}$ and $c_s^{(1)}$; these are given by

$$C = \frac{\sigma - 1}{\sigma + 1}\overline{C} + \frac{2}{\sigma + 1}\sqrt{\overline{C}(2\overline{U} - \overline{C})}, \tag{4.12a}$$

$$U = \sigma C + \overline{U} - \sigma\overline{C}, \tag{4.12b}$$

$$c_s^{(1)} = f'(t)\,\frac{4\overline{C}}{(\sigma+1)C(\overline{C}-\overline{U}+U+C)} - x\,\frac{\overline{U}}{(\sigma+1)^2(1-\overline{U}^2)C}\left\{\sigma\overline{C}(\overline{U}+\overline{C}) + \frac{2\overline{C}(\sigma\overline{C}-\overline{U})(3\overline{C}+\overline{U}-U-C)+\overline{U}(U+C-\overline{U}-\overline{C})^2}{2(\overline{C}-\overline{U}+U+C)}\right\}, \tag{4.13a}$$

$$u_s^{(1)} = f'(t)\,\frac{4\sigma\overline{C}}{(\sigma+1)U(\overline{C}-\overline{U}+U+C)} + x\,\frac{\sigma\overline{U}}{(\sigma+1)^2(1-\overline{U}^2)U}\left\{\overline{C}(\overline{U}+\overline{C}) - \frac{2\overline{C}(\sigma\overline{C}-\overline{U})(3\overline{C}+\overline{U}-U-C)+\overline{U}(U+C-\overline{U}-\overline{C})^2}{2(\overline{C}-\overline{U}+U+C)}\right\}. \tag{4.13b}$$

Substituting equations (4.13) into equations (4.7) gives expressions of the following form for the flow quantities on the downstream side of the shock:

$$\left.\begin{aligned} u_s &= U + \epsilon E_3 f'(t) + \epsilon E_4 x, \\ c_s &= C + \epsilon E_1 f'(t) + \epsilon E_2 x. \end{aligned}\right\} \tag{4.14}$$

The E_1 are given by:

$$\left.\begin{aligned} E_1 &= \frac{4\overline{C}}{(\sigma+1)(\overline{C}-\overline{U}+U+C)}, \\ E_2 &= -\frac{\overline{U}}{(\sigma+1)^2(1-\overline{U}^2)}\left\{\sigma\overline{C}(\overline{U}+\overline{C}) + \frac{2\overline{C}(\sigma\overline{C}-\overline{U})(3\overline{C}+\overline{U}-U-C)+\overline{U}(U+C-\overline{U}-\overline{C})^2}{2(\overline{C}-\overline{U}+U+C)}\right\}, \\ E_3 &= \frac{4\sigma\overline{C}}{(\sigma+1)(\overline{C}-\overline{U}+U+C)}, \\ E_4 &= \frac{\sigma\overline{U}}{(\sigma+1)^2(1-\overline{U}^2)}\left\{\overline{C}(\overline{U}+\overline{C}) - \frac{2\overline{C}(\sigma\overline{C}-\overline{U})(3\overline{C}+\overline{U}-U-C)+\overline{U}(U+C-\overline{U}-\overline{C})^2}{2(\overline{C}-\overline{U}+U+C)}\right\}. \end{aligned}\right\} \tag{4.15}$$

Finally, substituting equation (4.1) into equations (4.14) gives

$$\left.\begin{aligned} u_s &= U + \epsilon E_3 f'(t) + \epsilon^2 E_4 f(t), \\ c_s &= C + \epsilon E_1 f'(t) + \epsilon^2 E_2 f(t). \end{aligned}\right\} \tag{4.16}$$

These are the conditions on the downstream side of the shock and are, therefore, the boundary conditions to be satisfied on this side of the shock path. It is of interest to note that the effects of shock velocity appear as terms of first order in ϵ, whereas the effects of shock displacement appear as terms of second order.

Having obtained the conditions on the downstream side of the shock, we now proceed to determine the flow field downstream of the moving shock. A solution of equations (2.37) is sought under the boundary conditions given by equations (4.16). The boundary conditions are to be satisfied in the following manner: The shock path is to be mapped on $\alpha = \beta$ such that $t = \alpha = \beta$; that is,

$$\left.\begin{aligned} &x^{(0)}(\alpha,\alpha) = x^{(0)}(\beta,\beta) = 0; \\ &x^{(1)}(\alpha,\alpha) = f(\alpha),\ x^{(1)}(\beta,\beta) = f(\beta); \\ &x^{(n)}(\alpha,\alpha) = x^{(n)}(\beta,\beta) = 0, \qquad n > 1; \end{aligned}\right\} \tag{4.17}$$

$$\left.\begin{aligned} &t^{(0)}(\alpha,\alpha) = \alpha,\ t^{(0)}(\beta,\beta) = \beta; \\ &t^{(n)}(\alpha,\alpha) = t^{(n)}(\beta,\beta) = 0, \qquad n > 0; \end{aligned}\right\} \tag{4.18}$$

and

$$\left.\begin{aligned} &u^{(0)}(\alpha,\alpha) = u^{(0)}(\beta,\beta) = U; \\ &u^{(1)}(\alpha,\alpha) = E_3 f'(\alpha),\ u^{(1)}(\beta,\beta) = E_3 f'(\beta); \\ &u^{(2)}(\alpha,\alpha) = E_4 f(\alpha),\ u^{(2)}(\beta,\beta) = E_4 f(\beta); \\ &u^{(n)}(\alpha,\alpha) = u^{(n)}(\beta,\beta) = 0, \qquad n > 2; \end{aligned}\right\} \tag{4.19}$$

$$\left.\begin{aligned} &c^{(0)}(\alpha,\alpha) = c^{(0)}(\beta,\beta) = C; \\ &c^{(1)}(\alpha,\alpha) = E_1 f'(\alpha),\ c^{(1)}(\beta,\beta) = E_1 f'(\beta); \\ &c^{(2)}(\alpha,\alpha) = E_2 f(\alpha),\ c^{(2)}(\beta,\beta) = E_2 f(\beta); \\ &c^{(n)}(\alpha,\alpha) = c^{(n)}(\beta,\beta) = 0, \qquad n > 2. \end{aligned}\right\} \tag{4.20}$$

The solutions up to second order are:

$$\left.\begin{aligned} u^{(0)} &= U, \\ u^{(1)} &= U_1^{(1)}(\alpha - \beta) + U_2^{(1)} f'(\beta), \\ u^{(2)} &= U_1^{(2)}(\alpha - \beta)^2 + U_2^{(2)} f(\alpha) + U_3^{(2)} f(\beta) - \\ &\qquad U_4^{(2)}(\alpha - \beta) f'(\beta); \end{aligned}\right\} \tag{4.21a}$$

$$\left.\begin{aligned} c^{(0)} &= C, \\ c^{(1)} &= -C_1^{(1)}(\alpha - \beta) + C_2^{(1)} f'(\beta), \\ c^{(2)} &= -C_1^{(2)}(\alpha-\beta)^2 + C_2^{(2)} f(\alpha) + C_3^{(2)} f(\beta) + C_4^{(2)}(\alpha-\beta) f'(\beta); \end{aligned}\right\} \tag{4.21b}$$

$$\left.\begin{aligned} t^{(0)} &= T_1^{(0)}\beta - T_2^{(0)}\alpha, \\ t^{(1)} &= -T_1^{(1)}(\alpha-\beta)^2 + T_2^{(1)}\left[f(\beta) - f(\alpha)\right] + T_3^{(1)}(\alpha-\beta) f'(\beta), \\ t^{(2)} &= -T_1^{(2)}(\alpha-\beta)^3 - T_2^{(2)}(\alpha-\beta)\left[f'(\beta)\right]^2 - T_3^{(2)}\int_\alpha^\beta f(\tau)\,d\tau + \\ &\qquad T_4^{(2)}\int_\alpha^\beta \left[f'(\tau)\right]^2 d\tau - T_5^{(2)}(\alpha-\beta) f(\beta) - T_6^{(2)}(\alpha-\beta) f(\alpha) - \\ &\qquad T_7^{(2)}(\alpha-\beta)^2 f'(\beta) + T_8^{(2)} f'(\beta)\left[f(\alpha) - f(\beta)\right]; \end{aligned}\right\} \tag{4.21c}$$

$$
\left.
\begin{aligned}
x^{(0)} &= - X_1^{(0)}(\alpha - \beta), \\
x^{(1)} &= - X_1^{(1)}(\alpha-\beta)^2 + X_2^{(1)}f(\beta) + X_3^{(1)}f(\alpha) + X_4^{(1)}(\alpha-\beta)f'(\beta), \\
x^{(2)} &= - X_1^{(2)}(\alpha-\beta)^3 + X_2^{(2)}(\alpha-\beta)\left[f'(\beta)\right]^2 + X_3^{(2)}\int_\alpha^\beta f(\tau)d\tau + \\
&\quad X_4^{(2)}\int_\alpha^\beta \left[f'(\tau)\right]^2 d\tau + X_5^{(2)}(\alpha-\beta)f(\beta) - X_6^{(2)}(\alpha-\beta)f(\alpha) + \\
&\quad X_7^{(2)}(\alpha-\beta)^2 f'(\beta) + X_8^{(2)}f'(\beta)\left[f(\alpha) - f(\beta)\right].
\end{aligned}
\right\} \quad (4.21d)
$$

The coefficients are given by (use has been made of the fact that $E_3 = \sigma E_1$):

$$
\left.
\begin{aligned}
U_1^{(1)} &= UC/2 \\
U_2^{(1)} &= E_3 \\
U_1^{(2)} &= \frac{U(\sigma C^2 - U^2)}{8\sigma} \\
U_2^{(2)} &= \frac{E_3}{4\sigma C}(\sigma C + U)(U + C) + \frac{1}{2}(E_4 - \sigma E_2) \\
U_3^{(2)} &= \frac{1}{2}(E_4 + \sigma E_2) - \frac{E_3}{4\sigma C}(\sigma C + U)(U + C) \\
U_4^{(2)} &= \frac{E_3}{4\sigma C}(U - C)(\sigma C + U)
\end{aligned}
\right\} \quad (4.22a)
$$

$$
\left.
\begin{aligned}
C_1^{(1)} &= U^2/2\sigma \\
C_2^{(1)} &= E_3/\sigma \\
C_1^{(2)} &= U^2 C/4\sigma \\
C_2^{(2)} &= \frac{U}{2\sigma} - E_3\frac{(U + C)^2}{4\sigma C} - \frac{1}{2\sigma}(E_4 - \sigma E_2) \\
C_3^{(2)} &= E_3\frac{(U + C)^2}{4\sigma C} - \frac{U}{2\sigma} + \frac{1}{2\sigma}(E_4 + \sigma E_2) \\
C_4^{(2)} &= E_3\frac{(U - C)^2}{4\sigma C}
\end{aligned}
\right\} \quad (4.22b)
$$

$$T_1^{(0)} = \frac{U + C}{2C}$$

$$T_2^{(0)} = \frac{U - C}{2C}$$

$$T_1^{(1)} = \frac{U}{8\sigma C}(\sigma C^2 + U^2)$$

$$T_2^{(1)} = E_3 \frac{\sigma - 1}{4\sigma C^2}(U + C) - \frac{1}{2C}$$

$$T_3^{(1)} = E_3 \frac{(\sigma + 1)(U - C)}{4\sigma C^2}$$

$$T_1^{(2)} = \frac{U}{48\sigma^2 C^3}(\sigma C^2 + U^2)(\sigma C^2 + 2U^2)$$

$$T_2^{(2)} = E_3^2 \frac{(\sigma + 1)(\sigma + 3)}{16\sigma^2 C^3}(U - C)$$

$$T_3^{(2)} = \frac{E_3}{16\sigma^2 C^3}\left[5(\sigma+1)U^3 + \sigma(3-5\sigma)UC^2 + (4\sigma^2+5\sigma-3)U^2C + \sigma(3-\sigma)C^3\right] - E_4 \frac{\sigma - 1}{4\sigma C} - E_2 \frac{(\sigma - 1)U}{4C^2} + \frac{\sigma - 1}{4\sigma}\frac{U}{C}$$

$$T_4^{(2)} = E_3^2 \frac{\sigma - 1}{16\sigma^2 C^3}\left[(3\sigma - 1)C + (\sigma - 3)U\right] - E_3 \frac{\sigma - 1}{4\sigma C^2}$$

$$T_5^{(2)} = \frac{E_3}{8\sigma^2 C^3}\left[(\sigma+3)U^3 + (2\sigma^2-\sigma-1)U^2C - \sigma(3\sigma+1)UC^2 - \sigma(\sigma-1)C^3\right] - (E_4 + \sigma E_2)\frac{(\sigma + 1)(U - C)}{8\sigma C^2} + \frac{U[(\sigma - 1)C + 2U]}{8\sigma C^2}$$

$$T_6^{(2)} = \frac{E_3(U + C)}{16\sigma^2 C^3}\left[\sigma(\sigma + 1)C^2 + 4\sigma UC + (3\sigma - 1)U^2\right] + (E_4 - \sigma E_2)\frac{(\sigma + 1)(U + C)}{8\sigma C^2} + \frac{U[(\sigma - 1)C - 2U]}{8\sigma C^2}$$

$$T_7^{(2)} = E_3 \frac{\sigma + 1}{32\sigma^2 C^3}\left[\sigma C^2(C - 3U) + U^2(3C - 5U)\right]$$

$$T_8^{(2)} = E_3^2 \frac{(\sigma^2 - 1)}{8\sigma^2}\frac{U + C}{C^3} - E_3 \frac{\sigma + 1}{4\sigma C^2}$$

(4.22c)

$$X_1^{(0)} = \frac{U^2 - C^2}{2C} \qquad X_2^{(1)} = E_3 \frac{\sigma - 1}{4\sigma C^2}(U + C)^2 - \frac{U - C}{2C}$$

$$X_1^{(1)} = \frac{U^2}{8\sigma C^2}\left[(2\sigma+1)C^2 + U^2\right] \qquad X_3^{(1)} = \frac{U + C}{2C} - E_3 \frac{\sigma - 1}{4\sigma C^2}(U + C)^2$$

$$X_4^{(1)} = E_3 \frac{\sigma + 1}{4\sigma C^2}(U - C)^2$$

$$X_1^{(2)} = \frac{U^2}{48\sigma^2 C^3}\left\{(\sigma C^2+U^2)(\sigma C^2+2U^2) + \sigma C^2\left[(3\sigma+2)C^2 + U^2\right]\right\}$$

$$X_2^{(2)} = \frac{E_3^2}{16\sigma^2 C^3}(\sigma + 1)(U - C)\left[(3\sigma + 1)C - (\sigma + 3)U\right]$$

$$X_3^{(2)} = \frac{-E_3}{16\sigma^2 C^3}\left\{U^3\left[(3\sigma+7)C + 5(\sigma+1)U\right] - \sigma UC^2\left[(3\sigma-1)C + (5\sigma-3)U\right] + U^2C\left[(4\sigma^2 + 3\sigma - 1)C + (4\sigma^2 + 5\sigma - 3)U\right] + \sigma C^3\left[(\sigma + 1)C + (3 - \sigma)U\right]\right\} +$$
$$E_4 \frac{(\sigma - 1)U}{2\sigma C} + E_2 \frac{\sigma - 1}{4C^2}(U^2 + C^2) - \frac{\sigma - 1}{4\sigma} \cdot \frac{U^2}{C}$$

$$X_4^{(2)} = \frac{E_3^2}{16\sigma^2 C^2}(\sigma-1)(U+C)\left[(3\sigma-1)C + (\sigma-3)U\right] - \frac{E_3}{4\sigma C^2}(\sigma-1)(U+C)$$

$$X_5^{(2)} = \frac{E_3 U}{8\sigma^2 C^3}\left[4\sigma^2 C^3 + (2\sigma^2 + \sigma + 1)UC^2 - 2(\sigma^2 + 1)U^2C - (\sigma+3)U^3\right] +$$
$$(E_4 + \sigma E_2)\frac{\sigma + 1}{8\sigma}\left(\frac{U - C}{C}\right)^2 - \frac{U}{8\sigma C^2}\left[(\sigma+1)C^2 + (\sigma-1)UC + 2U^2\right]$$

$$X_6^{(2)} = E_3 \frac{(U + C)}{16\sigma^2 C^3}\left[\sigma(\sigma+1)C^3 + 3\sigma(\sigma+1)UC^2 + (5\sigma+1)U^2C + (3\sigma-1)U^3\right] +$$
$$(E_4 - \sigma E_2)\frac{\sigma + 1}{8\sigma}\left(\frac{U + C}{C}\right)^2 - \frac{U}{8\sigma C^2}\left[(\sigma+1)C^2 - (\sigma-1)UC + 2U^2\right]$$

$$X_7^{(2)} = \frac{\sigma + 1}{32\sigma^2}\frac{E_3}{C^3}\left\{\sigma C^2\left[C^2 - 8UC + 3U^2\right] + U^2\left[(4\sigma-1)C^2 - 4UC + 5U^2\right]\right\}$$

$$X_8^{(2)} = E_3^2 \frac{\sigma^2 - 1}{8\sigma^2}\frac{(U^2 - C^2)}{C^3} - E_3 \frac{\sigma + 1}{4\sigma}\frac{(U - C)}{C^2} .$$

(4.22d)

These equations give the flow field behind a shock moving on an arbitrary path in an "epsilon duct." The only conditions placed on the shock path are those of equations (4.3) and (4.4) and the fact that the shock does not leave the supersonic portion of the duct.

B. Examples

1. The "exponential" path. - The shock paths obtained in section III were described as "exponential decays" to their final position. Therefore, the first shock path investigated was chosen so that it would have an "exponential-decay" approach to a final position. Such a path is given by

$$f(t) = \begin{cases} B\left[1 - e^{-bt}(bt + 1)\right], & t \geq 0; \\ 0, & t < 0. \end{cases} \tag{4.23}$$

This path obviously satisfies equations (4.3) and (4.4). The coefficient B determines the magnitude of the excursion of the shock, and b (sometimes called a "time constant") determines the rate at which the shock approaches its final position. For convenience, the path given by equation (4.23) will be referred to as the "exponential" path.

The first case investigated was for a shock initially at a Mach number of 1.5 in a duct with $\epsilon = 0.1$. The amplitude B was taken as 3.5, and b was chosen to be 0.2. The shock path for these values is shown in figure (4.1). The shock starts its motion at zero velocity, accelerates, reaching a maximum velocity at $t = 1/b$, then gradually decelerates and approaches its terminal position. Over the time interval shown, the shock has traversed 91 percent of its total excursion.

For an initial upstream Mach number of 1.5, the values of $\overline{U}$ and $\overline{C}$ are -1.36458 and 0.90972, respectively ($\sigma = 5$). The corresponding conditions downstream of the shock (using the approximate shock transition relations) are $U = -0.73655$ and $C = 1.03533$. The variation of the downstream flow conditions along the shock path is shown in figure (4.2). As the shock accelerates, the particle velocity decreases in magnitude rather rapidly and then increases as it gradually approaches a final value greater than its initial value. The sonic speed rapidly increases and then decays to a final value somewhat greater than the initial value. The values of the downstream flow conditions shown in figure (4.2) were obtained by setting $\alpha = \beta$ in equations (4.21). The values of the coefficients of equations (4.21) (cf. eqs. (4.22)) for this case are given in table (4.1).

Equations (4.21) were programmed for computation on an IBM type-650 digital computer. The equations were programmed to compute the values of the flow variables at constant values of x, that is, at constant distances downstream of the initial shock location. The variation of particle velocity and sonic speed at $x = -0.5, -1.0, -1.5$ for the shock path under consideration is shown as the curves in figures (4.3), (4.4), and (4.5), respectively, and is listed in table (4.2). At all cross sections, the history of the flow variables is similar. The particle velocity decreases rapidly, reaches a minimum, and then gradually approaches a final value lower than its initial value. The sonic speed undergoes a rapid increase, reaches a maximum, and then decreases as it slowly approaches a final value greater than the initial value. From this, it is apparent that the downstream disturbance that would cause the assumed shock motion consists of a compression followed by an expansion. The amplification of the disturbance as it moves upstream is evident in the figures. At $x = -1.5$, the magnitude of the maximum change in u is 0.0223 units or 3.87 percent of the initial value of the variable. At $x = -0.5$, the maximum change in u is 0.0360, which is 4.55 percent of its initial value. Also of interest is the fact that the greater part of the change in the flow variables occurs in the first 5 to 6 units of time. During this interval the shock wave has completed only about one-third of its total movement.

One of the purposes of the computation of the flow field behind a moving shock was to determine the u,c-relation on lines of constant x. Figures (4.3) to (4.5) have been cross-plotted, and the resulting u,c-relations are shown in figure (4.6). At all values of x, the u,c-relation consists of an almost linear variation during the compression process. At the beginning of the expansion process, the curve folds back on itself and follows an almost straight path slightly displaced from that during the compression process. At the larger values of $|x|$, the portion of the curve representing the expansion process moves closer to the section representing the compression (i.e., the "hairpin" becomes narrower).

In section III it was assumed that, in the flow field behind the shock, the value of Q at a fixed x remained constant throughout the transient. This requires, first, that the u,c-relation at constant x should be a straight line and, second, that the slope of the straight line be equal to σ. In figure (4.6) the u,c-relation is not straight throughout the entire transient. This is principally the result of the fact that the shock path chosen requires an expansion as well as a compression in the downstream disturbance. (Succeeding examples will show that, for shock paths which can be produced by compressive disturbances, the relation can be approximated by a straight line.) The portion of the curves of figure (4.6) representing the compression process are approximately straight lines. For these portions of the curves, the slopes have been measured and are listed below.

x	du/dc
-0.5	5.00
-1.0	5.12
-1.5	5.26

5239

The value of σ for the example is 5. From the table, it is seen that close to the initial shock location the perturbation-series solution gives a value of 5 for du/dc. At greater distances, the slope increases. Therefore, only close to the initial location of the shock does the u,c-relation during the compression approximate Q = constant. Thus, for the region of applicability of the first-order interaction solution of section III, the assumption of constant Q appears to be reasonable.

Since, for the shock to move in the prescribed fashion, the disturbance causing the motion consists of a compression followed by an expansion, the shock comes to rest sooner than it would if the disturbance were purely compressive in nature. If the path were such that a longer time interval were required for the same over-all shock displacement, the disturbance should approach a pure compression. To demonstrate this, another case was computed for the same initial conditions and shock excursion, but with $b = 0.1$, one-half the previous value. The shock path for this value of b is shown in figure (4.7). The time interval for the shock to complete 91 percent of its travel is approximately twice that for $b = 0.2$. The history of the flow variables on the downstream side of the shock during its motion is shown in figure (4.8). (The coefficients of eqs. (4.21) are again given by table (4.1)). Comparison of this figure with figure (4.2) ($b = 0.2$) shows that, although the curves are quite similar in shape, the magnitude of the maximum excursion in the flow variables is much less in the present case. This reflects the smaller shock velocities during the transient for the lower value of b.

The variations of u and c with time at constant x for this example are shown in figures (4.9) and (4.10) for $x = -0.5$ and $x = -2.0$, respectively, and are listed in table (4.3). At $x = -0.5$, the flow variables exhibit a sharp rise followed by a gradual approach to their terminal values. At this section the disturbance is purely compressive. Over 80 percent of the change in the flow variables occurs in the first ten to twelve units of time. During this time period, the shock has moved but one-third of its total travel. At $x = -2.0$, a slight expansion follows the compression process. The magnitude of this expansion is, however, a much smaller proportion of the total change in the variables in this case than for that with $b = 0.2$.

The u,c-relation at the two values of x is shown in figure (4.11). At x = -0.5, the relation is essentially a straight line over most of the range of the variables. The fold, characteristic of the expansion in the first example, does not exist. There is, however, an increase of curvature towards the very end of the transient. At this value of x, the slope of the straight portion of the curve is 5.00, as it was at the same station for the larger value of b. At x = -2.0 (fig. (4.11b)), where there is an expansion process of small magnitude following the compression, the u,c-relation folds back on itself as in the first example. The major portion of this curve is essentially a straight line with a slope of 5.48; this again indicates the increase of the slope of the straight portion of the u,c-relation with distance from the initial shock location.

2. Comparison with the method-of-characteristics solution. - To check the accuracy of the representation of the flow field behind a moving shock wave afforded by the perturbation-series solution, the flow field was computed by the method of characteristics. For this computation the conditions on the downstream side of the moving shock wave were determined from the approximate shock transition relations (eqs. (3.1) and (3.2)) so that the comparison could be made for the same initial conditions. The characteristic net for the "exponential" shock path with B = 3.5, b = 0.2, and an initial shock Mach number of 1.5, is shown in figure (4.12). The values of the flow variables at constant x were obtained by linear interpolation between the net points and are shown as the data symbols on figures (4.3) to (4.5). At all values of x, the variation of u an c with time as determined by the method of characteristics is quite similar to that given by the perturbation-series solution. There is an initial rapid compression followed by an expansion process. At x = -0.5, the two solutions are in excellent agreement during the first eight units of time. After this time period, the values of c given by the method of characteristics are greater and the values of u smaller than those of the perturbation-series solution. At greater distances from the initial shock location these errors increase. The magnitude of the differences is always greatest towards the end of the transient. Further, the errors are proportionally greater for the sonic speed than they are for the particle velocity.

These errors result primarily from the representation of the underlying steady flow afforded by the perturbation series rather than from the representation of the transient process. It will be recalled from section II that the convergence and accuracy of the series solution for steady subsonic flow were poorest when the boundary conditions were specified at x = L, that is, at a high-velocity section. This is seen in figure (2.13), where even the third-order solution is accurate only for relatively short distances downstream from the boundary. This figure also shows that the accuracy of the representation of the sonic speed is much poorer than that of the particle velocity. The rather rapid decrease

in accuracy with distance from an upstream boundary causes not only the errors at the beginning of the transient but also accounts for the increase of the error with time at a given value of x.

The coordinate axes for the inverse-shock problem are located so that the origin coincides with the initial shock location. Therefore, during the course of the transient the shock wave, or carrier of the initial data, moves upstream from the origin, and a constant x corresponds to greater distances from the initial data carrier as time increases. The error in the magnitudes of the flow variables should, therefore increase with time at a constant x, as observed in figures (4.3) to (4.5).

To indicate the order of magnitude of the error that can be expected in the original steady flow, the second-order steady-flow solution was computed for a duct with $\epsilon = 0.1$, with the initial data given at the cross section with a Mach number of 0.7. This Mach number is close to that behind a shock at Mach 1.5 for $\sigma = 5$. The results are shown in figure (4.13) as the solid curves. The exact values are shown as the dashed curves. The rapid increase of the error in c with $|x|$ is quite apparent. From these curves it is easily seen that a large proportion of the error in the flow variables observed in figures (4.3) to (4.5) is attributable to the inaccuracy of the representation of the underlying steady flow.

To illustrate the effect of initial shock Mach number on the results, an example was calculated for an "exponential" shock path with $B = 3$, $b = 0.1$, $\epsilon = 0.1$ and an initial shock Mach number of 1.4. The shock path for this case is shown in figure (4.14) and the flow conditions on the downstream side of the shock in figure (4.15). The coefficients of equations (4.21) for this case are given in table (4.4). The variation of the flow variables at $x = -0.5$ and -1.0 are shown in figures (4.16) and (4.17), respectively, and are listed in table (4.5). The histories of the flow variables for this case are very similar in nature to those given previously for a shock initially at Mach 1.5 moving on an exponential path with $b = 0.1$. At $x = -0.5$, the disturbance is entirely compressive with the major portion of the change in the flow variables occurring in the first ten units of time. At $x = -1.0$, the compression process is followed by a very slight expansion process. The amplification of the disturbance as it moves upstream is quite evident. The u,c-relations at the two values of x are shown in figure (4.18). Again, these curves are almost straight lines with that at $x = -1.0$ showing the characteristic fold that indicates the expansion process.

This case was also solved by the method of characteristics. The results are shown as the data symbols in figures (4.16) and (4.17). As in the earlier example, the representation of the particle velocity is more accurate than that of the sonic speed. Again, the history of the

flow variables given by the method-of-characteristics solution is very similar to that from the series solution. The errors increase with time at a fixed value of x and are greater at the larger value of x. In this case the errors are relatively larger than those observed for an initial Mach number of 1.5. The increase in relative error is caused by the fact that, for an initial shock Mach number of 1.4, the downstream flow is specified at a cross section with higher subsonic velocity than for a shock at Mach 1.5. This further diminishes the accuracy of the series representation of the underlying steady flow.

3. The "cosine" path. - The examples presented thus far have all been for the "exponential" shock path given by equation (4.23). For this path it was seen that the u,c-relation at constant x could be approximated by straight lines for the compression and expansion phases of the disturbance. To demonstrate that such an approximation holds for other shock paths, equations (4.21) were evaluated for a path given by

$$f(t) = \begin{cases} \frac{1}{2} B(1 - \cos \omega t), & 0 \leqslant \omega t \leqslant \pi; \\ 0, & \omega t < 0; \\ B, & \omega t > \pi. \end{cases} \qquad (4.24)$$

This path satisfies equations (4.3) and (4.4), and the magnitude of the excursion of the shock is given by the coefficient B. For convenience, this path will be referred to as the "cosine" path.

The case investigated was for $B = 3.5$ and $\omega = \pi/20$ with an initial shock Mach number of 1.5. The total shock motion and initial shock Mach number are the same as those of the first example for the "exponential" path. As the coefficients of equations (4.21) are functions of the initial conditions only, the values given in table (4.1) apply to the present example. The history of the flow variables at $x = -0.5$ and -1.0 are shown in figures (4.19) and (4.20), respectively, and are listed in table (4.6). For the shock to move on the prescribed path, the disturbance consists of a compression followed by an expansion process. The trigonometric nature of the shock path function is reflected in the appearance of the variations of u and c. The variation of u and c have the appearance of slightly distorted, displaced cosine functions.

The u,c-relations at constant x are shown in figure (4.21). For the "cosine" path, the relation again consists of an almost straight section followed by an abrupt fold to a second straight section, characteristic of the expansion process. Again, the slope of the straight portion of the u,c-curve increases with distance from the initial shock location. The character of the relation between the downstream flow variables is thus seen to be relatively independent of the nature of the shock path.

C. Discussion

From the examples presented, it can be seen that the perturbation-series solution gives a fairly accurate picture of the history of the flow variables downstream of a moving shock wave. The agreement of the series solution with the method-of-characteristics solution is not as good as that observed for the unsteady-flow examples given in section II. However, the discrepancies were shown to arise primarily from the series representation of the underlying steady flow. For subsonic flow specified on an upstream boundary at which the flow velocity is high, the series representation of the steady flow is much less accurate than that for a flow specified at a low-speed downstream boundary.

For an "exponential" shock path (which approximates that obtained in section III for the direct interaction problem) the greater part of the change in the flow variables was seen to occur during the early part of the transient. During this early part of the transient, the shock moved but a small part of its total travel. This is similar to the result obtained in section III, where it was found that, for the disturbance function employed, most of the shock motion occurred after the downstream conditions had ceased to vary. For the "exponential" path with $b = 0.1$, the variation of the flow variables at constant x (cf. fig. (4.9)) can be reasonably approximated by the disturbance function given by equation (3.33). The largest discrepancies for such an approximation would occur in the region of the "knee" of the curves of figure (4.9).

The u,c-relations at constant x were seen to be approximately straight-line relations for the "exponential" paths that did not require expansion processes to bring the shock to rest. For values of x close to the initial shock location, the u,c-relation can be approximated by the Q = constant relation employed in section III. At greater distances from the initial shock location, the slope of straight portion of the u,c-relation increases; this indicates that the constant Q assumption employed in section III is reasonably accurate only for short distances downstream of the shock.

For shock paths requiring an expansion process to arrest the motion of the shock, the u,c-relation at constant x is almost a straight line during the compression process. At the peak of the compression, the u,c-relation abruptly folds back on itself and follows a slightly different, but again almost straight, path during the expansion process. This was true not only for the "exponential" path but also for the "cosine" path; this indicates that the relationship between the dependent variables is not greatly influenced by the nature of the shock path.

To compute the series solution at a given value of x required about 7 minutes of digital computer time. Therefore, to compute the solution at three values of x required about 21 minutes of machine time. The method-of-characteristics solution required 145 minutes of machine time to compute the net points covering the same range of x and t. To this time must be added that required to perform the necessary interpolations. The series solution offers, therefore, a considerable saving in computational effort for the solution of this problem.

Lewis Flight Propulsion Laboratory
National Advisory Committee for Aeronautics
Cleveland, Ohio, Aug. 22, 1958

APPENDIX - SYMBOLS

A	cross-sectional area of cut
B	amplitude
B_i	coefficients, eq. (3.32)
b	dimensionless constant
C	initial value of sonic speed
$\overline{C}$	sonic speed immediately upstream of stationary shock
C+	characteristic of family with slope u + c
C-	characteristic of family with slope u - c
$C_j^{(k)}$	coefficient of j-th member of k-th order terms in series for sonic speed
c	sonic speed
$\overline{c}$	sonic speed upstream of shock
D_i	coefficients, eq. (3.36)
E_i	coefficients, eq. (4.14)
K	eqs. (2.46) and (2.47)
L	duct length
M	Mach number
N	eqs. (2.46) and (2.47)
p	pressure
Q	Riemann invariant, u - σc
R_i	coefficients, eq. (3.26)
S_i	coefficients, eq. (3.29)
T	time

$T_j^{(k)}$	coefficient of j-th member of k-th order terms in series for time
t	time
U	initial value of particle velocity
$\overline{U}$	particle velocity immediately upstream of stationary shock
$U_j^{(k)}$	coefficient of j-th member of k-th order terms in series for particle velocity
u	particle velocity
$\overline{u}$	particle velocity upstream of shock
V	dimensionless shock velocity
v	shock velocity
$X_j^{(k)}$	coefficient of j-th member of k-th order terms in series for space coordinate
x	space coordinate
y	space coordinate, two-dimensional steady flow
α	characteristic parameter of family with slope $u - c$
β	characteristic parameter of family with slope $u + c$
γ	ratio of specific heat at constant pressure to specific heat at constant volume
δ	period
ϵ	"smallness" parameter
ζ	eq. (2.23)
η	eq. (2.31)
λ	index
ξ	parameter
σ	$2/(\gamma - 1)$

τ parameter

ω circular frequency

Subscripts:

s at shock location

* critical condition

5239

REFERENCES

1. Rudinger, George: Wave Diagrams for Nonsteady Flow in Ducts. D. Van Nostrand Co., Inc., 1955.

2. Kantrowitz, Arthur: The Formation and Stability of Normal Shock Waves in Channel Flows. NACA TN 1225, 1947.

3. Meyer, R. E.: On Waves of Finite Amplitude in Ducts. Quart. Jour. Mech. and Appl. Math., vol. 5, 1952, pp. 257-269; 270-291.

4. Lin, C. C.: On a Perturbation Theory Based on the Method of Characteristics. Jour. Math. and Phys., vol. 33, no. 2, July 1954, pp. 117-134.

5. Friedrichs, K. O.: Formation and Decay of Shock Waves. Communications on Pure and Appl. Math., vol. 2, Sept. 1948, pp. 211-245.

6. Courant, R., and Friedrichs, K. O.: Supersonic Flow and Shock Waves. Interscience Pub., Inc., 1948.

7. Fox, P. A.: On the Use of Coordinate Perturbations in the Solution of Physical Problems. Tech. Rep. No. 1, Proj. for Machine Methods of Computation and Numerical Analysis, M.I.T., Nov. 1953.

8. Roberts, R. C., and Lin, C. C.: The Method of Characteristics in Compressible Flow. Pt. II - Unsteady Flow. Tech. Rep. No. F-TR-1173D-ND (GDAM A-9-M 11/2), WADC, 1947.

9. Wolontis, V. M.: A Complete Floating-Decimal Interpretive System for the IBM 650 Magnetic Drum Calculator. Tech. Newsletter No. 11, IBM Appl. Sci. Div., Mar. 1956.

BIBLIOGRAPHY

1. Courant, R., and Hilbert, D.: Methoden der Mathematischen Physik. Vol. II. Julius Springer (Berlin), 1937. (Reprinted by Interscience Pub., 1943.)

2. Sauer, R.: Écoulements des Fluides Compressibles. Librairie Polytechnique Ch. Béranger (Paris), 1951.

3. Oswatitsch, K.: Gas Dynamics. Academic Press, 1956. (English version by G. Kuerti.)

4. Sears, W. R., ed.: General Theory of High Speed Aerodynamics. Vol. VI of High Speed Aerodynamics and Jet Propulsion, Princeton Univ. Press, 1954.

5. Oswatitsch, K.: Über die charakteristikenverfahren der Hydrodynamik. Z.A.M.M. Bd. 25/27, Heft 7, Oct. 1947; Bd. 25/27, Heft 8/9, Nov./Dec. 1947.

6. Guderley, G.: Nonstationary Gas Flow in Thin Pipes of Variable Cross Section. NACA TM 1196, 1948.

7. Neice, Stanford E.: A Method for Stabilizing Shock Waves in Channel Flow by Means of a Surge Chamber. NACA TN 2694, 1953.

8. Kahane, A., et al.: A Theoretical and Experimental Study of Finite Amplitude Wave Interactions with Channels of Varying Area. Jour. Aero. Sci., vol. 21, no. 8, Aug. 1954, pp. 505-524.

9. Chester, W.: Unsteady Compressible Flow in Ducts. Quart. Jour. Mech. and Appl. Math., vol. 7, pt. 2, 1954, pp. 247-256.

10. Trimpi, Robert L.: An Analysis of Buzzing in Supersonic Ram Jets by a Modified One-Dimensional Nonstationary Wave Theory. NACA TN 3695, 1956. (Supersedes NACA RM L52A18.)

TABLE 2.1. - COEFFICIENTS OF EQUATIONS (2.58) FOR

$U = -0.37879$, $C = 1.08226$, AND $\sigma = 5$ $(\gamma = 7/5)$

$X_j^{(k)}$

j \ k	0	1	2
1	+0.47484	-0.03989	-0.01455
2		+1.36687	+0.47507
3		+0.31687	-0.10007
4		+1.12250	+0.16204
5			+0.46192
6			+0.88876
7			+0.02252
8			-0.17960
9			-2.19853
10			-0.74323
11			+1.82431

$T_j^{(k)}$

j \ k	0	1	2
1	+0.32500	+0.04851	+0.00918
2	+0.67500	+0.45044	-0.20309
3		-0.93554	-0.00182
4		-0.32339	-0.10492
5			-0.16017
6			-0.60830
7			+0.03201
8			-1.35535
9			+0.86443
10			-0.41621
11			+0.67234

$U_j^{(k)}$

j \ k	1	2
1	-0.20497	-0.05409
2	+2.50000	-0.47044
3		+0.84923
4		+0.56818

$C_j^{(k)}$

j \ k	1	2
1	-0.01434	-0.00776
2	+0.50000	+0.05715
3		+0.24655
4		+0.30370

TABLE 2.2. - COEFFICIENTS OF EQUATIONS (2.69) FOR

$U = -0.37879$, $C = 1.08226$, AND $\sigma = 5$ ($\gamma = 7/5$)

$X_j^{(k)}$

j \ k	0	1	2
1	+0.47484	-0.03989	-0.01455
2		+2.73375	+0.95014
3		+0.42249	-8.79412
4			+0.00953
5			+2.43241
6			+1.99698
7			-0.12190

$T_j^{(k)}$

j \ k	0	1	2
1	+0.32500	+0.04850	+0.00917
2	+0.67500	-1.87108	-0.40619
3		+0.60059	+3.45775
4			+0.20080
5			-1.66484
6			+2.83877
7			+0.33296

$U_j^{(k)}$

j \ k	1	2
1	-0.20497	-0.05409
2	+5.00000	+1.69846
3		-0.81778

$C_j^{(k)}$

j \ k	1	2
1	-0.01434	-0.00776
2	+1.00000	+0.49310
3		+0.11431

TABLE 3.1. - COEFFICIENTS OF EQUATIONS (2.69) FOR

$U = -0.73179$, $C = 1.04541$, $\sigma = 5$

$U_j^{(k)}$

j \ k	1	2
1	-0.38251	-0.09017
2	+5.00000	+1.91049
3		-0.33714

$C_j^{(k)}$

j \ k	1	2
1	-0.05355	-0.02799
2	+1.00000	+0.75531
3		+0.02352

$X_j^{(k)}$

j \ k	0	1	2
1	+0.26658	-0.15383	-0,05611
2		+4.33501	+2.04768
3		+0.09000	-13.17190
4			-0.09825
5			+1.46353
6			+0.90394
7			-0.14828

$T_j^{(k)}$

j \ k	0	1	2
1	+0.15000	+0.10044	+0.02093
2	+0.85000	-2.43924	-0.70069
3		+0.28697	+4.66657
4			+0.08572
5			-0.82350
6			+2.88229
7			+0.16470

TABLE 3.2. - NUMERICAL INTEGRATION OF EQUATION FOR SHOCK PATH FOR

$U = -0.73179$, $C = 1.04541$, $\bar{U} = -1.36458$, $\bar{C} = 0.90972$, AND $\bar{X} = 0.00700$

β	First order			Second order		
	α	x	t	α	x	t
0	0.02629	0.00700	0.02236	0.02629	0.00700	0.02236
2	2.12527	.03421	2.10595	2.12536	.03424	2.10602
4	4.26928	.07525	4.22668	4.26996	.07542	4.22724
6	6.42758	.11844	6.36060	6.42942	.11895	6.36214
8	8.56341	.15490	8.47593	8.56651	.15576	8.47852
10	10.67989	.18570	10.57512	10.68403	.18685	10.57859
12	12.77972	.21177	12.66034	12.78450	.21308	12.66436
14	14.86522	.23386	14.73349	14.87020	.23521	14.73769
16	16.93839	.25258	16.79622	16.94315	.25386	16.80022
18	19.00099	.26846	18.84997	19.00513	.26957	18.85344
20	21.05451	.28195	20.89598	21.05770	.28280	20.89864
22	23.10025	.29340	22.93534	23.10223	.29393	22.93697
24	25.13932	.30314	24.96900	25.13990	.30330	24.96943
26	27.17268	.31141	26.99777	27.17174	.31118	26.99689
28	29.20115	.31845	29.02234	29.19863	.31781	29.02010
30	31.22545	.32443	31.04332	31.22132	.32339	31.03969
32	33.24618	.32952	33.06123	33.24046	.32808	33.05622
34	35.26387	.33386	35.07652	35.25657	.33202	35.07015
36	37.27895	.33754	37.08955	37.27015	.33533	37.08189
38	39.29181	.34068	39.10067	39.28158	.33812	39.09178
40	41.30277	.34335	41.11016	41.29121	.34046	41.10011
42	43.31211	.34563	43.11824	43.29930	.34242	43.10712
44	45.32008	.34756	45.12514	45.30612	.34408	45.11301
46	47.32686	.34921	47.13101	47.31185	.34547	47.11797
48	49.33265	.35062	49.13602	49.31667	.34663	49.12215
50	51.33758	.35181	51.14029	51.32072	.34762	51.12566
52	53.34178	.35283	53.14392	53.32413	.34844	53.12861
54	55.34536	.35370	55.14702	55.32699	.34913	55.13109
56	57.34840	.35443	57.14967	57.32940	.34972	57.13317
58	59.35100	.35506	59.15191	59.33142	.35021	59.13492
60	61.35321	.35560	61.15383	61.33313	.35062	61.13640
62	63.35510	.35605	63.15546	63.33456	.35096	63.13764

TABLE 3.3. - COEFFICIENTS OF EQUATIONS (2.69) FOR

$U = -0.63481$, $C = 1.05801$, $\sigma = 5$

$U_j^{(k)}$

j \ k	1	2
1	-0.33582	-0.08243
2	+5.00000	+1.86210
3		-0.46552

$C_j^{(k)}$

j \ k	1	2
1	-0.04030	-0.02132
2	+1.00000	+0.67713
3		+0.04232

$X_j^{(k)}$

j \ k	0	1	2
1	+0.33856	-0.11445	-0.04173
2		+3.84002	+1.69622
3			-11.79578
4			-0.09344
5			+1.81471
6			+1.20981
7			-0.16319

$T_j^{(k)}$

j \ k	0	1	2
1	+0.20000	+0.08507	+0.01716
2	+0.80000	-2.26841	-0.60600
3		+0.37806	+4.28808
4			+0.11520
5			-1.07201
6			+2.85871
7			+0.21440

TABLE 3.4. - NUMERICAL INTEGRATION OF EQUATION FOR SHOCK PATH FOR $U = -0.63481$, $C = 1.05801$, $\overline{U} = -1.36458$, $\overline{C} = 0.90972$, AND $\overline{X} = 0.83000$

β	First order			Second order		
	α	x	t	α	x	t
0	2.69884	0.83000	2.22018	2.72931	0.82999	2.24933
2	4.79665	.86977	4.29379	4.77498	.85655	4.27834
4	6.93161	.92103	6.39908	6.86908	.89706	6.34890
6	9.11598	.97238	8.55485	9.01770	.93749	8.47476
8	11.28114	1.01771	10.69487	11.14585	.97184	10.58363
10	13.42907	1.05779	12.82069	13.25611	1.00099	12.67757
12	15.56156	1.09326	14.93369	15.35078	1.02574	14.75841
14	17.68018	1.12468	17.03511	17.43191	1.04672	16.82784
16	19.78637	1.15253	19.12610	19.50134	1.06452	18.88736
18	21.88138	1.17723	21.20769	21.56065	1.07961	20.93828
20	23.96637	1.19915	23.28079	23.61126	1.09240	22.98179
22	26.04237	1.21861	25.34627	25.65440	1.10324	25.01891
24	28.11031	1.23589	27.40488	27.69113	1.11243	27.05056
26	30.17102	1.25125	29.45733	29.72238	1.12021	29.07750
28	32.22526	1.26490	31.50424	31.74895	1.12680	31.10042
30	34.27369	1.27703	33.54617	33.77152	1.13238	33.11991
32	36.31694	1.28781	35.58364	35.79069	1.13710	35.13646
34	38.35553	1.29740	37.61711	37.80696	1.14111	37.15052
36	40.38998	1.30593	39.64700	39.82077	1.14450	39.16245
38	42.42071	1.31352	41.67368	41.83247	1.14737	41.17257
40	44.44812	1.32027	43.69750	43.84240	1.14980	43.18116
42	46.47257	1.32627	45.71875	45.85081	1.15186	45.18844
44	48.49436	1.33162	47.73771	47.85795	1.15360	47.19461
46	50.51380	1.33637	49.75462	49.86399	1.15507	49.19984
48	52.53112	1.34060	51.76969	51.86911	1.15632	51.20427
50	54.54656	1.34437	53.78313	53.87345	1.15738	53.20802
52	56.56032	1.34772	55.79512	55.87712	1.15828	55.21120
54	58.57258	1.35070	57.80580	57.88023	1.15903	57.21389
56	60.58350	1.35335	59.81532	59.88287	1.15967	59.21618
58	62.59324	1.35571	61.82380	61.88510	1.16022	61.21811
60	64.60191	1.35782	63.83136	63.88699	1.16068	63.21974
62	66.60963	1.35969	65.83809	65.88859	1.16107	65.22113

TABLE 4.1. - COEFFICIENTS OF EQUATIONS (4.21) FOR

$\overline{U} = -1.36458$, $\overline{C} = 0.90972$, $U = -0.73655$, $C = 1.03533$,

$\epsilon = 0.1$, $\sigma = 5$, $E_2 = -0.000379$, $E_3 = 1.17851$, $E_4 = -0.54772$

$U_j^{(k)}$

j \ k	1	2
1	-0.38128	-0.08870
2	+1.17851	-0.19741
3		-0.35031
4		-0.44777

$C_j^{(k)}$

j \ k	1	2
1	+0.05425	+0.02808
2	+0.23570	-0.02415
3		+0.02377
4		+0.17869

$X_j^{(k)}$

j \ k	0	1	2
1	-0.25567	+0.15729	+0.05741
2		+0.87534	-0.74701
3		+0.12466	-0.08608
4		+1.03554	-0.01701
5			-0.32413
6			-0.15189
7			+0.48854
8			+0.50493

$T_j^{(k)}$

j \ k	0	1	2
1	+0.14429	-0.10307	-0.02171
2	-0.85571	-0.41724	-0.26610
3		-0.58443	+0.31446
4			-0.05693
5			+0.14965
6			-0.09983
7			+0.16785
8			-0.28497

TABLE 4.2. - SERIES SOLUTION FOR FLOW FIELD BEHIND

"EXPONENTIAL" SHOCK PATH

Initial Shock Mach Number = 1.5

B = 3.5, b = 0.2, ϵ = 0.1, σ = 5

β	x = -0.5				x = -1.0			
	α	t	-u	c	α	t	-u	c
0	-1.77450	-1.48721	0.67168	1.04407	-3.31655	-2.73255	0.61985	1.05022
1	-.73179	-.44361	.66077	1.04624	-2.23927	-1.65384	.61071	1.05200
2	.26073	.55106	.65302	1.04780	-1.22390	-.63541	.60419	1.05329
3	1.21853	1.51527	.64778	1.04887	-.24771	.34441	.59975	1.05418
4	2.15378	2.46068	.64443	1.04958	.70227	1.29955	.59692	1.05476
5	3.07584	3.39503	.64245	1.05002	1.63276	2.23926	.59529	1.05511
6	3.99107	4.32366	.64144	1.05026	2.55195	3.17023	.59449	1.05529
7	4.90392	5.25029	.64109	1.05037	3.46574	4.09718	.59428	1.05537
8	5.81751	6.17755	.64118	1.05039	4.37825	5.02342	.59444	1.05536
9	6.73401	7.10728	.64155	1.05036	5.29235	5.95130	.59484	1.05531
10	7.65486	8.04069	.64208	1.05028	6.21002	6.88238	.59538	1.05523
11	8.58100	8.97857	.64269	1.05019	7.13254	7.81769	.59599	1.05513
12	9.51292	9.92135	.64334	1.05009	8.06064	8.75781	.59662	1.05502
13	10.45084	10.86920	.64398	1.04998	8.99477	9.70307	.59725	1.05492
14	11.39474	11.82209	.64459	1.04988	9.93498	10.65348	.59784	1.05482
15	12.34443	12.77988	.64517	1.04978	10.88118	11.60894	.59839	1.05472
16	13.29964	13.74232	.64570	1.04970	11.83313	13.56923	.59890	1.05463
17	14.25998	14.70908	.64618	1.04961	12.79048	13.53404	.59936	1.05455
18	15.22507	15.67984	.64661	1.04954	13.75285	14.50304	.59978	1.05448
19	16.19447	16.65423	.64700	1.04947	14.71981	15.47585	.60014	1.05442
20	17.16778	17.63189	.64734	1.04941	15.69092	16.45212	.60047	1.05436

β	x = -1.5			
	α	t	-u	c
0	-4.72877	-3.83893	0.57608	1.05470
1	-3.62947	-2.73757	.56812	1.05619
2	-2.59981	-1.70367	.56243	1.05727
3	-1.61501	-.71374	.55857	1.05801
4	-.65878	.24769	.55610	1.05850
5	.27966	1.19117	.55467	1.05879
6	1.20404	2.12365	.55401	1.05893
7	2.11984	3.05046	.55387	1.05898
8	3.03222	3.97549	.55408	1.05895
9	3.94477	4.90146	.55451	1.05889
10	4.85995	5.83024	.55507	1.05880
11	5.77943	6.76306	.55568	1.05869
12	6.70423	7.70066	.55632	1.05858
13	7.63492	8.64340	.55693	1.05847
14	8.57172	9.59142	.55752	1.05836
15	9.51464	10.54464	.55807	1.05826
16	10.46348	11.50285	.55858	1.05817
17	11.41795	12.46577	.55903	1.05809
18	12.37766	13.43305	.55944	1.05801
19	13.34221	14.40433	.55981	1.05794
20	14.31115	15.37922	.56013	1.05788

TABLE 4.3. - SERIES SOLUTION FOR FLOW FIELD BEHIND

"EXPONENTIAL" SHOCK PATH

Initial Shock Mach Number = 1.5

B = 3.5, b = 0.1, ϵ = 0.1, σ = 5

β	x = -0.5				x = -2.0			
	α	t	-u	c	α	t	-u	c
0	-1.77449	-1.48721	0.67168	1.04407	-6.06210	-4.85682	0.53801	1.05789
2	.23813	.52627	.66604	1.04520	-4.01271	-2.80519	.53436	1.05854
4	2.20876	2.50203	.66169	1.04609	-2.01305	-.80075	.53157	1.05905
6	4.15117	4.45427	.65841	1.04678	-.04556	1.17249	.52949	1.05943
8	6.07667	6.39225	.65596	1.04731	1.89872	3.12480	.52800	1.05971
10	7.99307	8.32244	.65414	1.04771	3.82618	5.06339	.52697	1.05990
12	9.90582	10.24450	.65281	1.04802	5.74448	6.99577	.52630	1.06003
14	11.81868	12.17613	.65183	1.04826	7.65907	8.92565	.52587	1.06010
16	13.73423	14.10994	.65112	1.04844	9.57373	10.85190	.52562	1.06014
18	15.65416	16.03016	.65060	1.04858	11.49103	12.78483	.52550	1.06016
20	17.57950	17.97560	.65023	1.04869	13.41267	14.72463	.52546	1.06016
22	19.51081	19.91099	.64996	1.04877	15.33968	16.66934	.52548	1.06015
24	21.44832	21.86816	.64977	1.04883	17.27261	18.60309	.52554	1.06013
26	23.39199	23.81679	.64963	1.04888	19.21165	20.55725	.52562	1.06011
28	25.34159	25.77517	.64954	1.04892	21.15676	22.51121	.52571	1.06009
30	27.29682	27.74060	.64948	1.04895	23.10771	24.47308	.52580	1.06006
32	29.25727	29.70976	.64944	1.04897	25.06418	26.44001	.52590	1.06004
34	31.22253	31.67907	.64942	1.04898	27.02577	28.40870	.52599	1.06002
36	33.19213	33.65483	.64941	1.04899	28.99205	30.38558	.52607	1.05999
38	35.16565	35.63334	.64941	1.04900	30.96258	32.35703	.52616	1.05998
40	37.14270	37.61138	.64941	1.04901	32.93693	34.33950	.52623	1.05996

TABLE 4.4. - COEFFICIENTS OF EQUATIONS (4.21) FOR

$\overline{U} = -1.29987$, $\overline{C} = 0.92848$, $U = -0.77119$, $C = 1.03421$

$\epsilon = 0.1$, $\sigma = 5$, $E_2 = -0.04598$, $E_3 = 1.24223$, $E_4 = -0.77151$

$U_j^{(k)}$

j \ k	1	2
1	-0.39879	-0.09164
2	+1.24226	-0.20130
3		-0.57021
4		-0.47708

$C_j^{(k)}$

j \ k	1	2
1	+0.05947	+0.03075
2	+0.24845	-0.02711
3		-0.01887
4		+0.19576

$X_j^{(k)}$

j \ k	0	1	2
1	-0.22958	+0.17262	+0.06301
2		+0.88891	-0.85824
3		+0.11109	-0.08957
4		+1.13569	-0.01363
5			-0.53452
6			+0.16612
7			+0.54863
8			+0.54956

$T_j^{(k)}$

j \ k	0	1	2
1	+0.12716	-0.10815	-0.02299
2	-0.87284	-0.42236	-0.30224
3		-0.62905	+0.36264
4			-0.05181
5			+0.07735
6			-0.10428
7			+0.18565
8			-0.30440

TABLE 4.5. - SERIES SOLUTION FOR FLOW FIELD BEHIND "EXPONENTIAL" SHOCK PATH

Initial Shock Mach Number = 1.4

B = 3.0, b = 0.1, ϵ = 0.1, σ = 5

β	x = -0.5				x = -1.0			
	α	t	-u	c	α	t	-u	c
0	-1.92014	-1.63773	0.69799	1.04450	-3.53678	-2.96193	0.64161	1.05140
2	.09526	.37839	.69320	1.04545	-1.50456	-.92850	.63770	1.05215
4	2.06954	2.35679	.68953	1.04619	.48409	1.06267	.63473	1.05273
6	4.01594	4.31122	.68680	1.04675	2.44137	3.02605	.63252	1.05316
8	5.94544	6.25110	.68478	1.04717	4.37785	4.97192	.63094	1.05347
10	7.86566	8.18294	.68331	1.04749	6.30224	6.90760	.62981	1.05369
12	9.78194	10.11133	.68224	1.04772	8.22072	8.83829	.62902	1.05384
14	11.69800	12.03947	.68147	1.04789	10.13758	10.76764	.62848	1.05394
16	13.61640	13.96956	.68092	1.04801	12.05585	12.69820	.62812	1.05400
18	15.53883	15.90307	.68052	1.04810	13.97754	14.63166	.62788	1.05404
20	17.46637	17.84093	.68024	1.04816	15.90394	16.56914	.62773	1.05406
22	19.39958	19.78365	.68004	1.04821	17.83582	18.51127	.62764	1.05407
24	21.33873	21.73144	.67989	1.04824	19.77353	20.45836	.62759	1.05407
26	23.28381	23.68431	.67980	1.04827	21.71715	22.41047	.62758	1.05406
28	25.23462	25.64210	.67973	1.04828	23.66653	24.36749	.62758	1.05405
30	27.19089	27.60456	.67969	1.04829	25.62145	26.32921	.62760	1.05404
32	29.15223	29.57137	.67966	1.04830	27.58155	28.29533	.62762	1.05403
34	31.11824	31.54219	.67965	1.04831	29.54640	30.26549	.62765	1.05402
36	33.08849	33.51665	.67964	1.04831	31.51560	32.23935	.62767	1.05401
38	35.06256	35.49439	.67964	1.04831	33.48873	34.21654	.62770	1.05400
40	37.04004	37.47506	.67964	1.04831	35.46538	36.19672	.62773	1.05399

TABLE 4.6. - SERIES SOLUTION FOR FLOW FIELD BEHIND "COSINE" SHOCK PATH

Initial Shock Mach Number = 1.5

$B = 3.5$, $\omega = \pi/20$, $\epsilon = 0.1$, $\sigma = 5$

β	x = -0.5				x = -1.0			
	α	t	-u	c	α	t	-u	c
0	-1.77449	-1.48721	0.67168	1.04407	-3.31656	-2.73255	0.61985	1.05023
1	-.75764	-.47004	.66762	1.05488	-2.28658	-1.70208	.61646	1.05089
2	.24558	.53406	.66334	1.04574	-1.27007	-.68427	.61288	1.05159
3	1.23427	1.52548	.65900	1.04661	-.26692	.32079	.60923	1.05231
4	2.20861	2.50487	.65472	1.04749	.72269	1.31329	.60564	1.05303
5	3.16962	3.47304	.65063	1.04833	1.69787	2.29364	.60220	1.05372
6	4.11850	4.43099	.64684	1.04912	2.65942	3.26251	.59902	1.05436
7	5.05658	5.37981	.64344	1.04983	3.60841	4.22076	.59618	1.05495
8	5.98532	6.32066	.64053	1.05045	4.54611	5.16940	.59375	1.05545
9	6.90620	7.25476	.63817	1.05096	5.47392	6.10955	.59179	1.05586
10	7.82083	8.18342	.63638	1.05136	6.39340	7.04246	.59034	1.05617
11	8.73087	9.10800	.63522	1.05163	7.30619	7.96946	.58943	1.05637
12	9.63804	10.02992	.63468	1.05178	8.21407	8.89201	.58905	1.05647
13	10.54415	10.95066	.63475	1.05180	9.11886	9.81162	.58921	1.05646
14	11.45103	11.87178	.63542	1.05170	10.02260	10.72999	.58988	1.05636
15	12.36060	12.79489	.63665	1.05149	10.92722	11.64877	.59103	1.05616
16	13.27477	13.72163	.63840	1.05117	11.83482	12.56975	.59262	1.05587
17	14.19551	14.65369	.64062	1.05075	12.74750	13.49473	.59461	1.05550
18	15.12478	15.59276	.64324	1.05025	13.66733	14.42555	.59694	1.05506
19	16.06438	16.54044	.64622	1.04968	14.59633	15.36399	.59955	1.05457
20	17.01610	17.49829	.64947	1.04905	15.53644	16.31174	.60239	1.05403

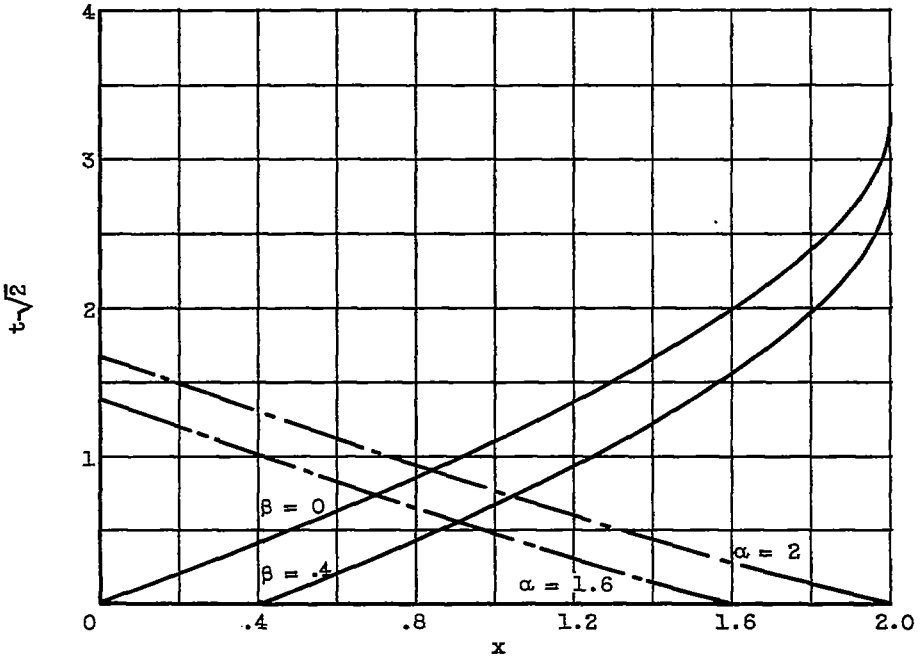

Figure 2.1. - Characteristics of steady duct flow. $A = e^{-b(x-2)}$, $b = 1$, $\sigma = 1$.

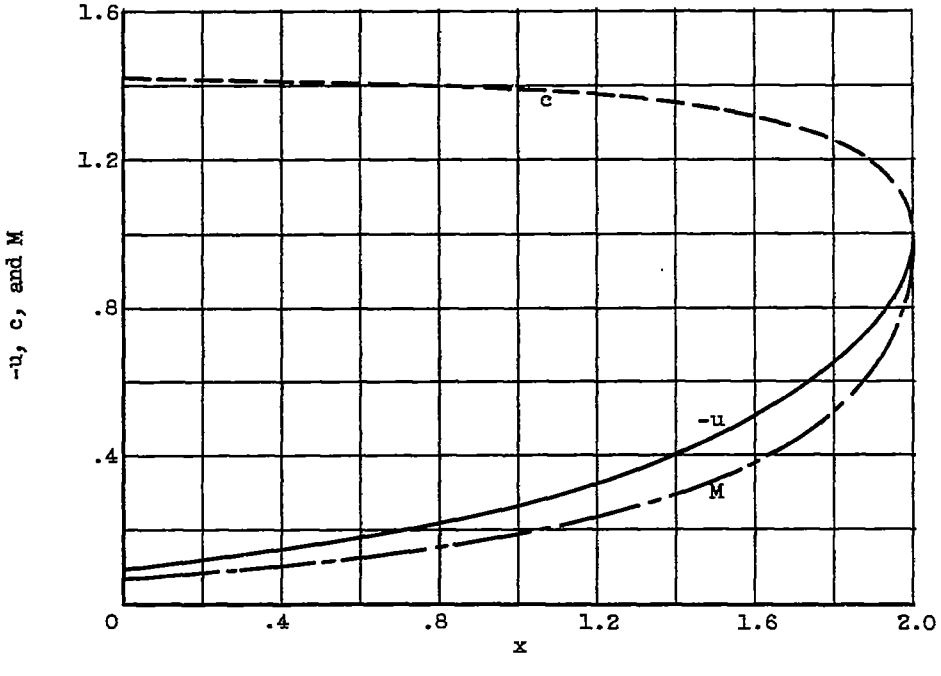

Figure 2.2 - Variation of flow parameters with x. $A = e^{-b(x-2)}$, $b = 1$, $\sigma = 1$.

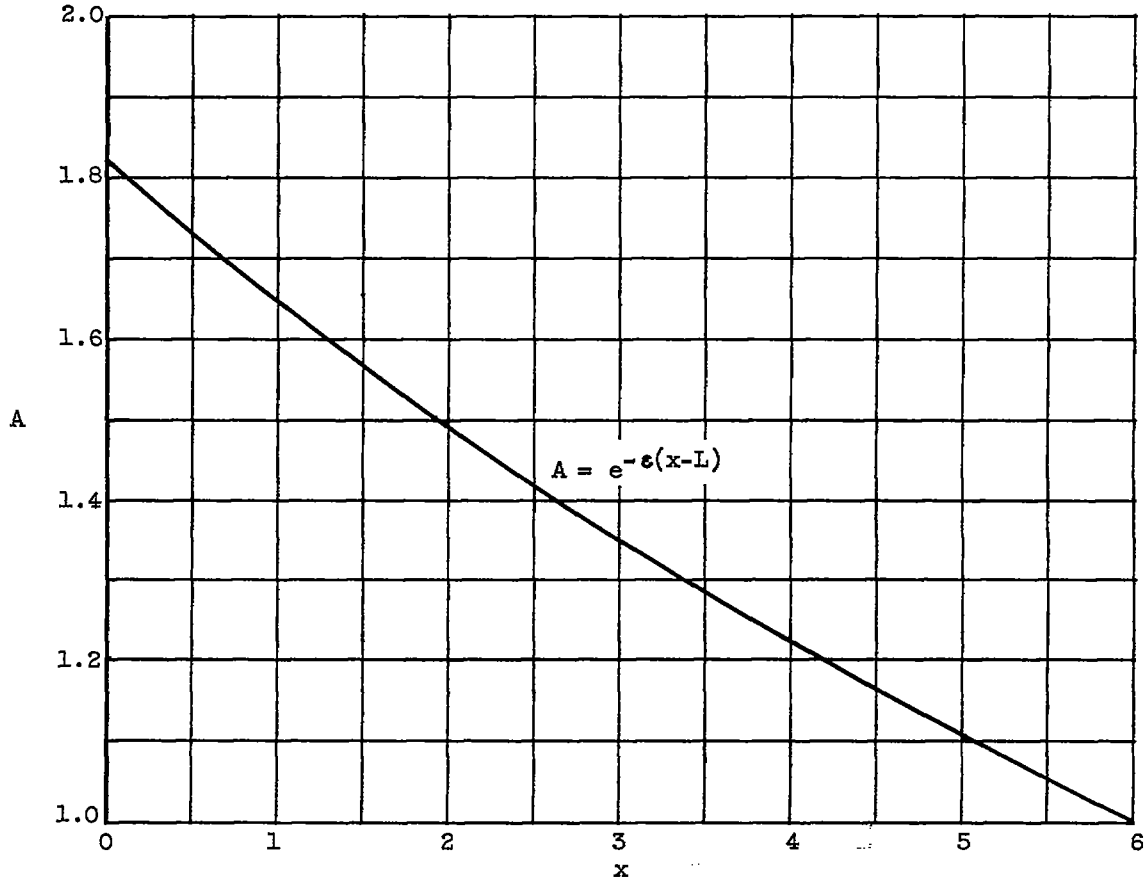

Figure 2.3. - Area variation for "epsilon duct"; $\varepsilon = 0.1$, $L = 6$.

5239

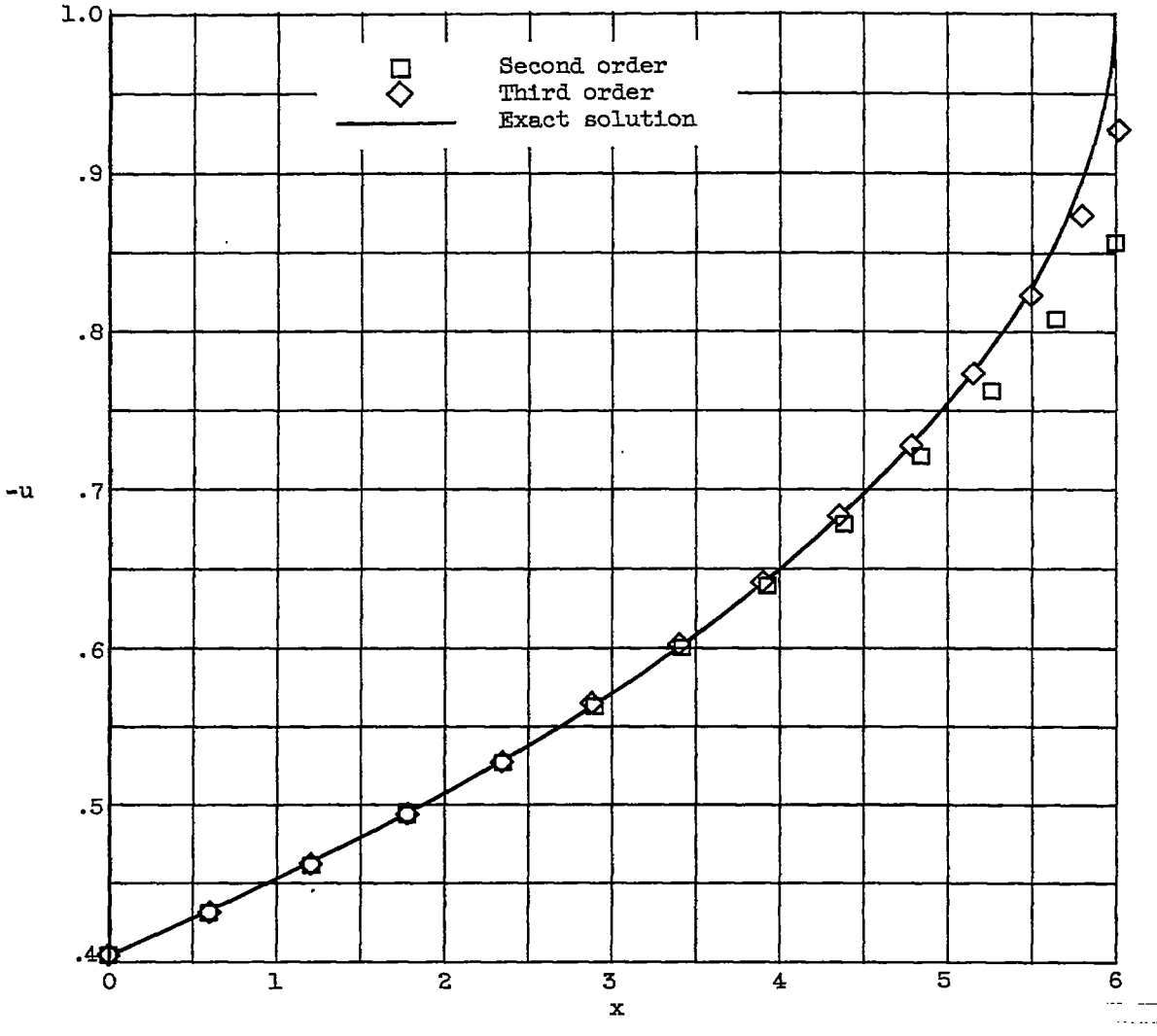

Figure 2.4. - Particle velocity as a function of x. Subsonic flow specified on x = 0. "Epsilon duct": $\varepsilon = 0.1$, $L = 6$, $\sigma = 1$.

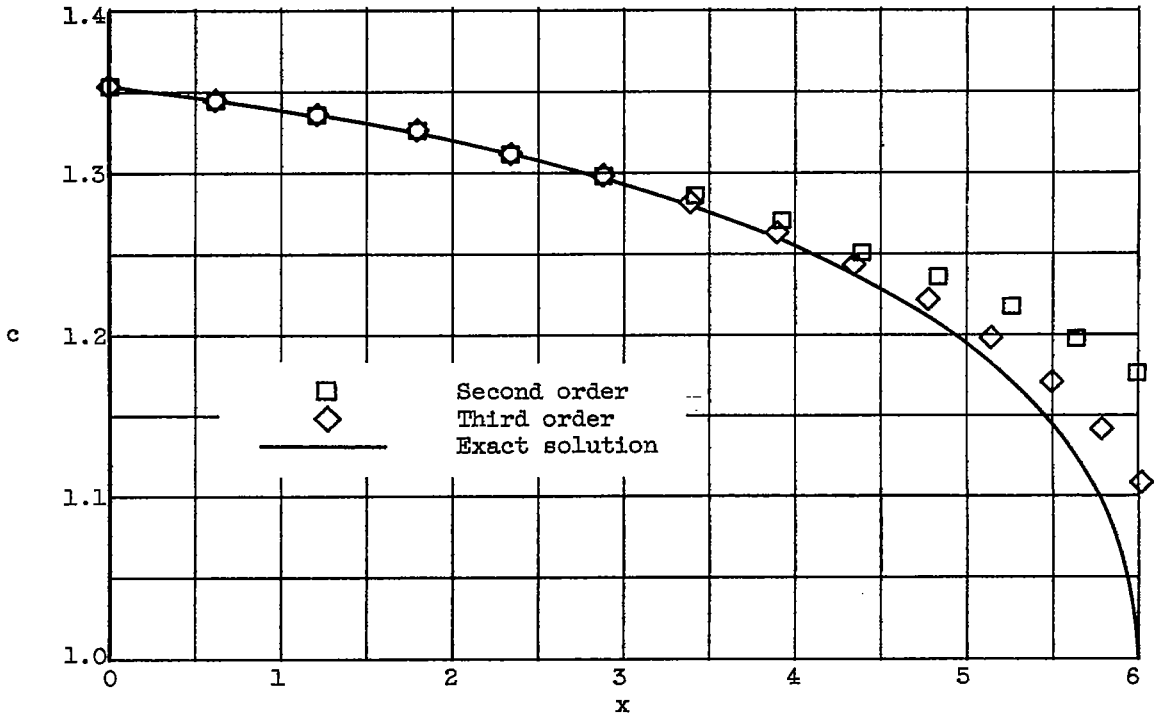

Figure 2.5. - Sonic speed as a function of x. Subsonic flow specified on x = 0. "Epsilon duct": $\varepsilon = 0.1$, L = 6, $\sigma = 1$.

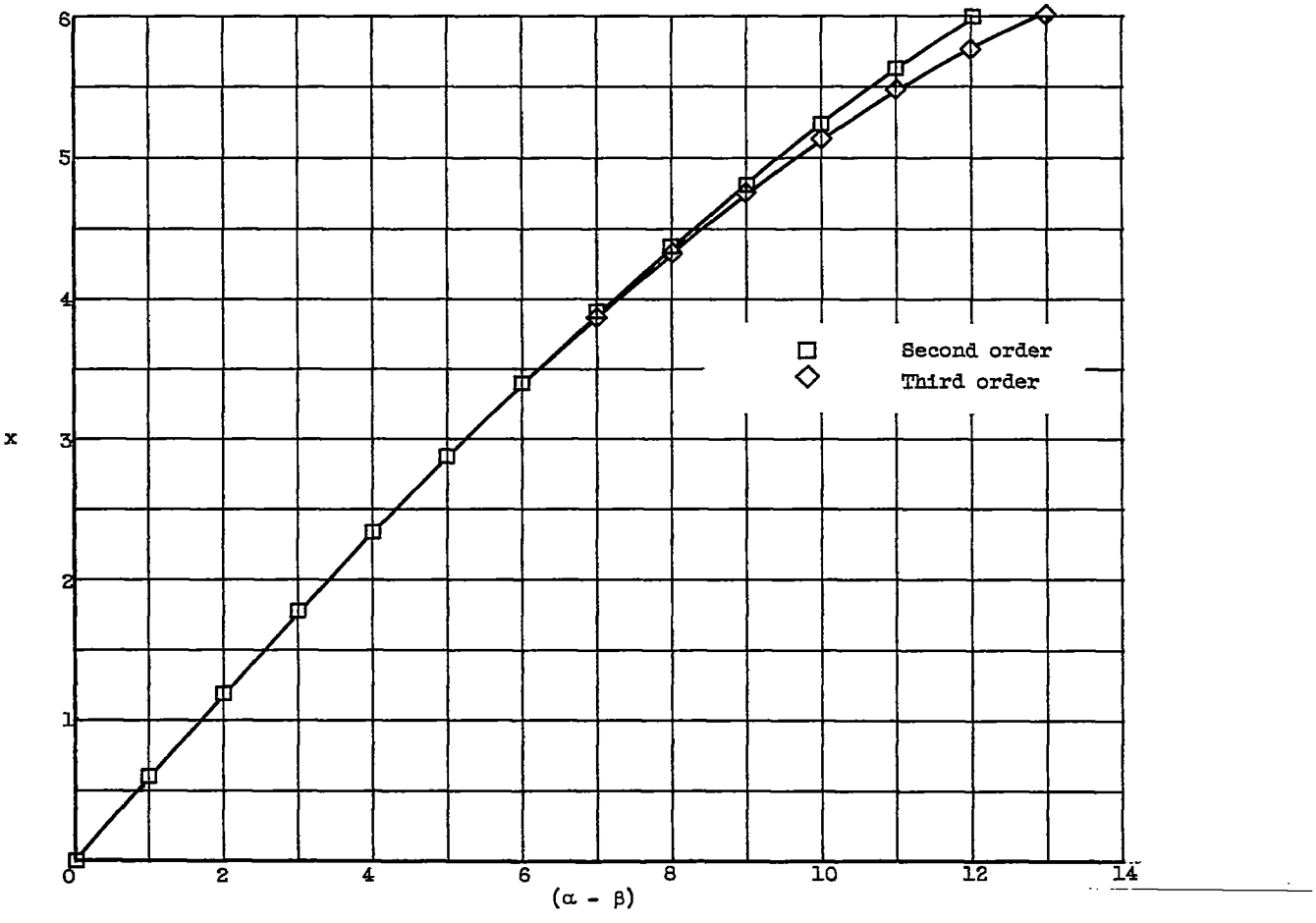

Figure 2.6. - x as a function of $(\alpha - \beta)$. Subsonic flow specified on $x = 0$. "Epsilon duct": $\varepsilon = 0.1$, $L = 6$, $\sigma = 1$.

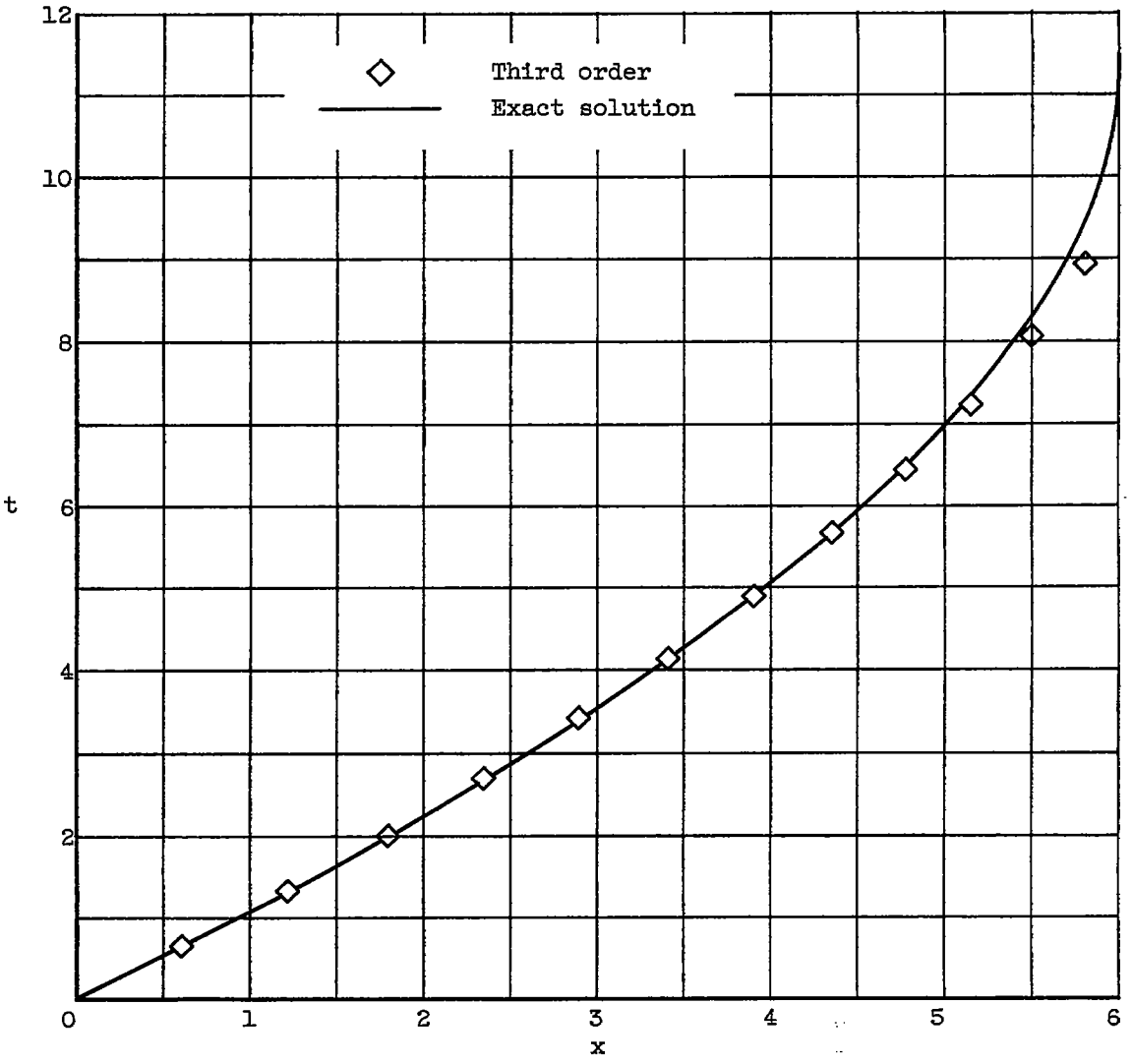

Figure 2.7. - $\beta = 0$ Characteristic. Subsonic flow specified on $x = 0$. "Epsilon duct": $\varepsilon = 0.1$, $L = 6$, $\sigma = 1$.

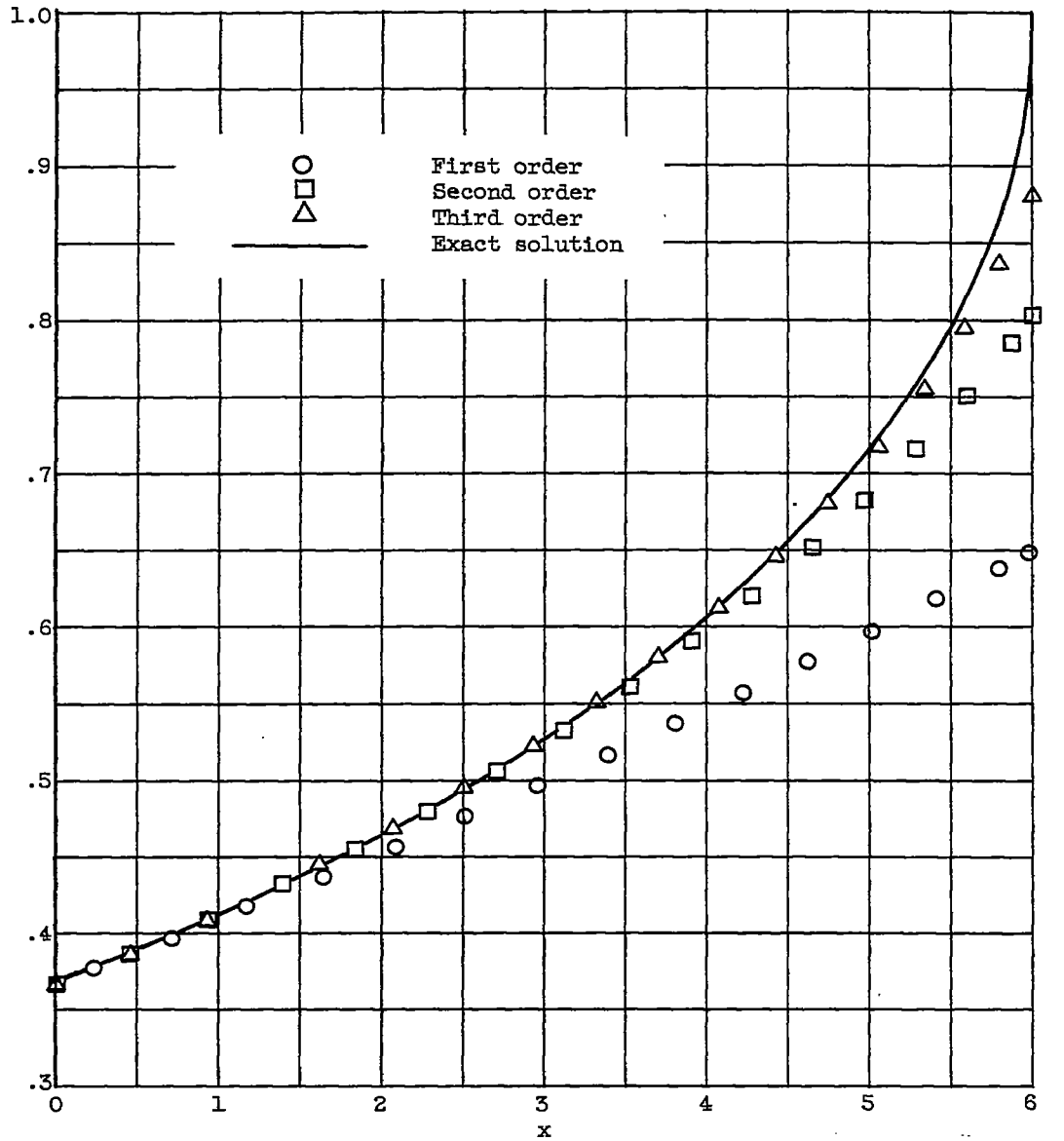

(a) Particle velocity.

Figure 2.8. - Flow variables as a function of x. Subsonic flow specified on x = 0. "Epsilon duct": $\varepsilon = 0.1$, L = 6, $\sigma = 5$.

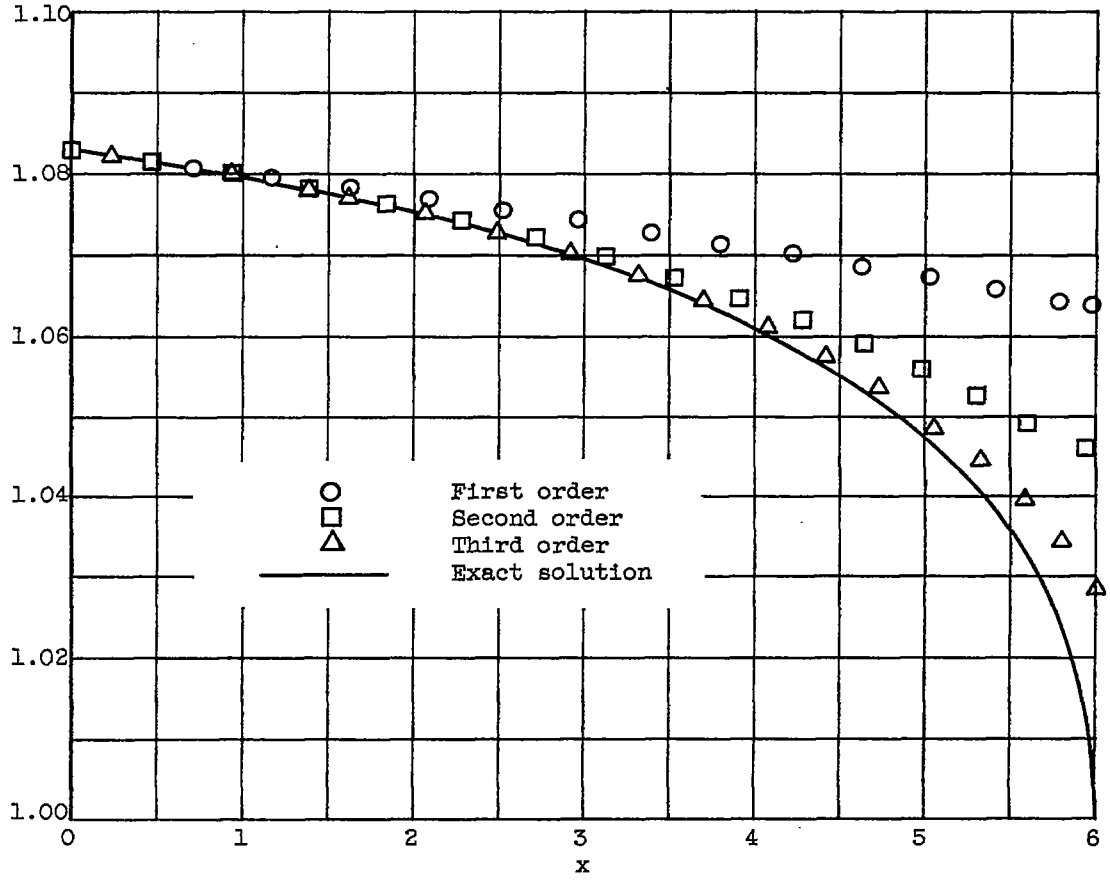

(b) Sonic speed.

Figure 2.8. - Concluded. Flow variables as a function of x. Subsonic flow specified on x = 0. "Epsilon duct": $\varepsilon = 0.1$, L = 6, $\sigma = 5$.

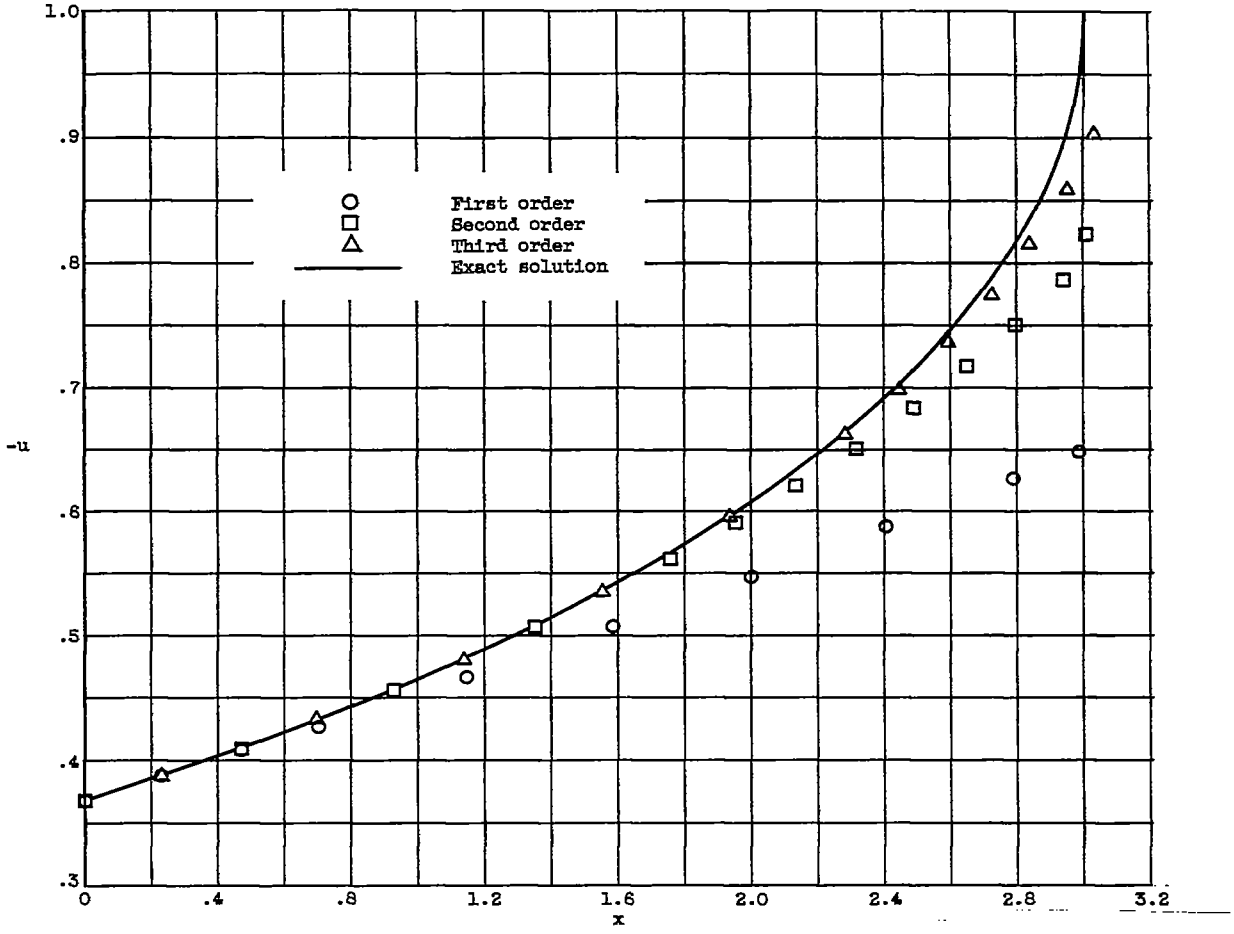

(a) Particle velocity.

Figure 2.9. - Flow variables as a function of x. Subsonic flow specified on x = 0. "Epsilon duct": $\epsilon = 0.2$, $L = 3$, $\sigma = 5$.

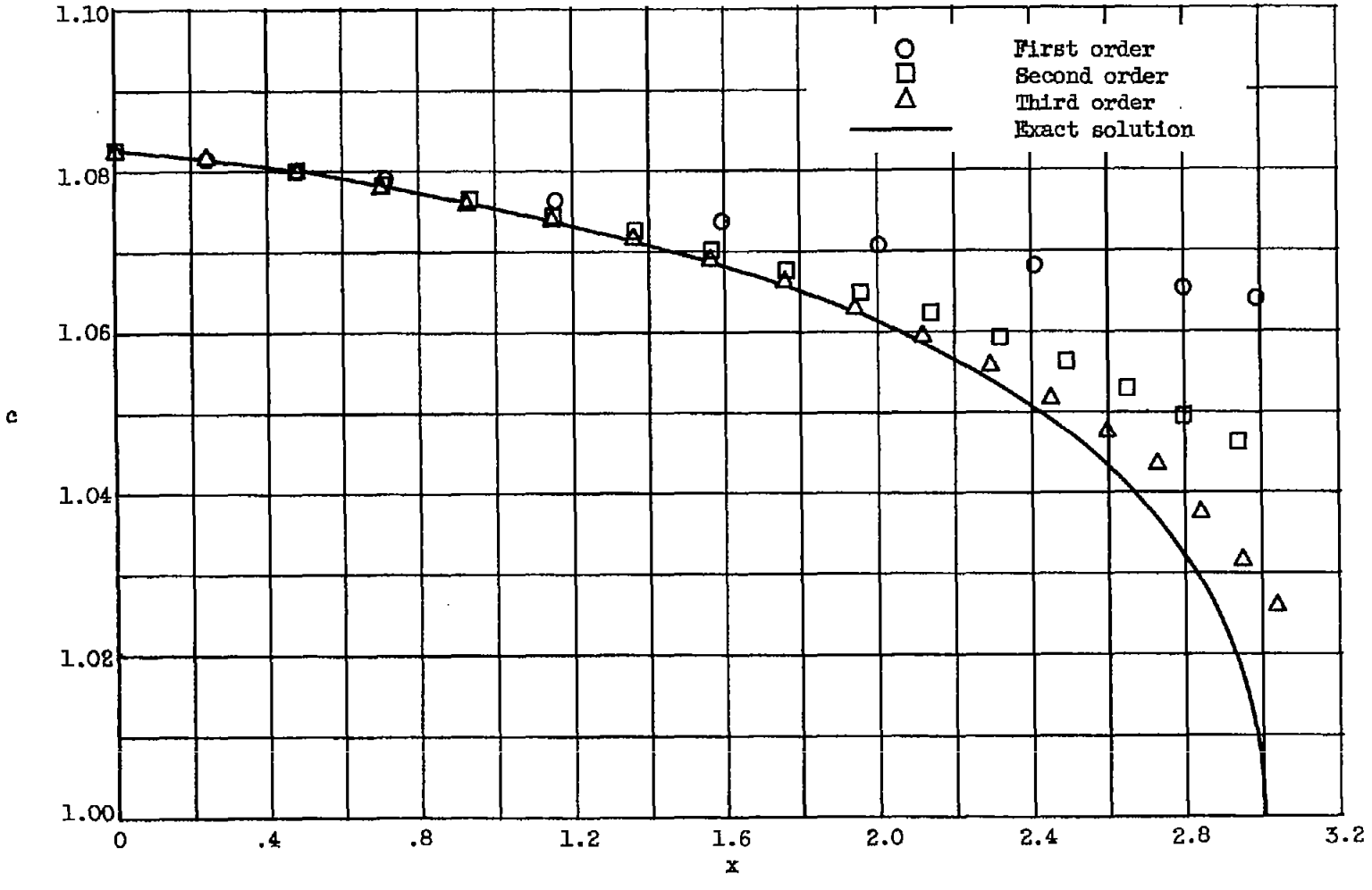

(b) Sonic speed.

Figure 2.9. - Concluded. Flow variables as a function of x. Subsonic flow specified on x = 0. "Epsilon duct": $\varepsilon = 0.2$, L = 3, $\sigma = 5$.

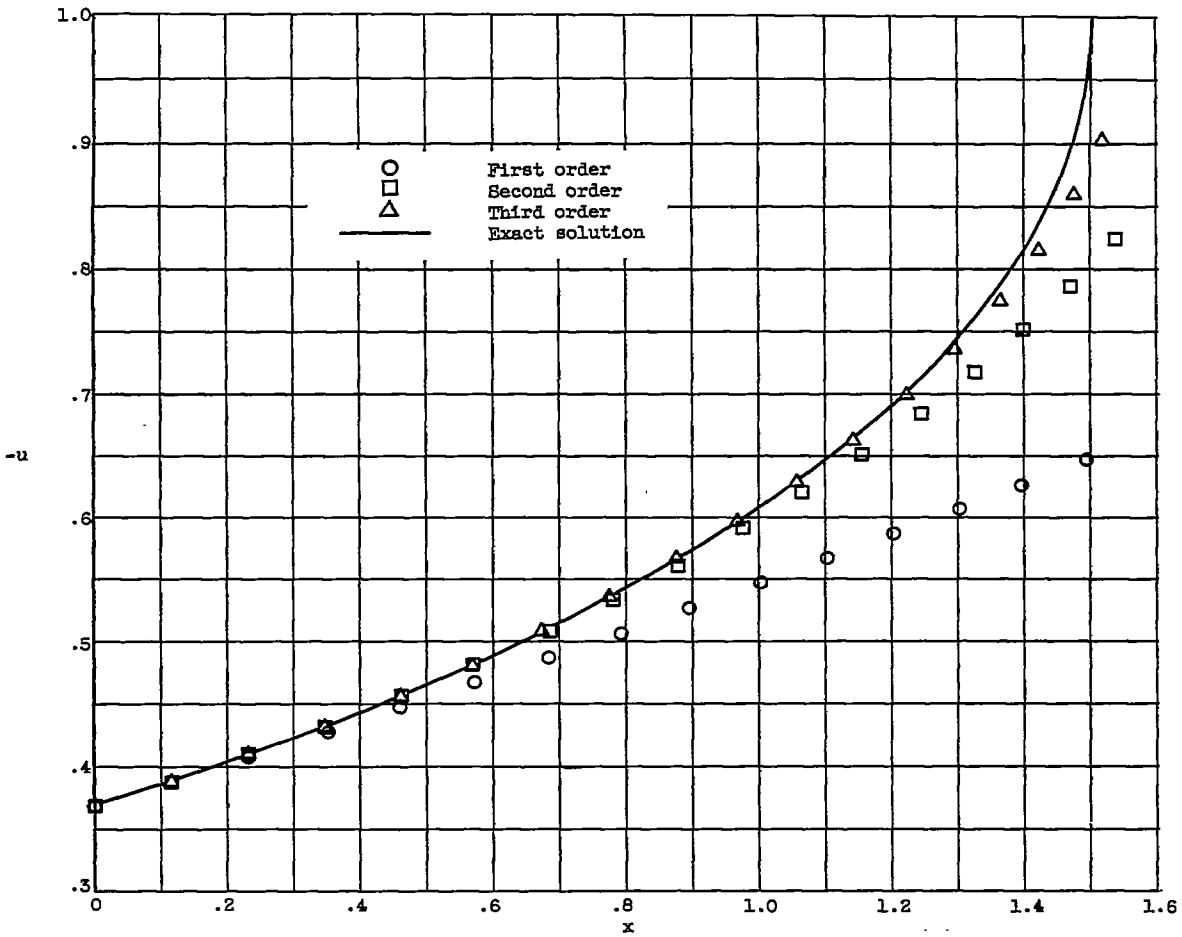

(a) Particle velocity.

Figure 2.10. - Flow variables as a function of x. Subsonic flow specified on x = 0. "Epsilon duct": $\varepsilon = 0.4$, $L = 1.5$, $\sigma = 5$.

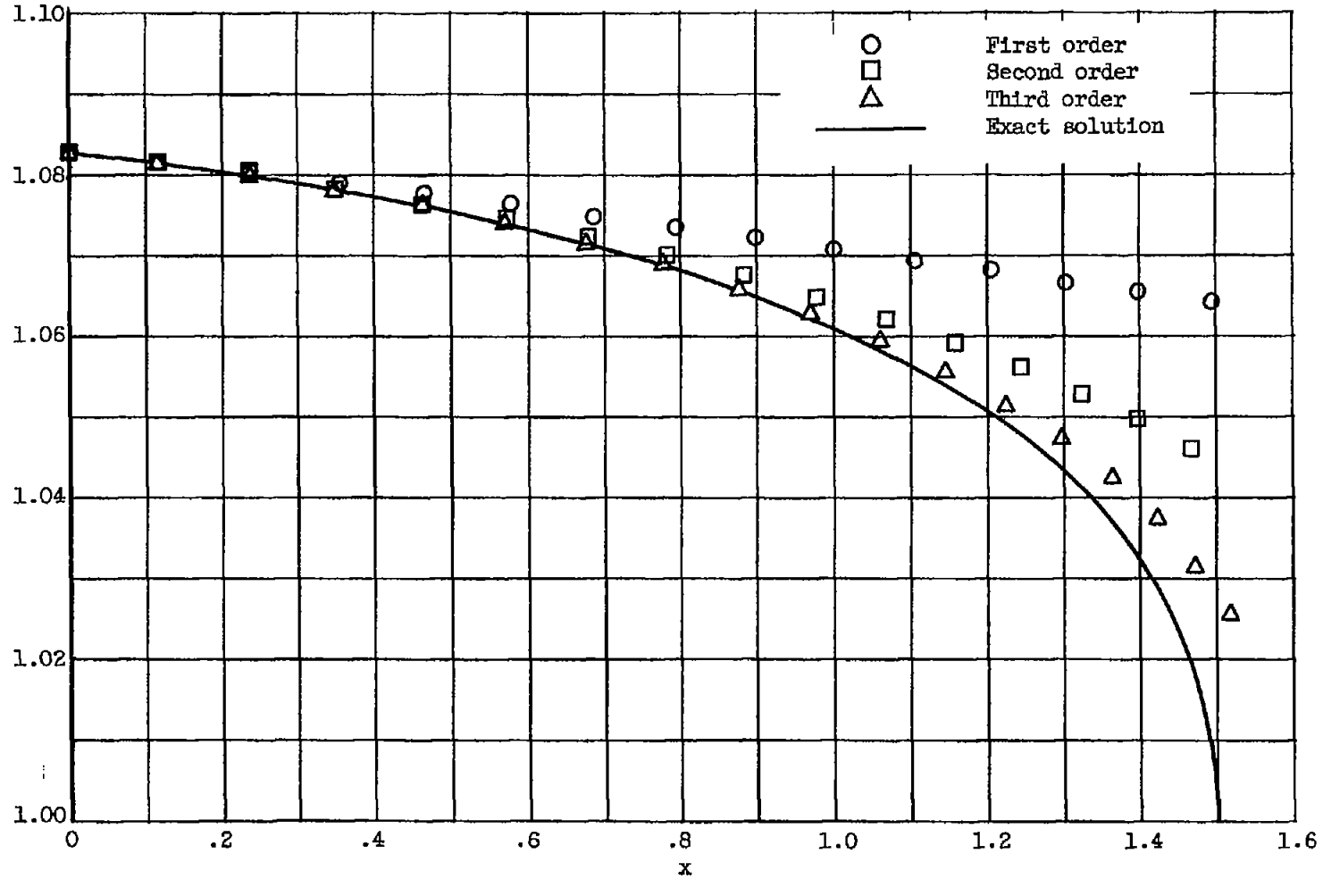

(b) Sonic speed.

Figure 2.10. - Concluded. Flow variables as a function of x. Subsonic flow specified on x = 0. "Epsilon duct": $\varepsilon = 0.4$, L = 1.5, $\sigma = 5$.

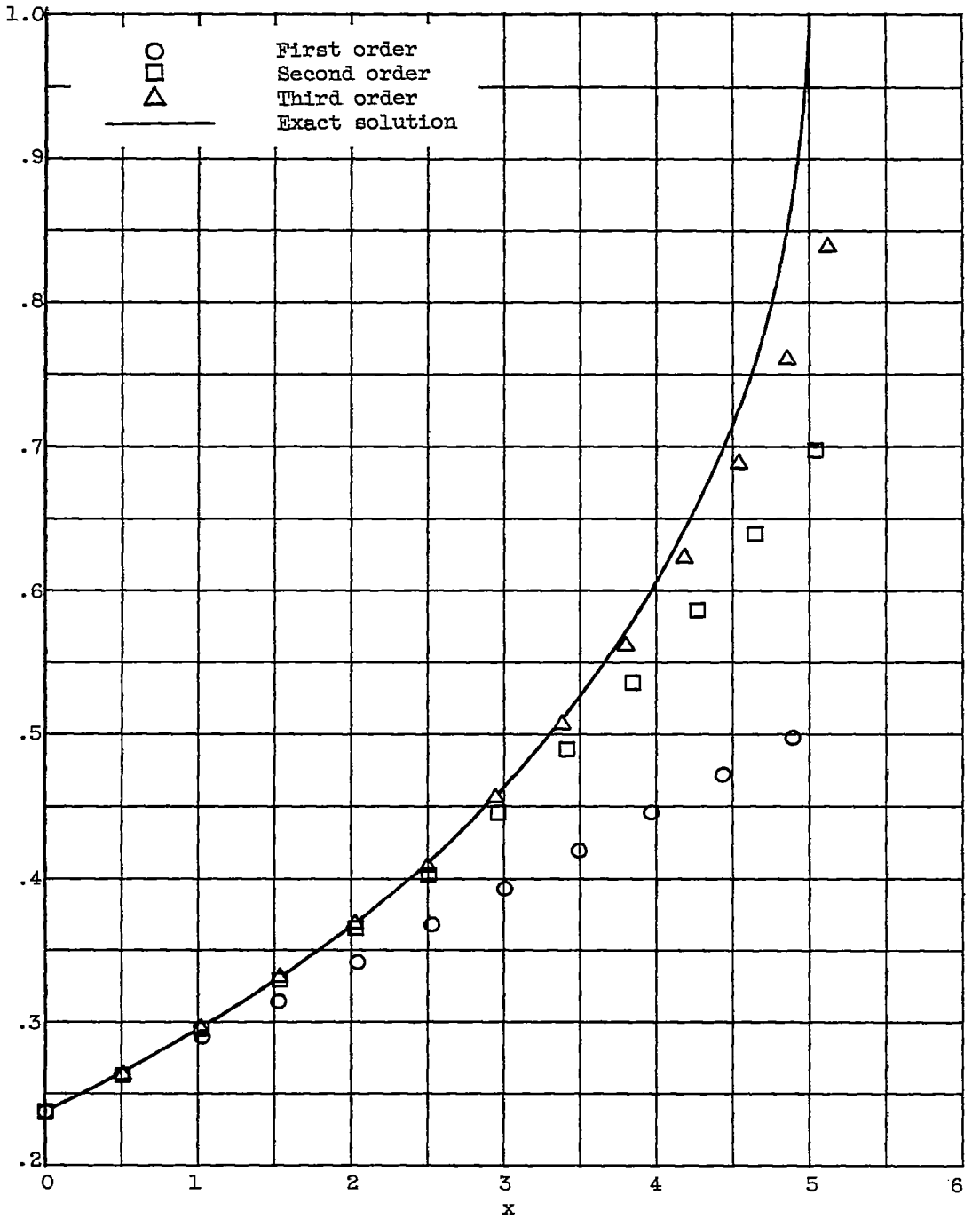

(a) Particle velocity.

Figure 2.11. - Flow variables as a function of x. Subsonic flow specified on x = 0. "Epsilon duct": $\varepsilon = 0.2$, L = 5, $\sigma = 5$.

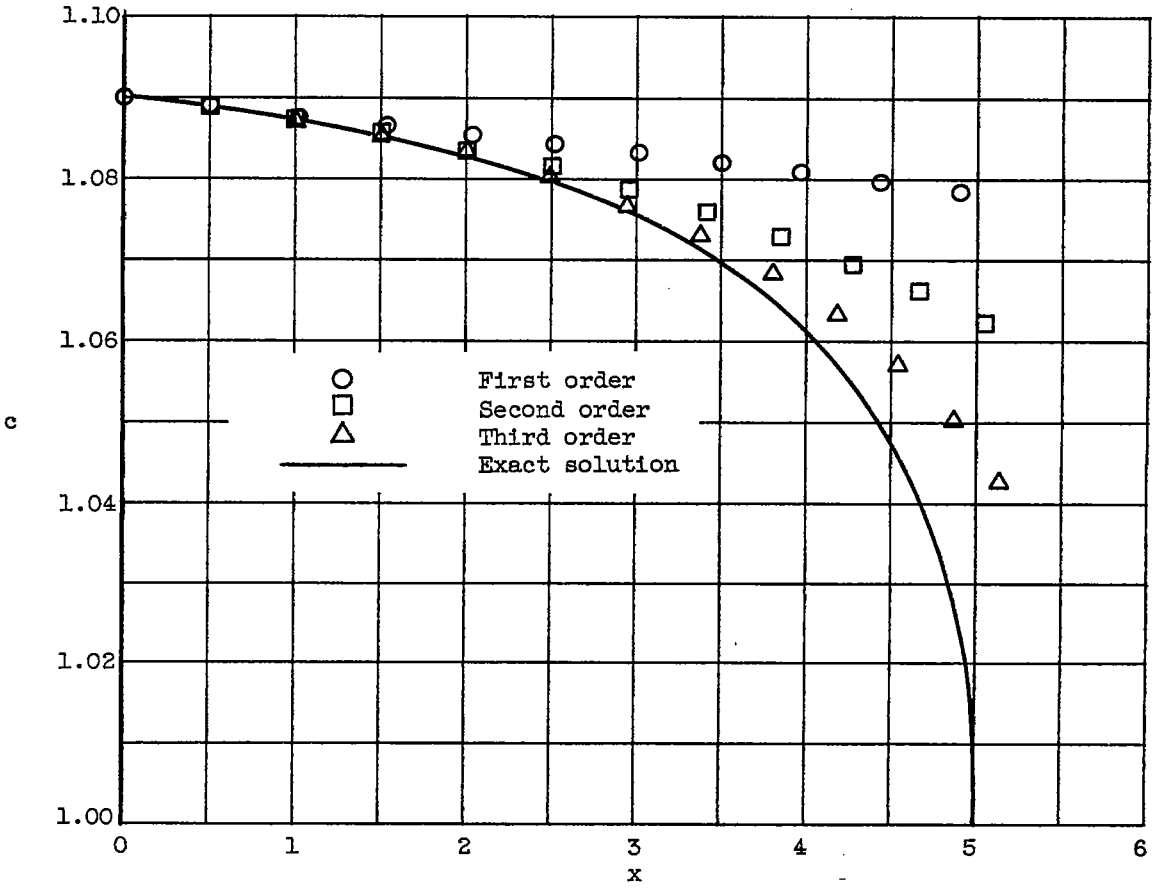

(b) Sonic speed.

Figure 2.11. - Concluded. Flow variables as a function of x. Subsonic flow specified on x = 0. "Epsilon duct": $\varepsilon = 0.2$, L = 5, $\sigma = 5$.

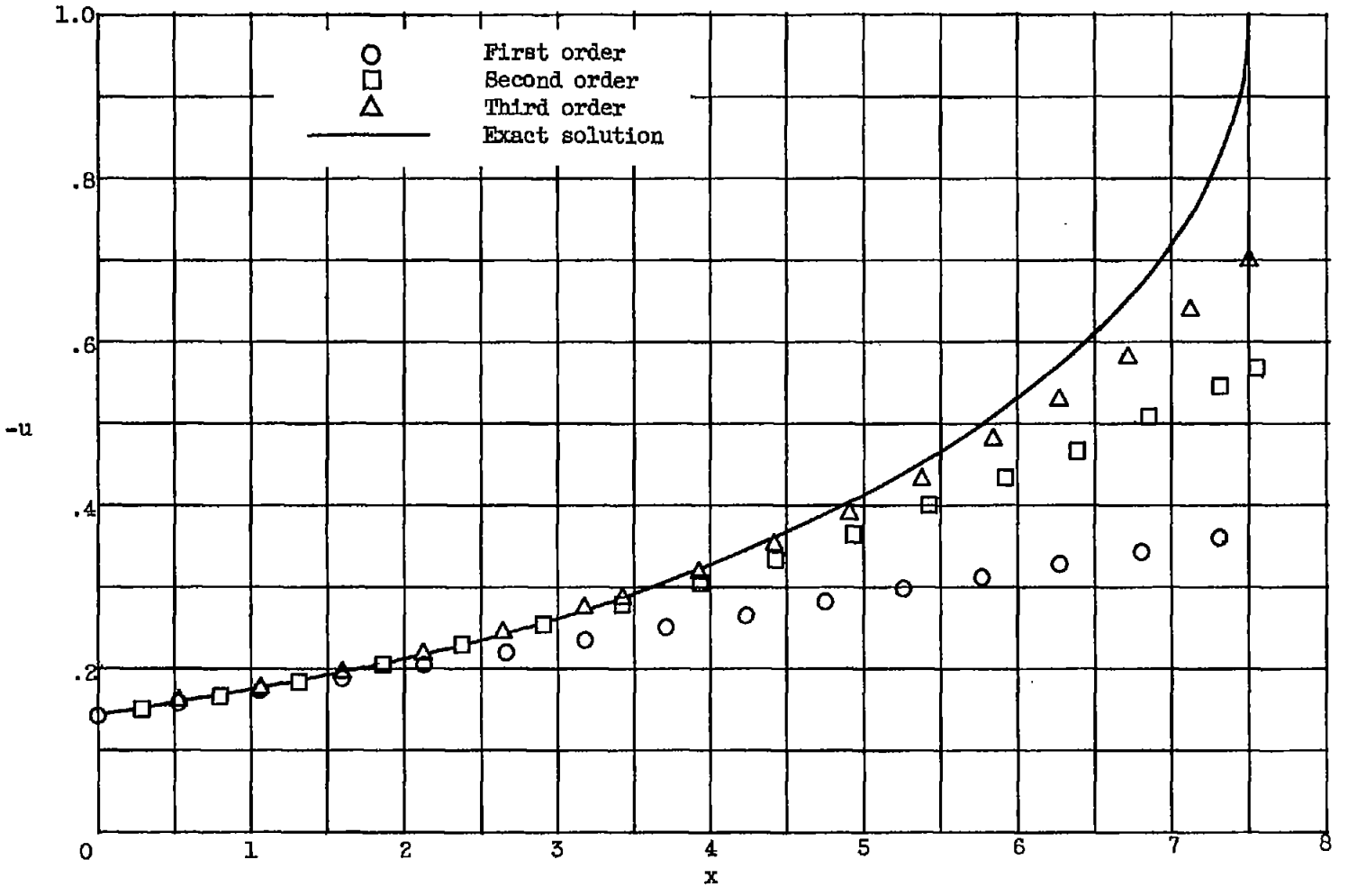

(a) Particle velocity.

Figure 2.12. - Flow variables as a function of x. Subsonic flow specified on x = 0. "Epsilon duct": $\epsilon = 0.2$, L = 7.5, $\sigma = 5$.

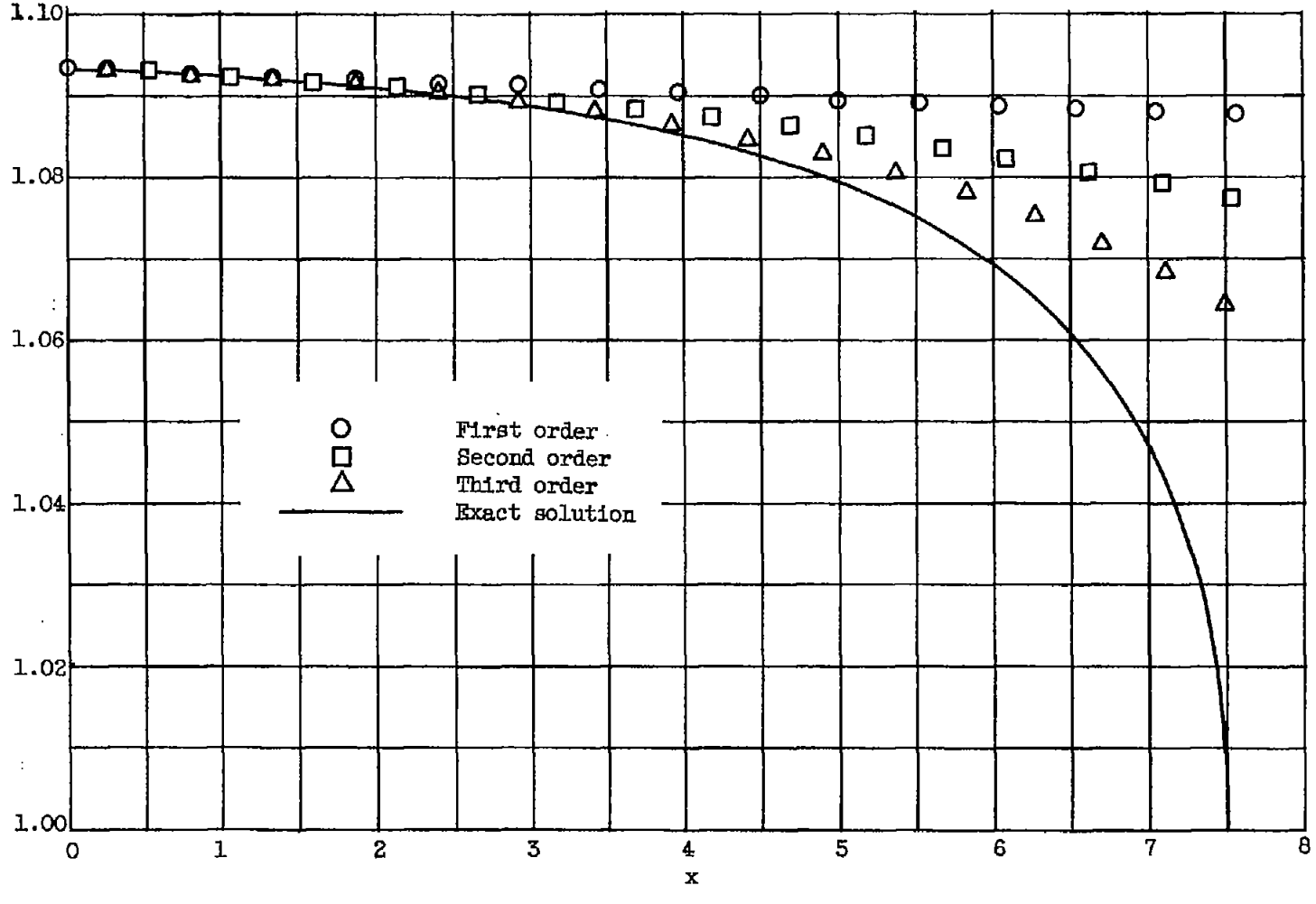

(b) Sonic speed.

Figure 2.12. - Concluded. Flow variables as a function of x. Subsonic flow specified on x = 0. "Epsilon duct": ε = 0.2, L = 7.5, σ = 5.

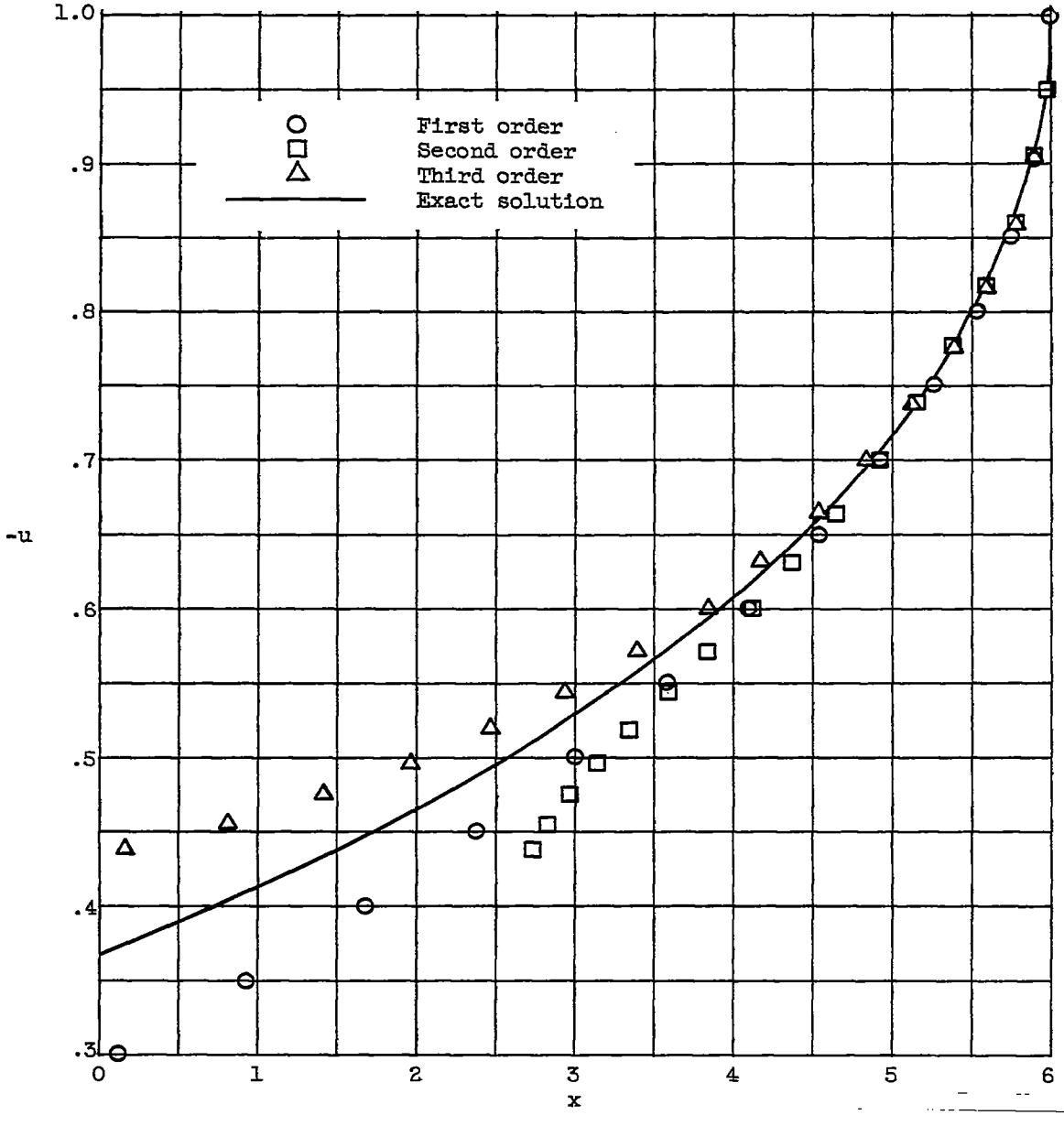

(a) Particle velocity.

Figure 2.13. - Flow variables as a function of x. Subsonic flow specified on x = L. "Epsilon duct": $\varepsilon = 0.1$, L = 6, $\sigma = 5$.

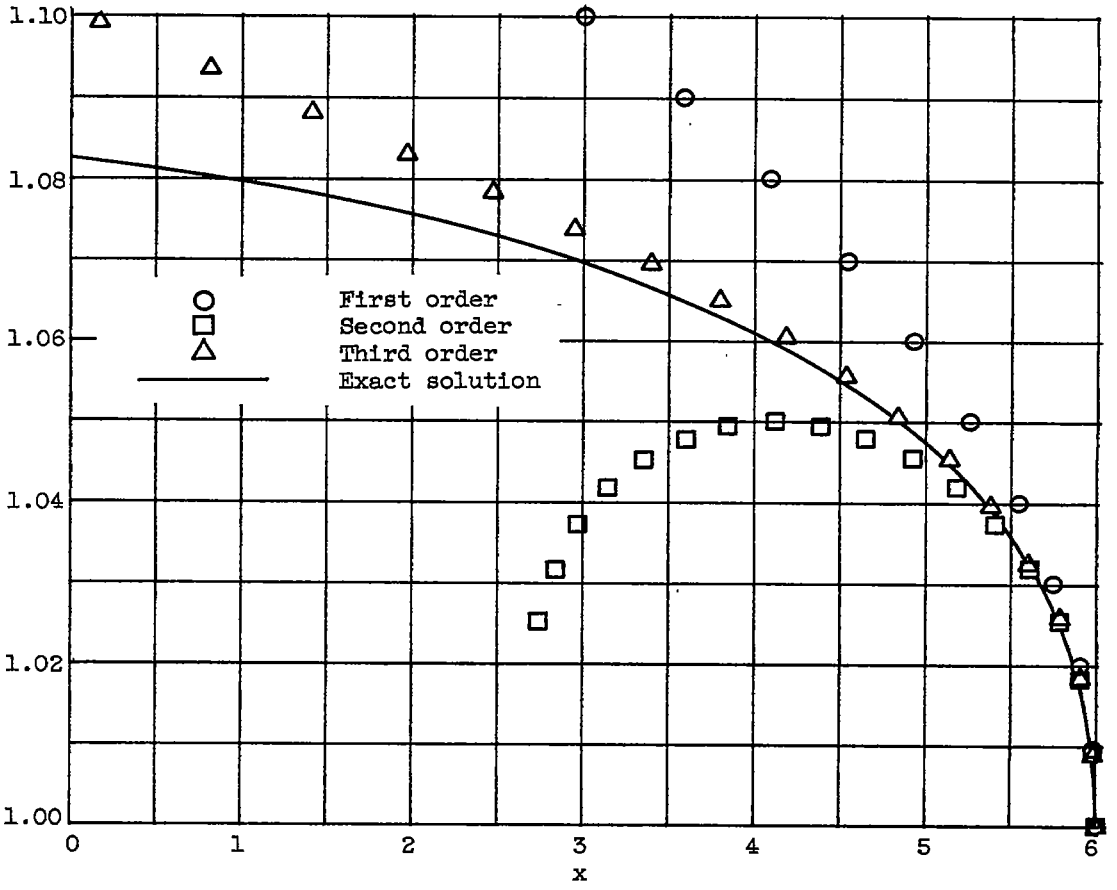

(b) Sonic speed.

Figure 2.13. - Concluded. Flow variables as a function of x. Subsonic flow specified on x = L. "Epsilon duct": $\epsilon = 0.1$, L = 6, $\sigma = 5$.

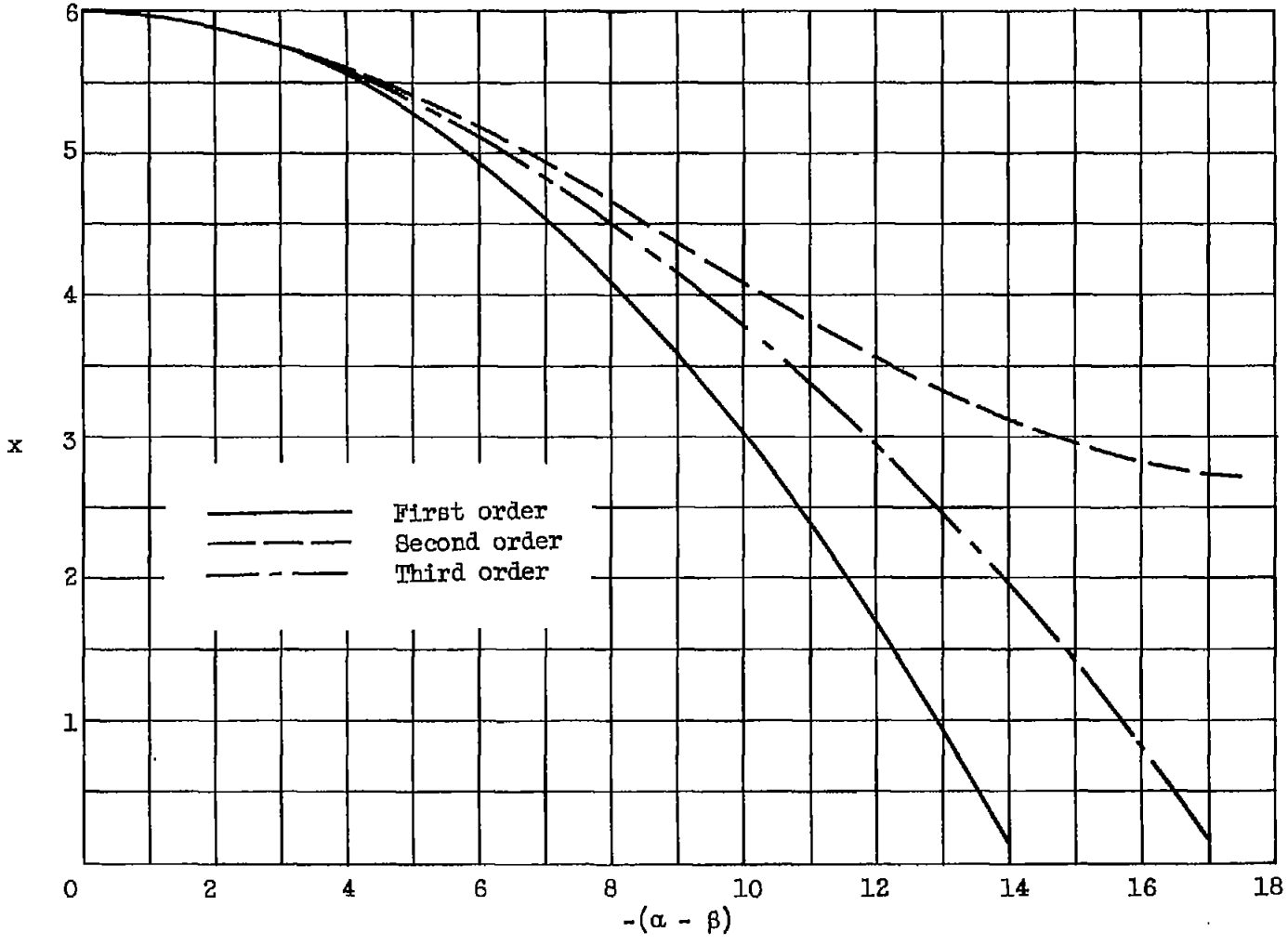

Figure 2.14. - x as a function of $(\alpha - \beta)$. Subsonic flow specified on x = L. "Epsilon duct": $\epsilon = 0.1$, L = 6, $\sigma = 5$.

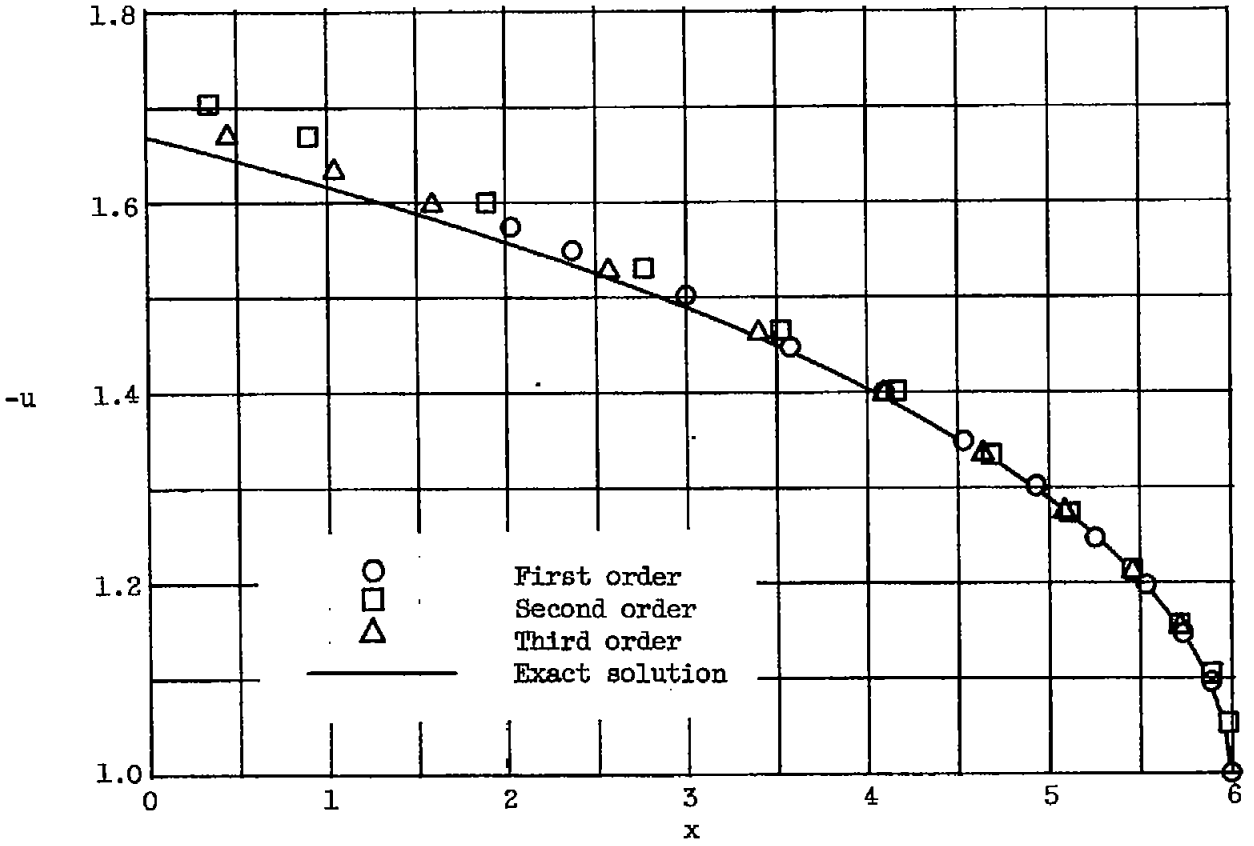

(a) Particle velocity.

Figure 2.15. - Flow variables as a function of x. Supersonic flow specified on x = L. "Epsilon duct": $\varepsilon = 0.1$, L = 6, $\sigma = 5$.

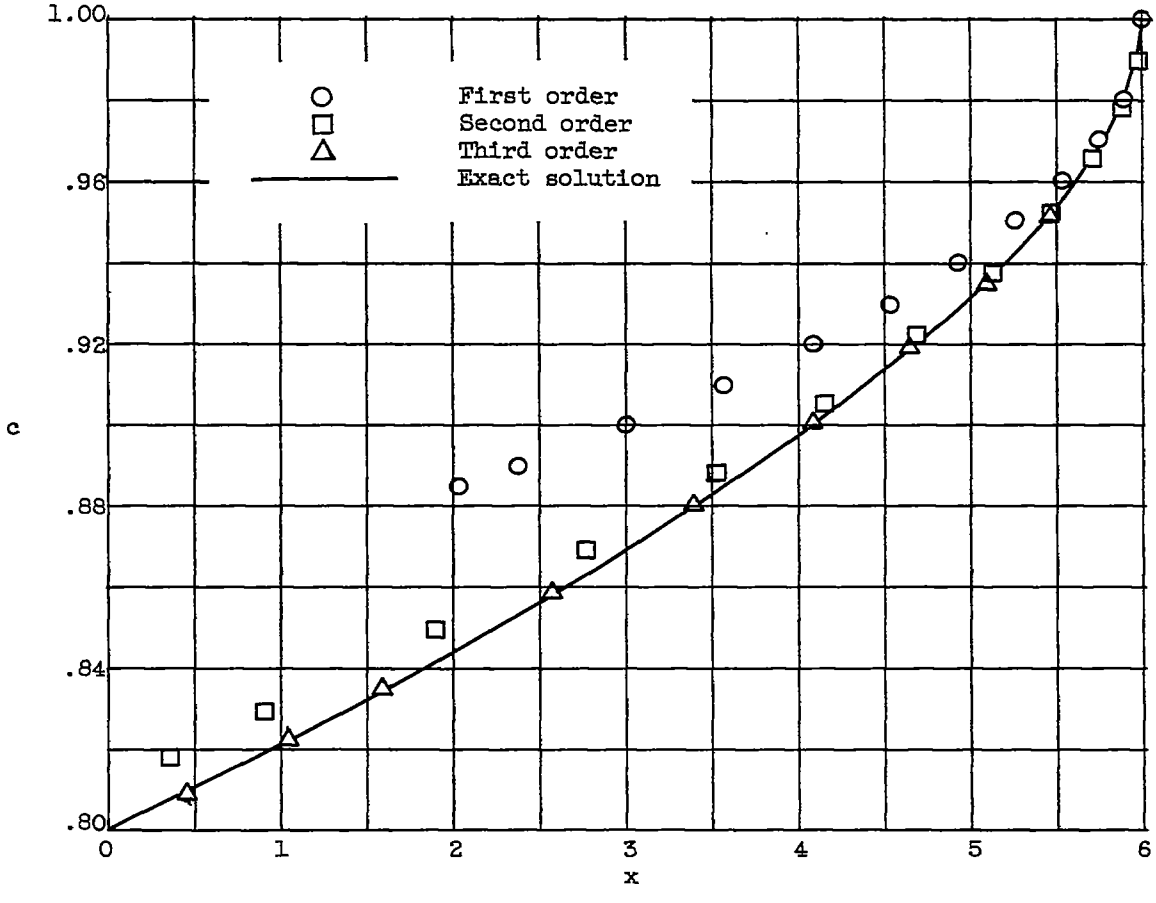

(b) Sonic speed.

Figure 2.15. - Concluded. Flow variables as a function of x. Supersonic flow specified on x = L. "Epsilon duct": $\varepsilon = 0.1$, L = 6, $\sigma = 5$.

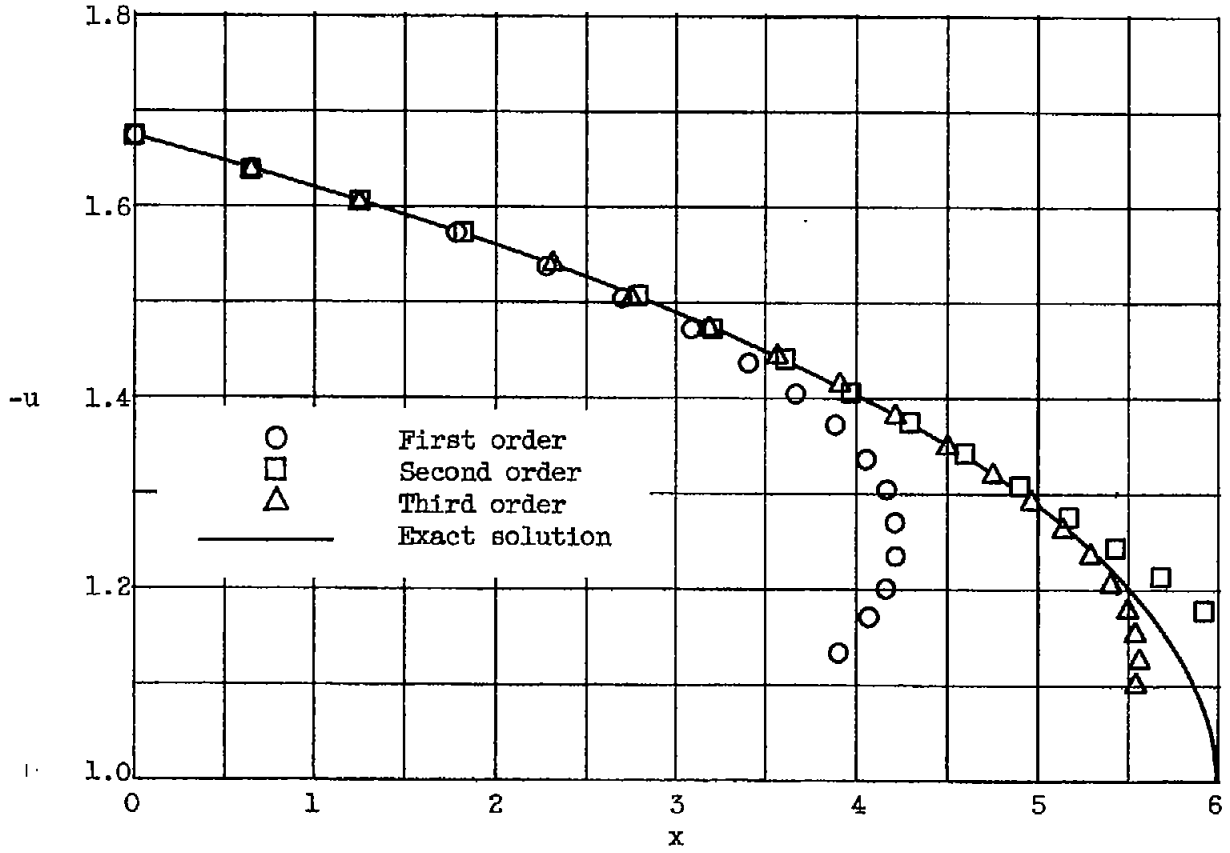

(a) Particle velocity.

Figure 2.16. - Flow variables as a function of x. Supersonic flow specified on x = 0. "Epsilon duct": $\varepsilon = 0.1$, L = 6, $\sigma = 5$.

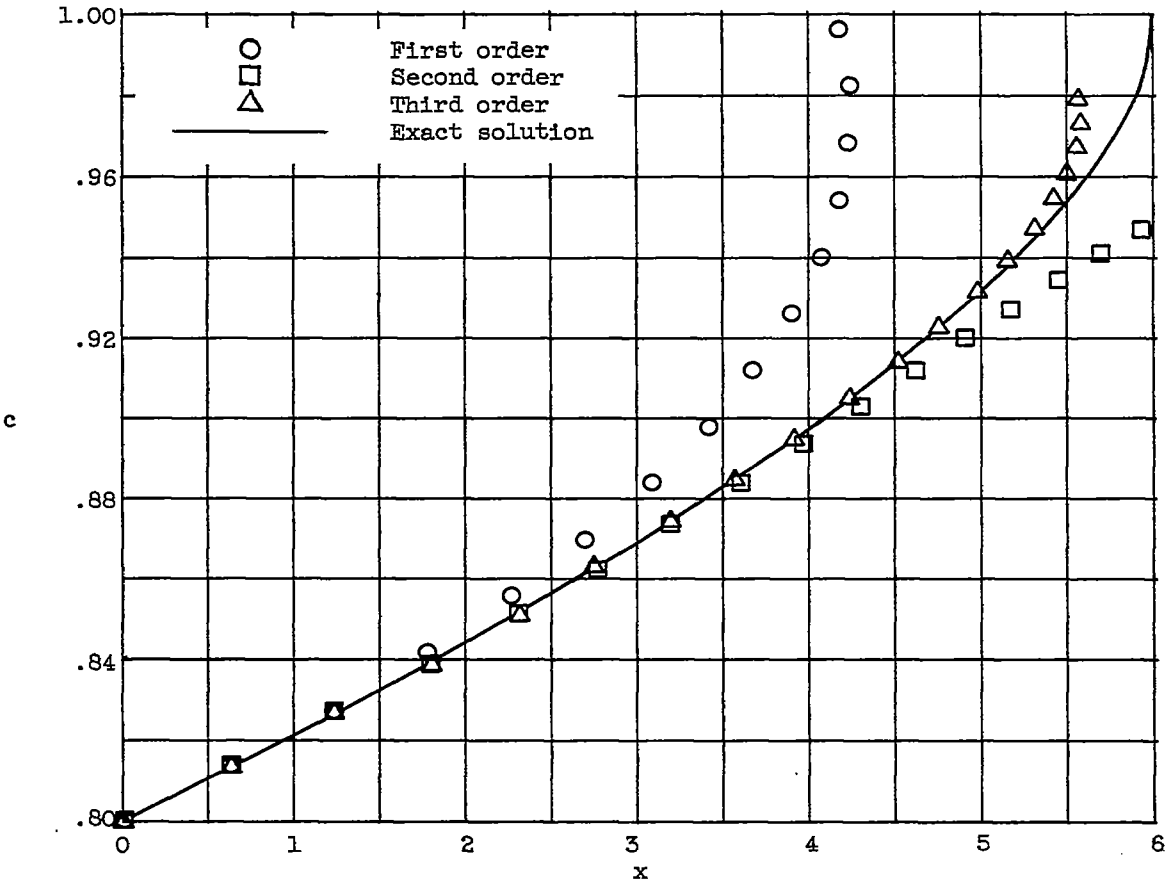

(b) Sonic speed.

Figure 2.16. - Concluded. Flow variables as a function of x. Supersonic flow specified on x = 0. "Epsilon duct": $\varepsilon = 0.1$, L = 6, $\sigma = 5$.

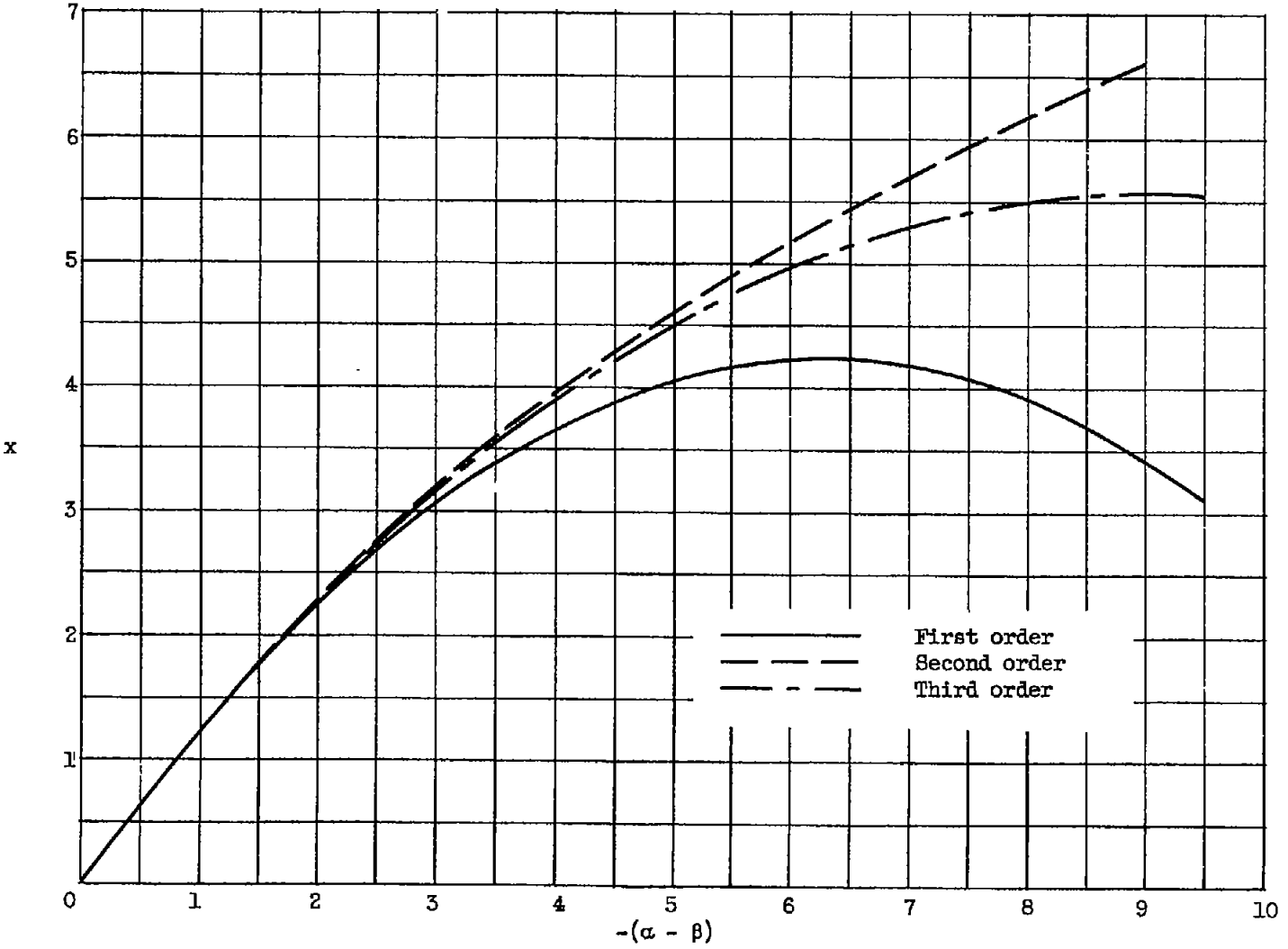

Figure 2.17. - x as a function of $(\alpha - \beta)$. Supersonic flow specified on $x = 0$. "Epsilon duct": $\varepsilon = 0.1$, $L = 6$, $\sigma = 5$.

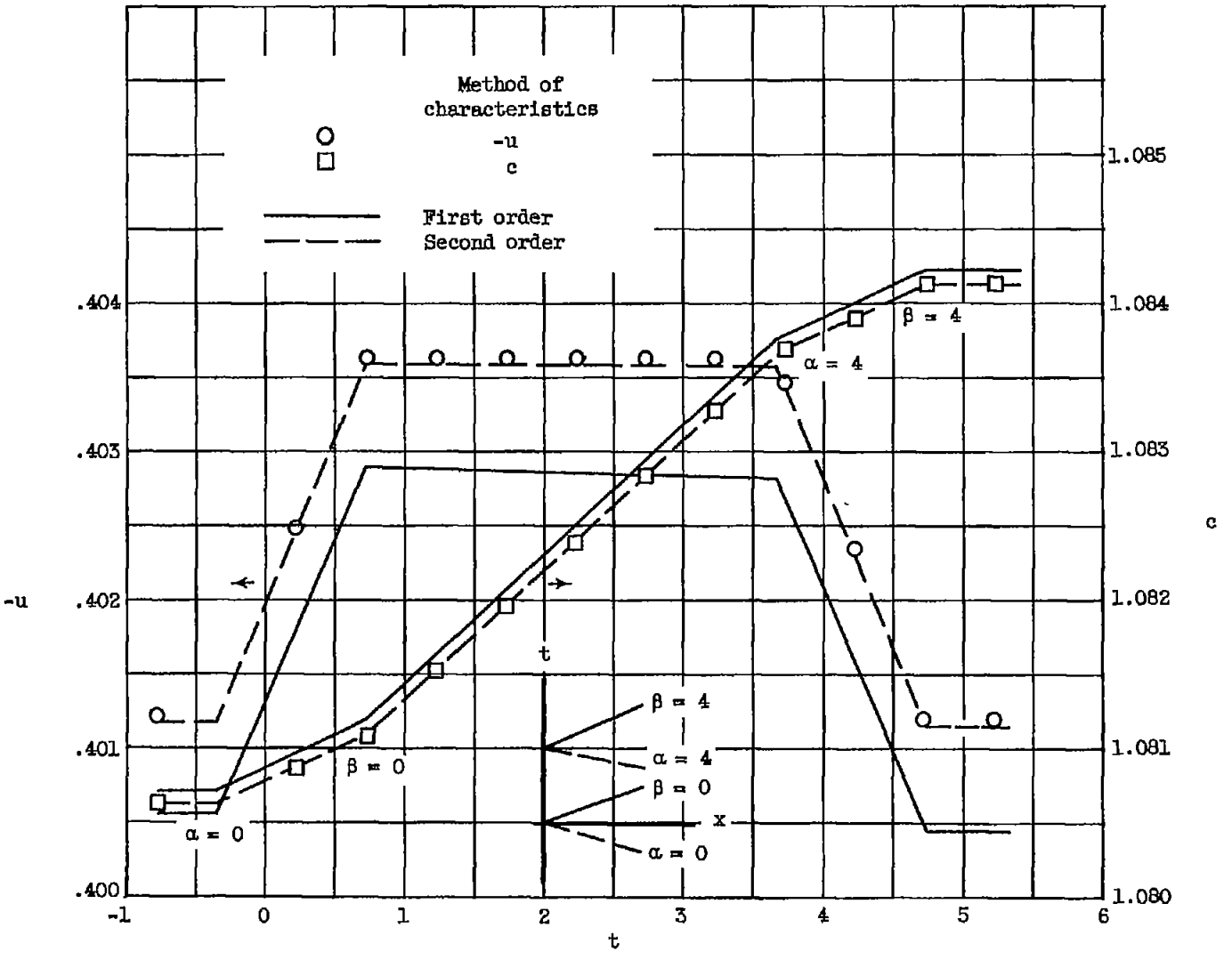

Figure 2.18. - Variation of u and c on x = 0.5 for disturbance in c alone on x = 0; ε = 0.1, σ = 5.

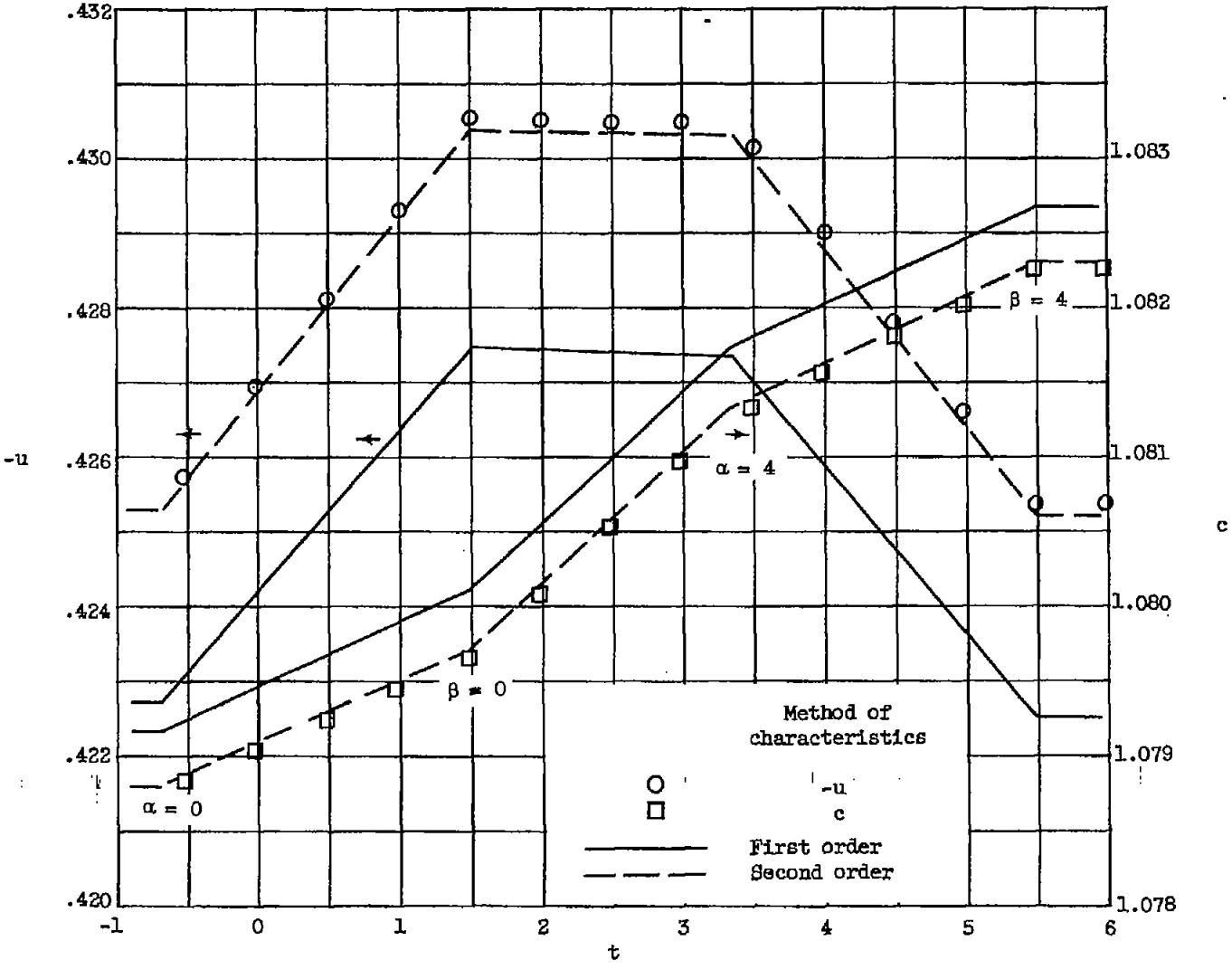

Figure 2.19. - Variation of u and c on x = 1.0 for disturbance in c alone on x = 0; $\varepsilon = 0.1$, $\sigma = 5$.

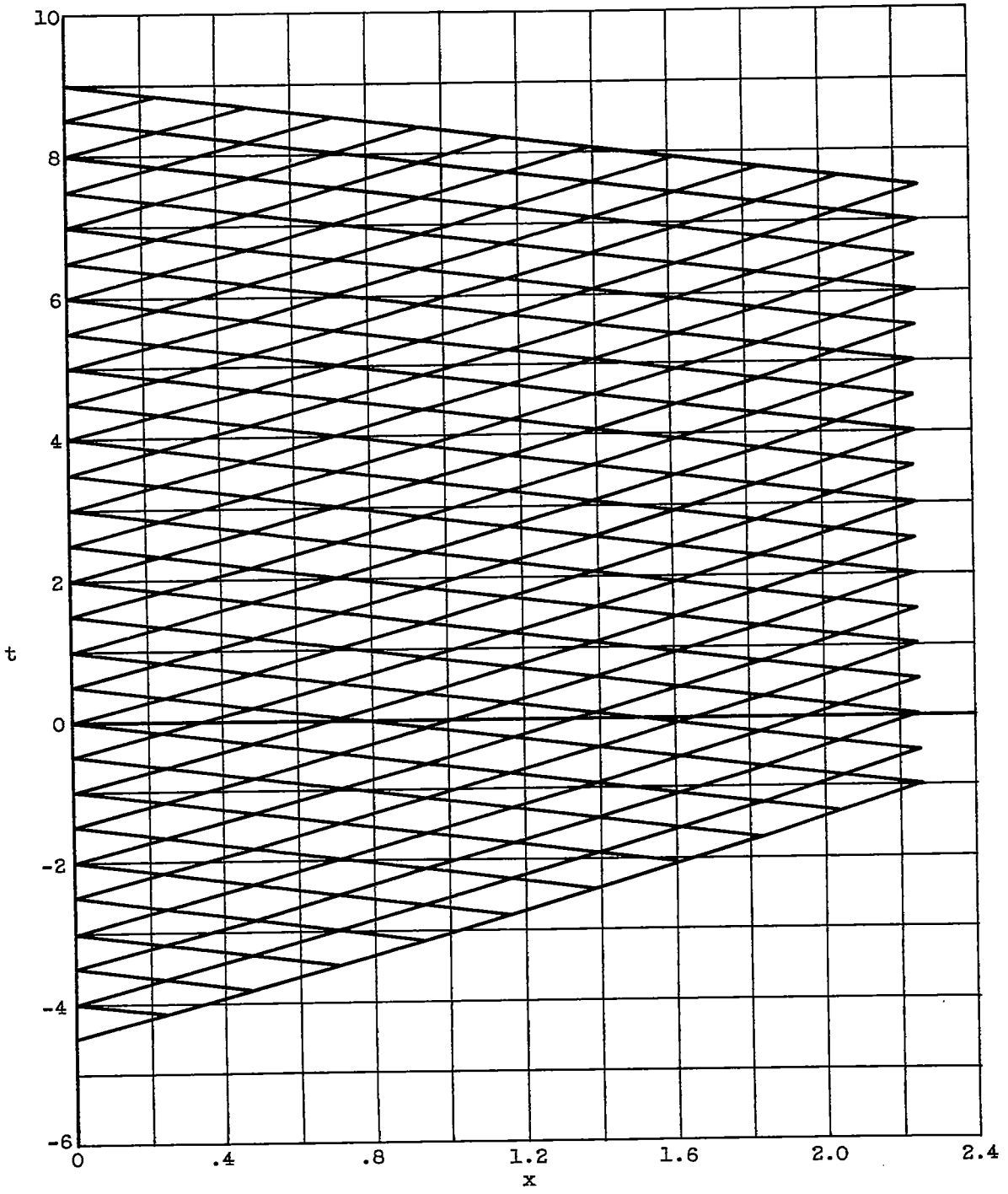

Figure 2.20. - Characteristics net for disturbance of c alone on x = 0; $\varepsilon = 0.1$, $\sigma = 5$.

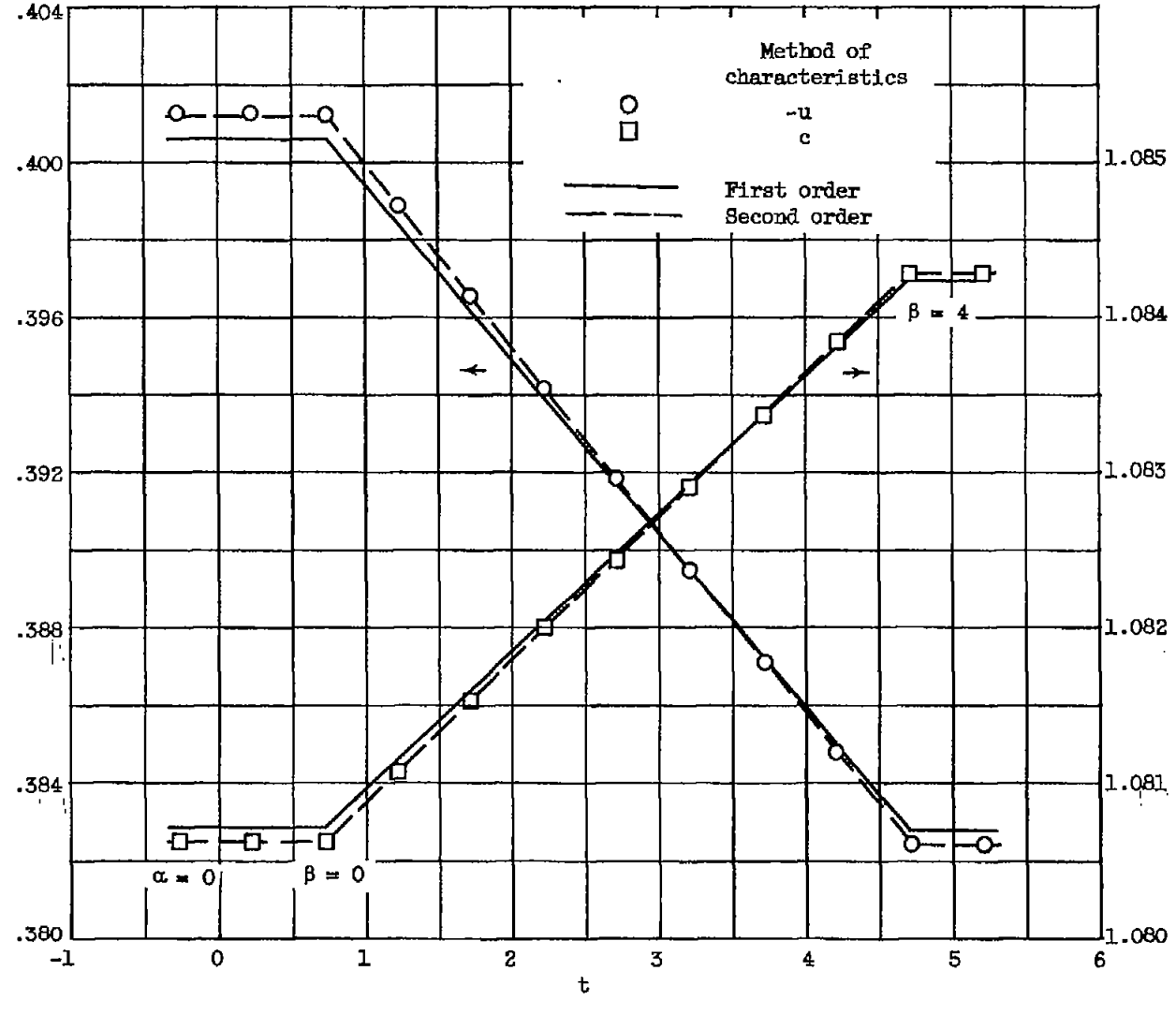

Figure 2.21 - Variation of u and c on x = 0.5 for "simple-wave-type" disturbance on x = 0; ε = 0.1, σ = 5.

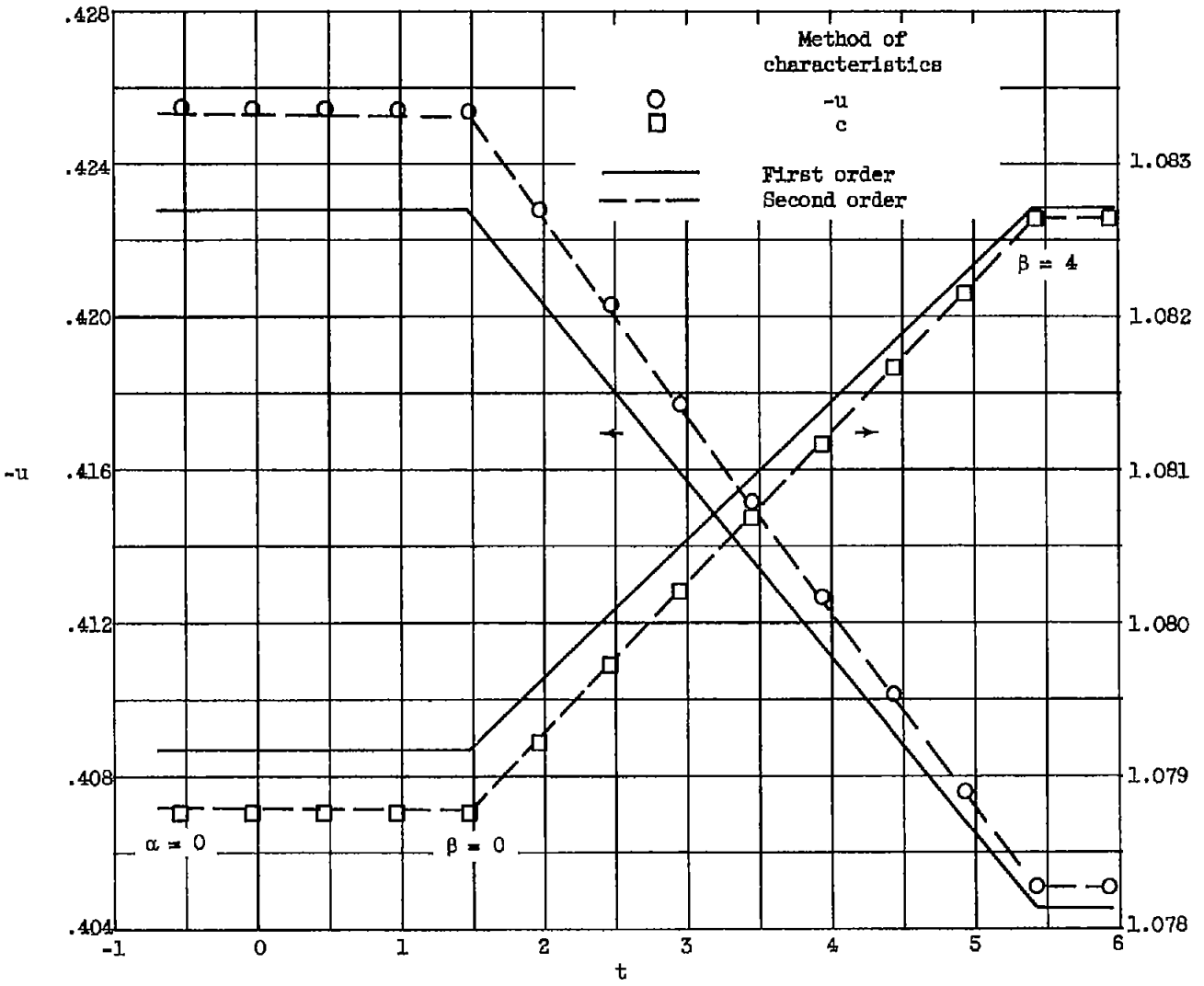

Figure 2.22 - Variation of u and c on x = 1.0 for "simple-wave-type" disturbance on x = 0; ε = 0.1, σ = 5.

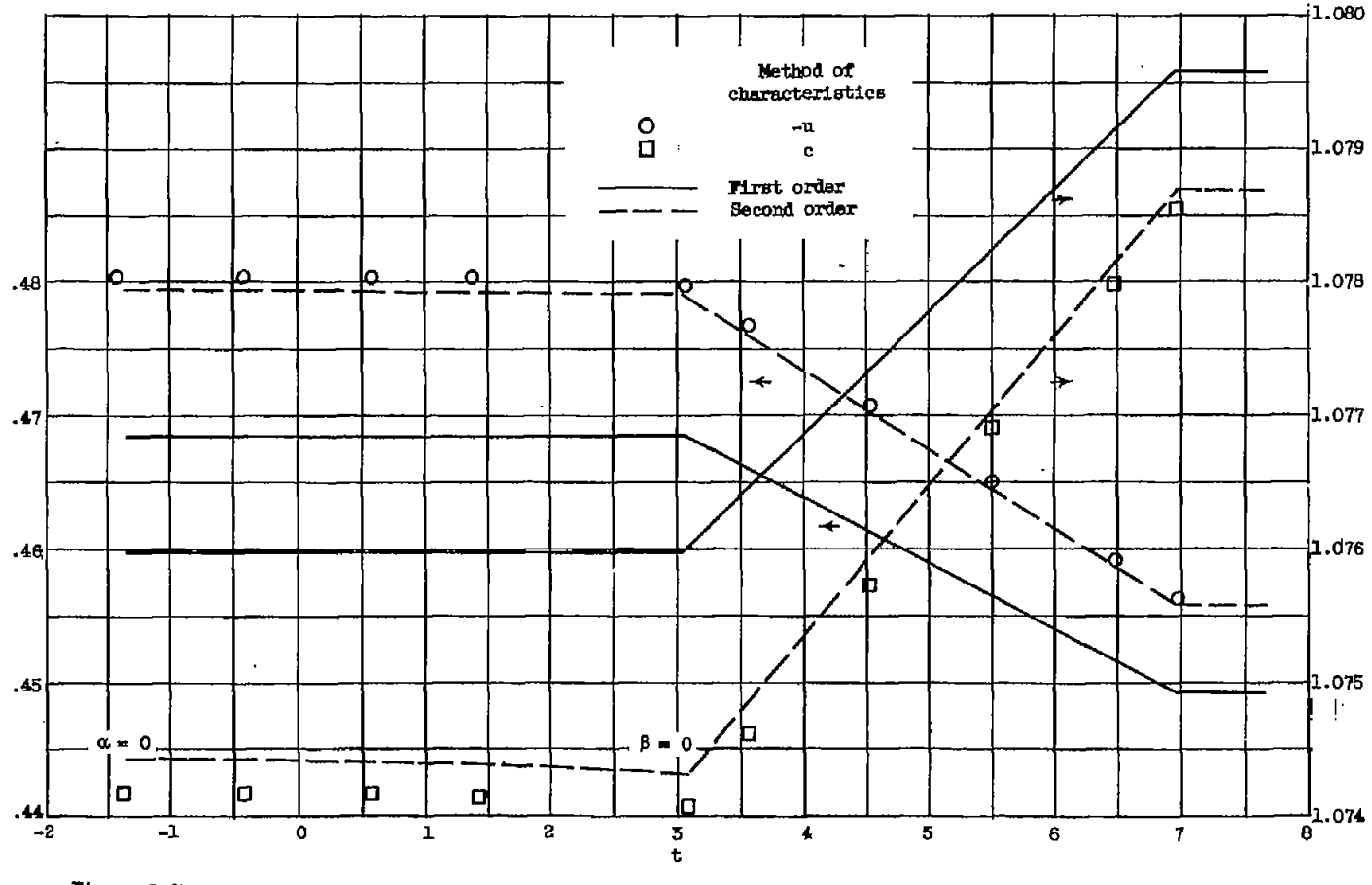

Figure 2.23. - Variation of u and c on x = 2.0 for "simple-wave-type" disturbance on x = 0; ε = 0.1, σ = 5.

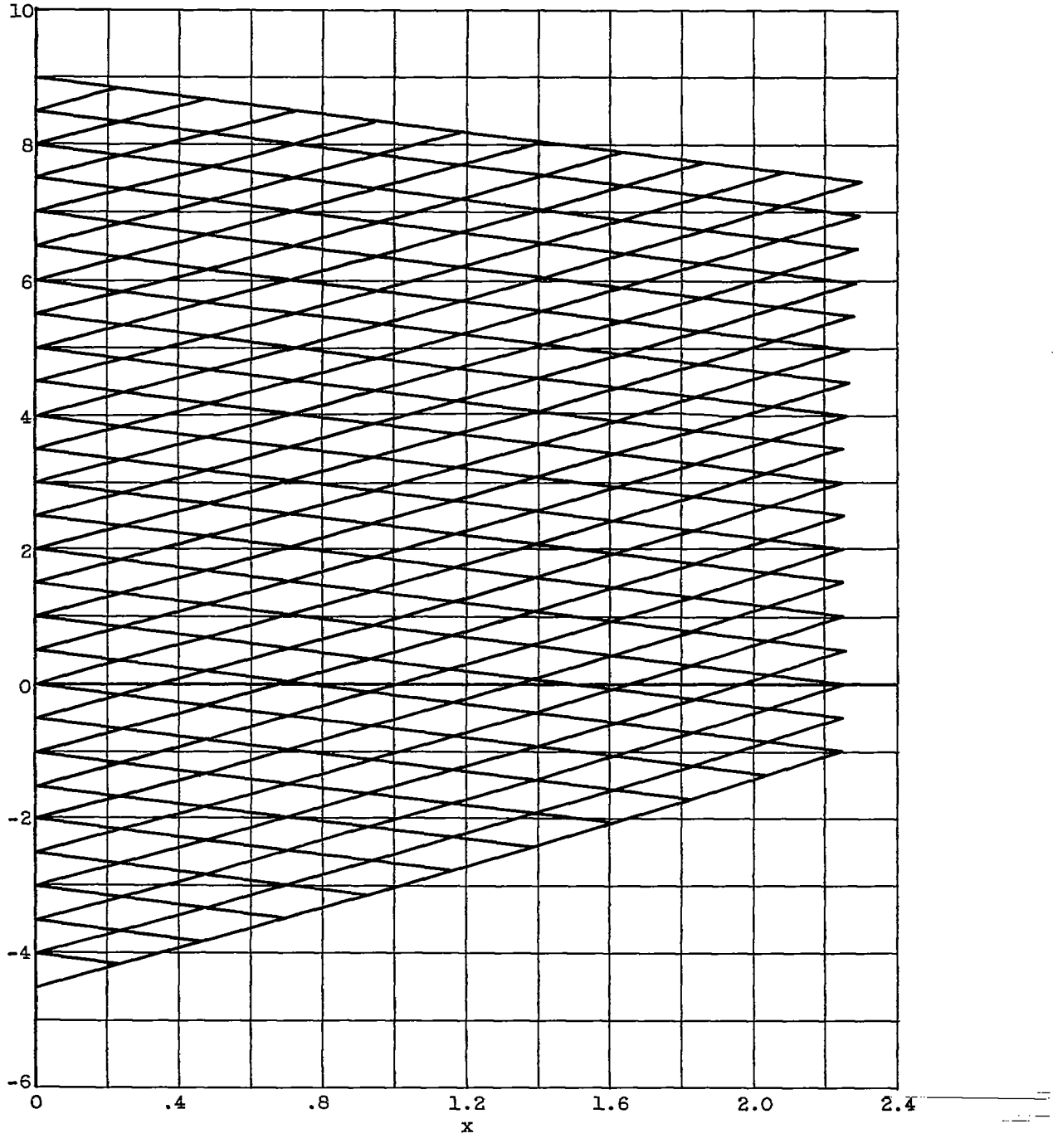

Figure 2.24. - Characteristics net for "simple-wave-type" disturbance on $x = 0$; $\epsilon = 0.1$, $\sigma = 5$.

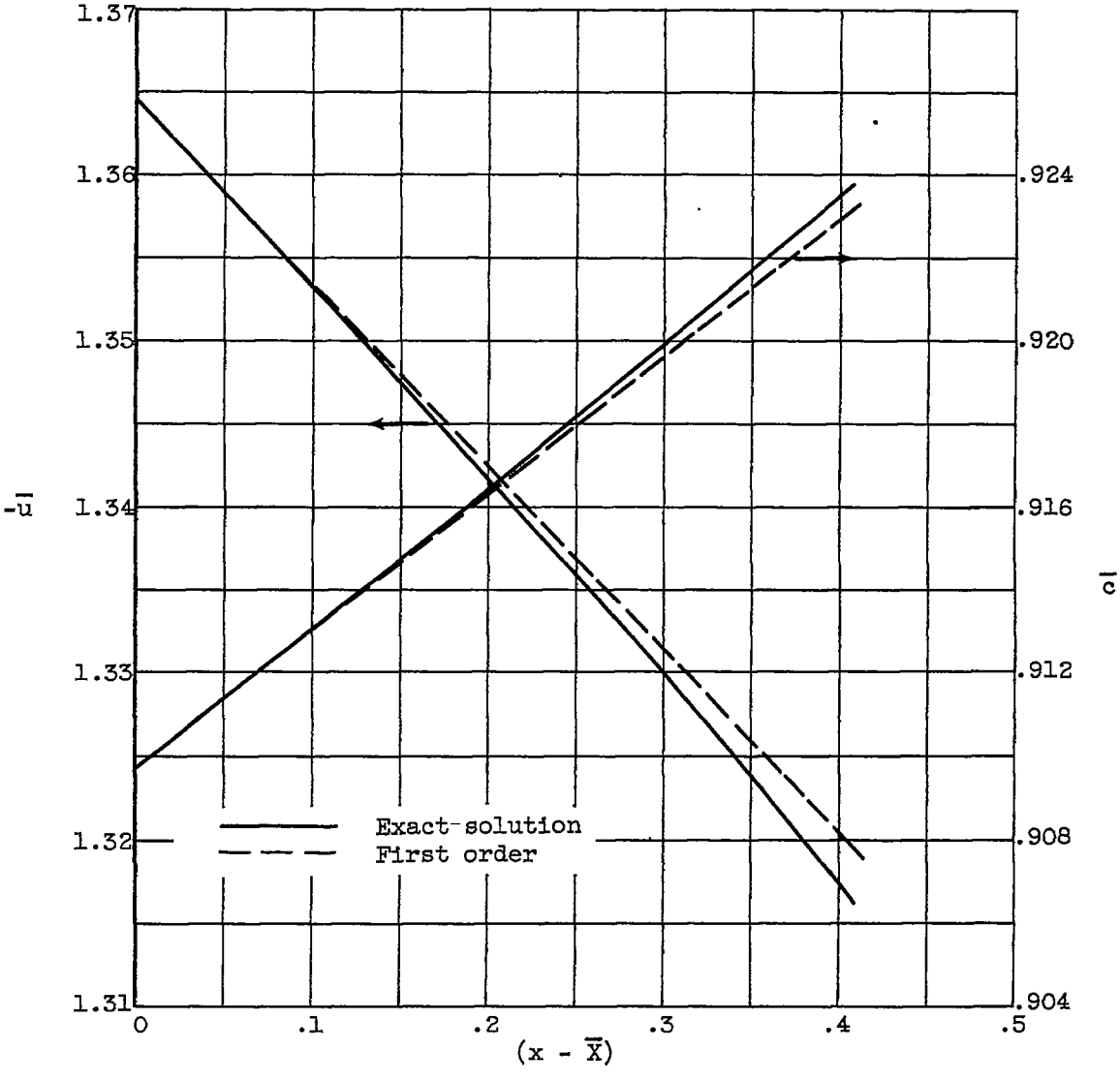

Figure 3.1. - Variation of flow variables upstream of a shock at Mach 1.5 in an "epsilon duct"; $\varepsilon = 0.1$, $\sigma = 5$. (Test of eq. (3.20)).

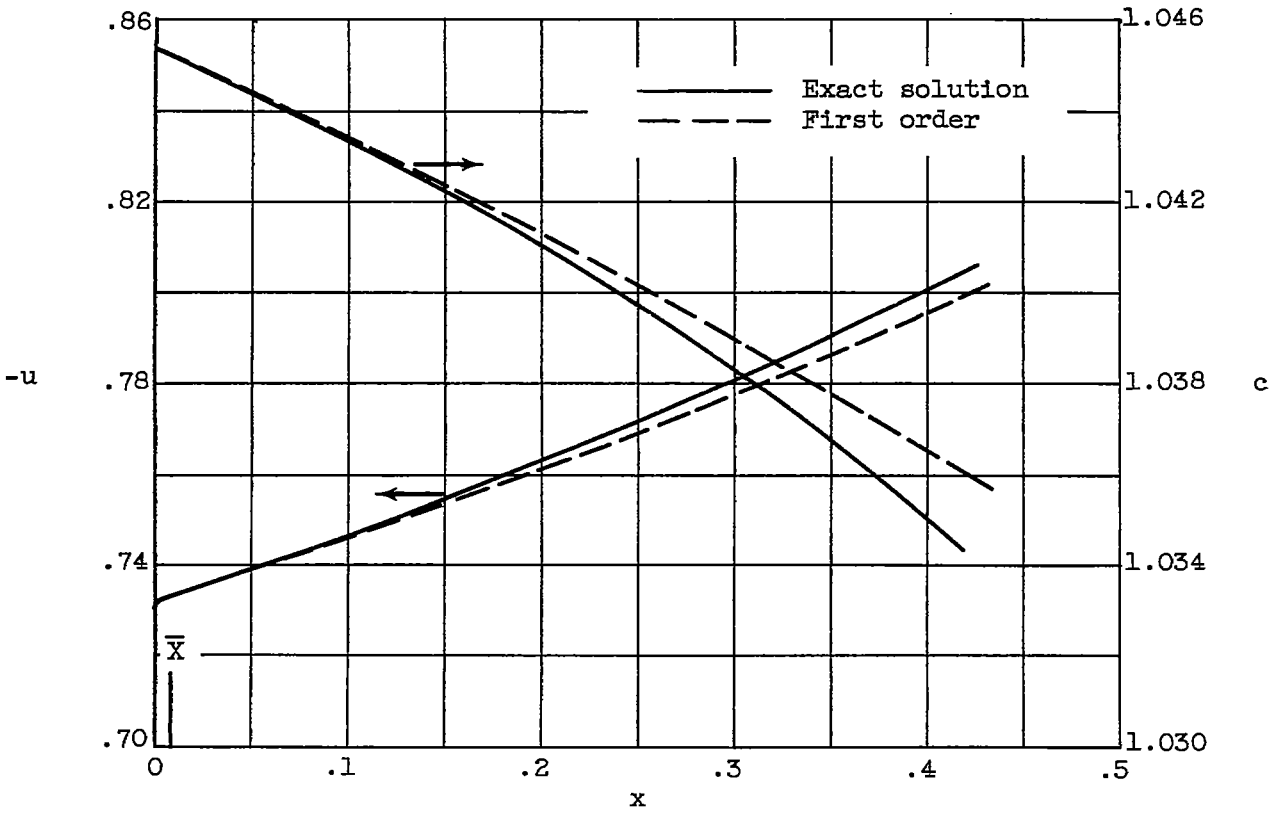

Figure 3.2. - Variation of downstream flow variables in an "epsilon duct". Boundary Mach number, 0.7; $\epsilon = 0.1$, $\sigma = 5$.

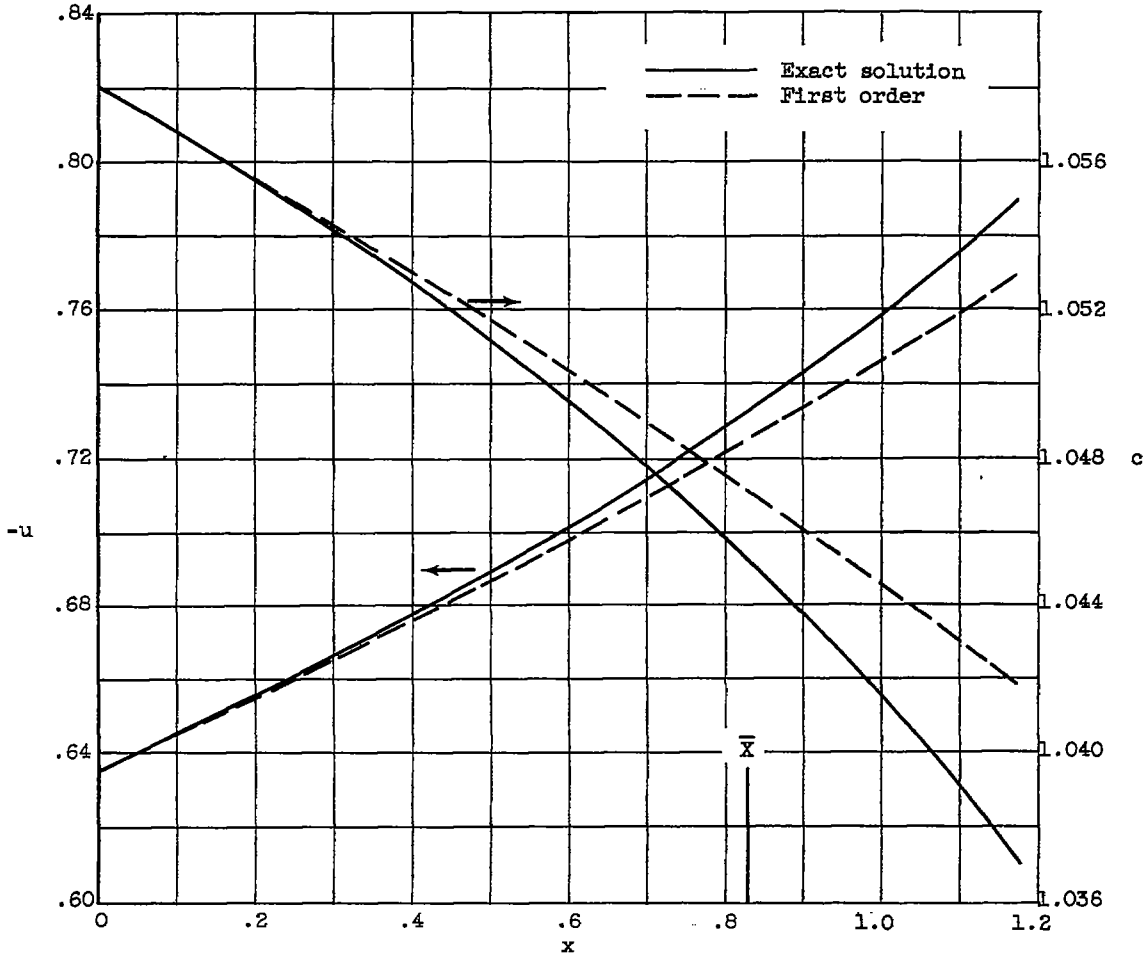

Figure 3.3. - Variation of downstream flow variables in an "epsilon duct". Boundary Mach number, 0.6; $\varepsilon = 0.1$, $\sigma = 5$.

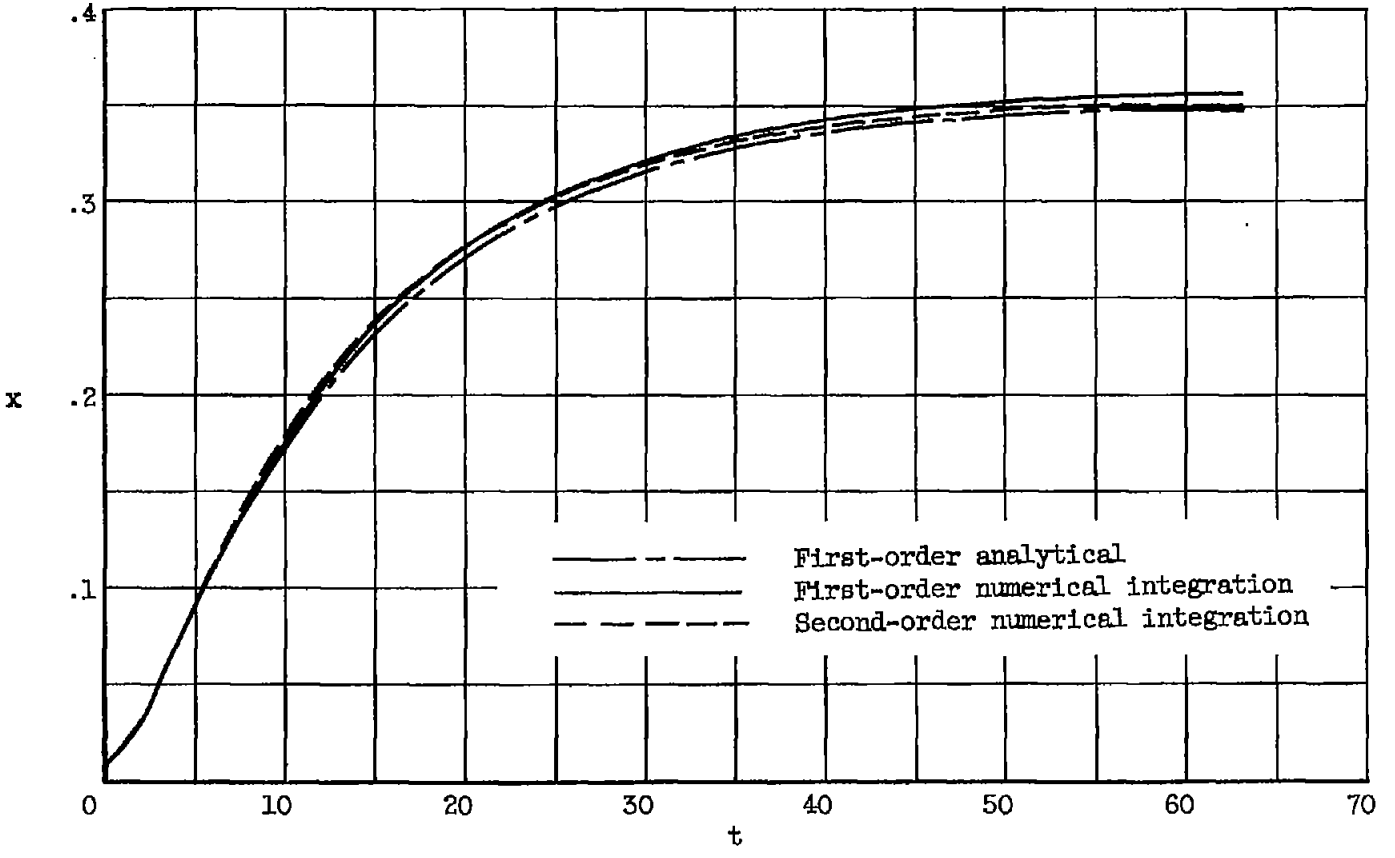

Figure 3.4. - Shock path for a "simple-wave-type" disturbance specified at a downstream Mach number of 0.7. Initial upstream Mach number, 1.5; $\varepsilon = 0.1$, $\sigma = 5$.

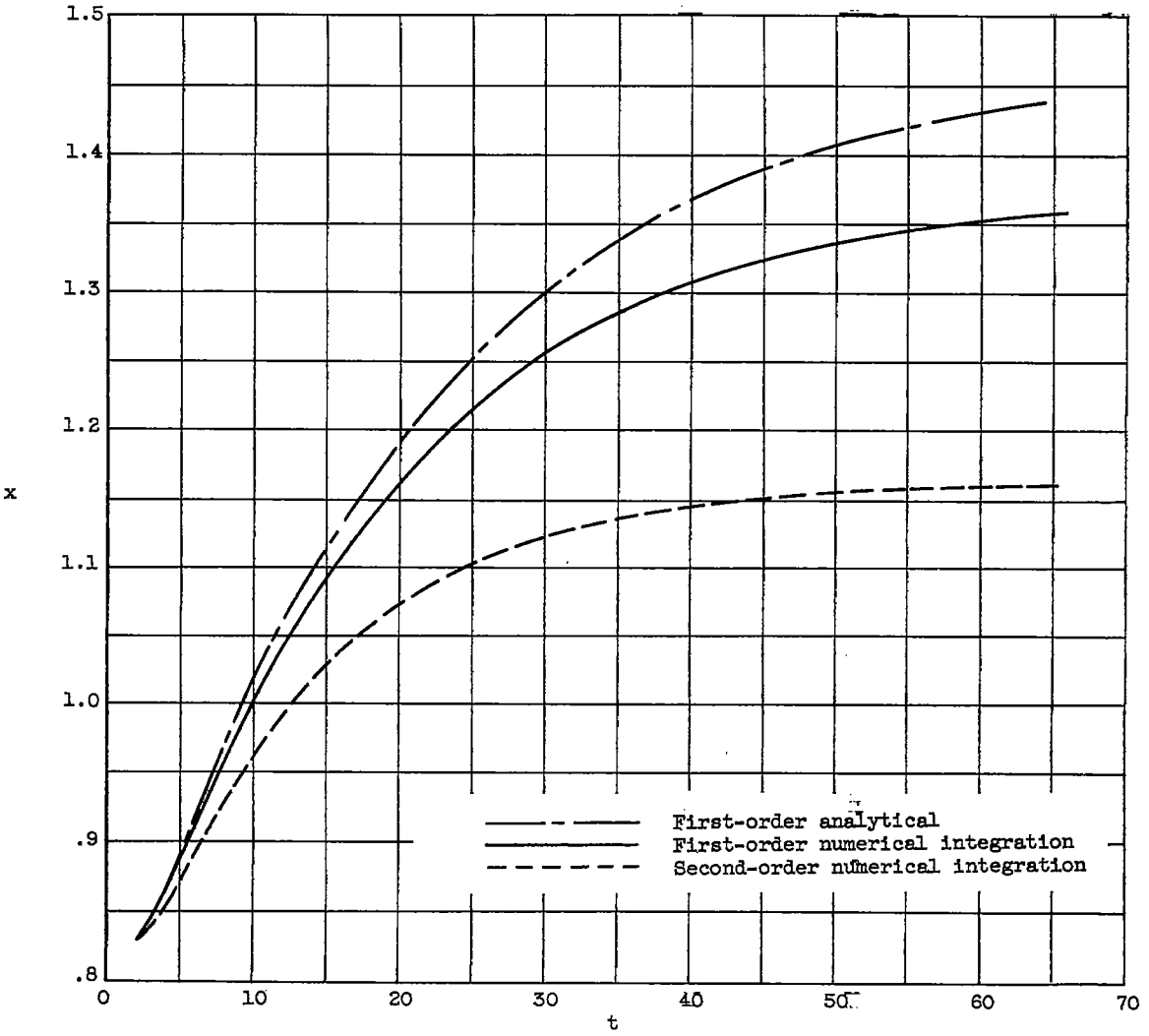

Figure 3.5. - Shock path for a "simple-wave-type" disturbance specified at a downstream Mach number of 0.6. Initial upstream Mach number, 1.5; $\varepsilon = 0.1$, $\sigma = 5$.

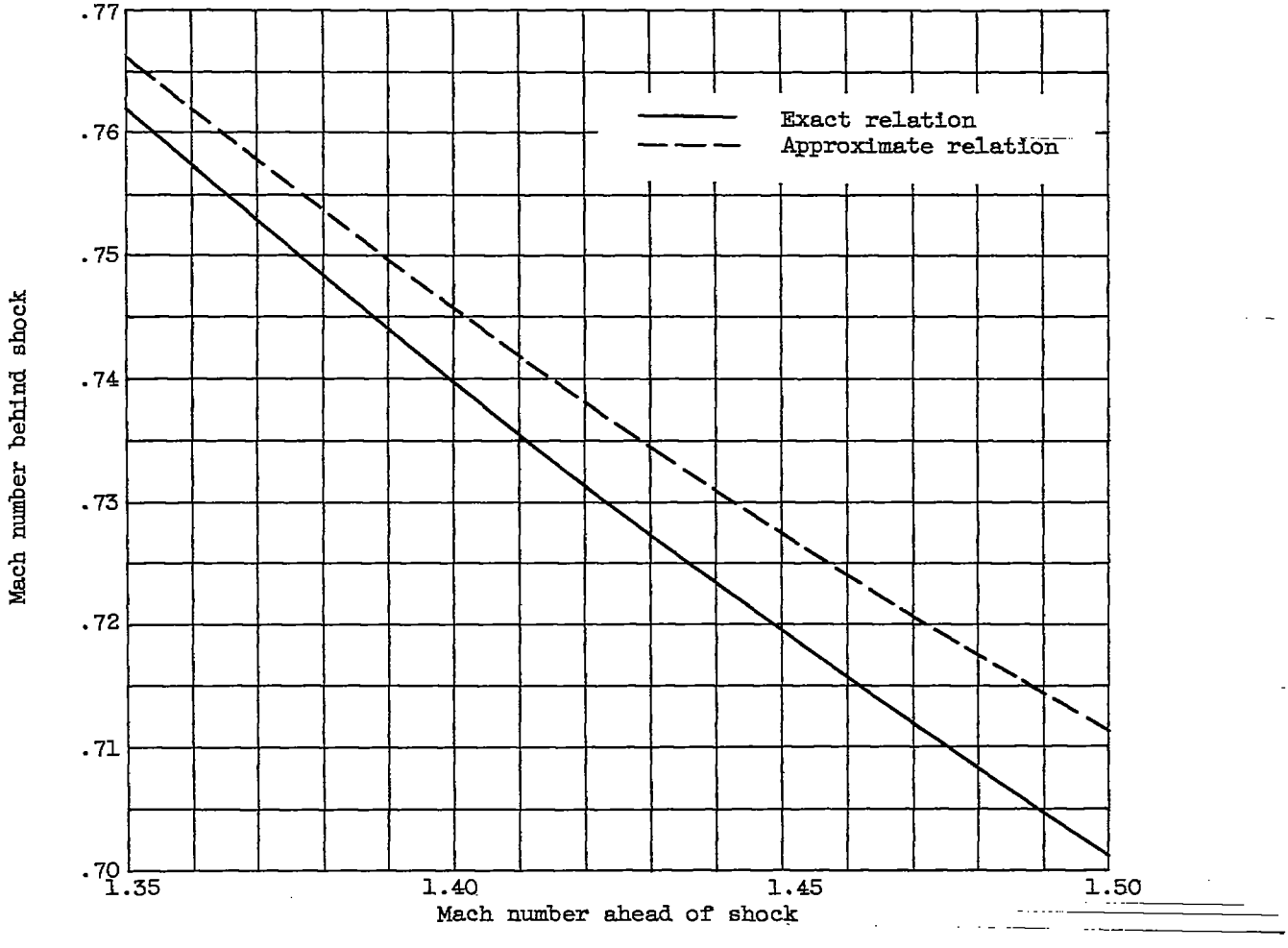

Figure 3.6. - Mach number behind shock as a function of Mach number ahead of shock; $\sigma = 5$.

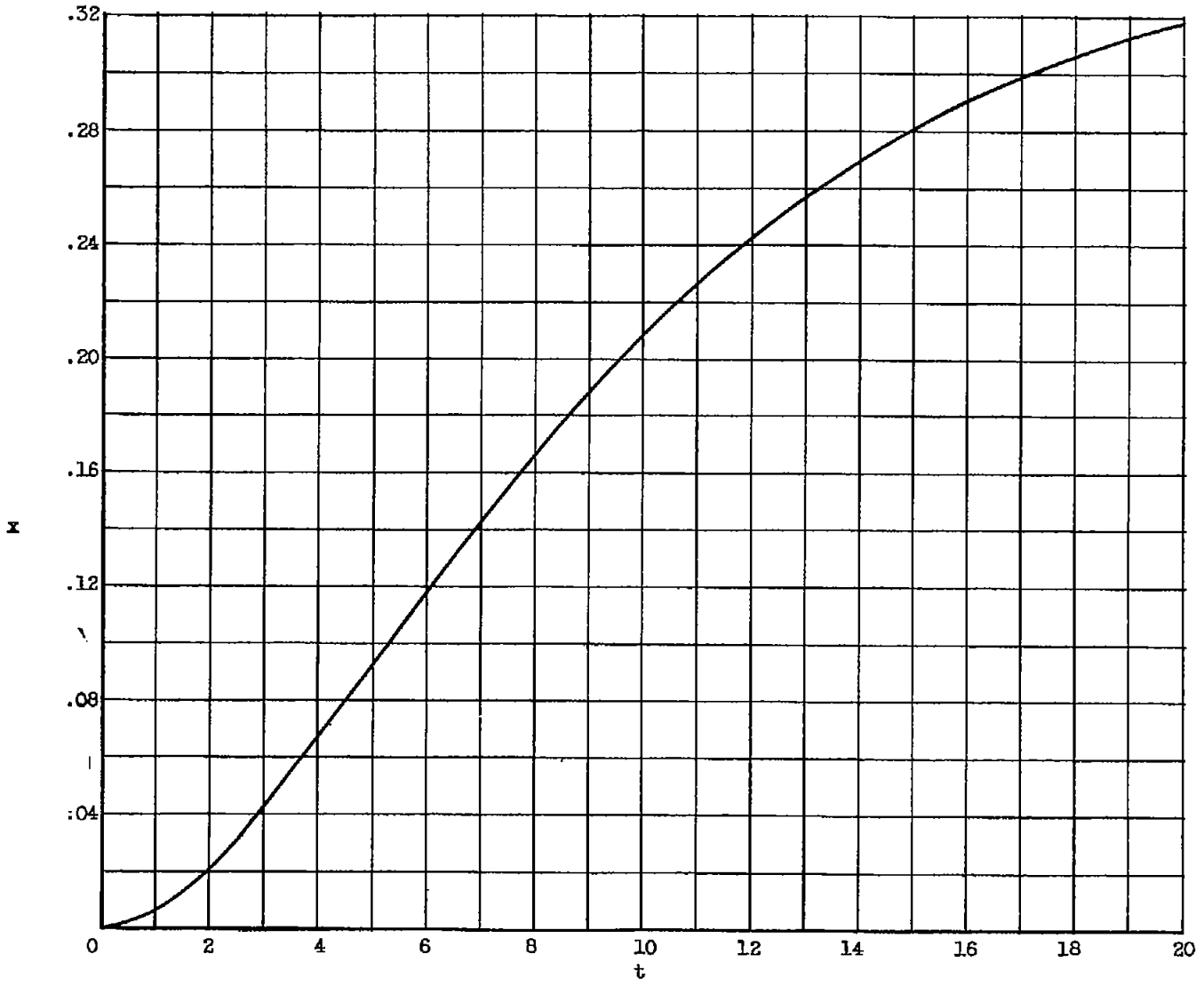

Figure 4.1. - Shock path for "exponential" function; B = 3.5, b = 0.2, ε = 0.1.

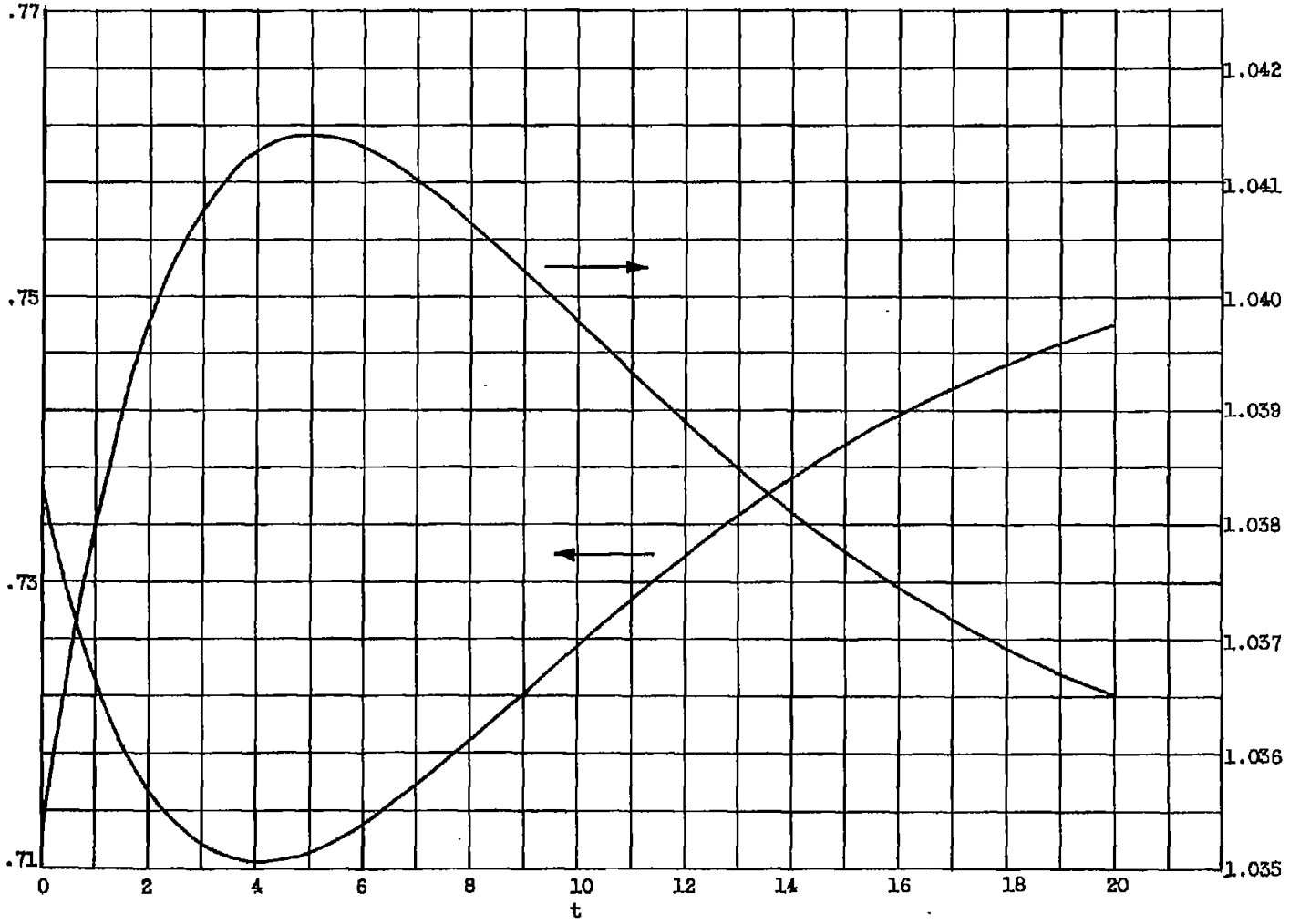

Figure 4.2. - Variation of downstream flow conditions along "exponential" shock path. Initial shock Mach number, 1.5; B = 3.5, b = 0.2, ε = 0.1.

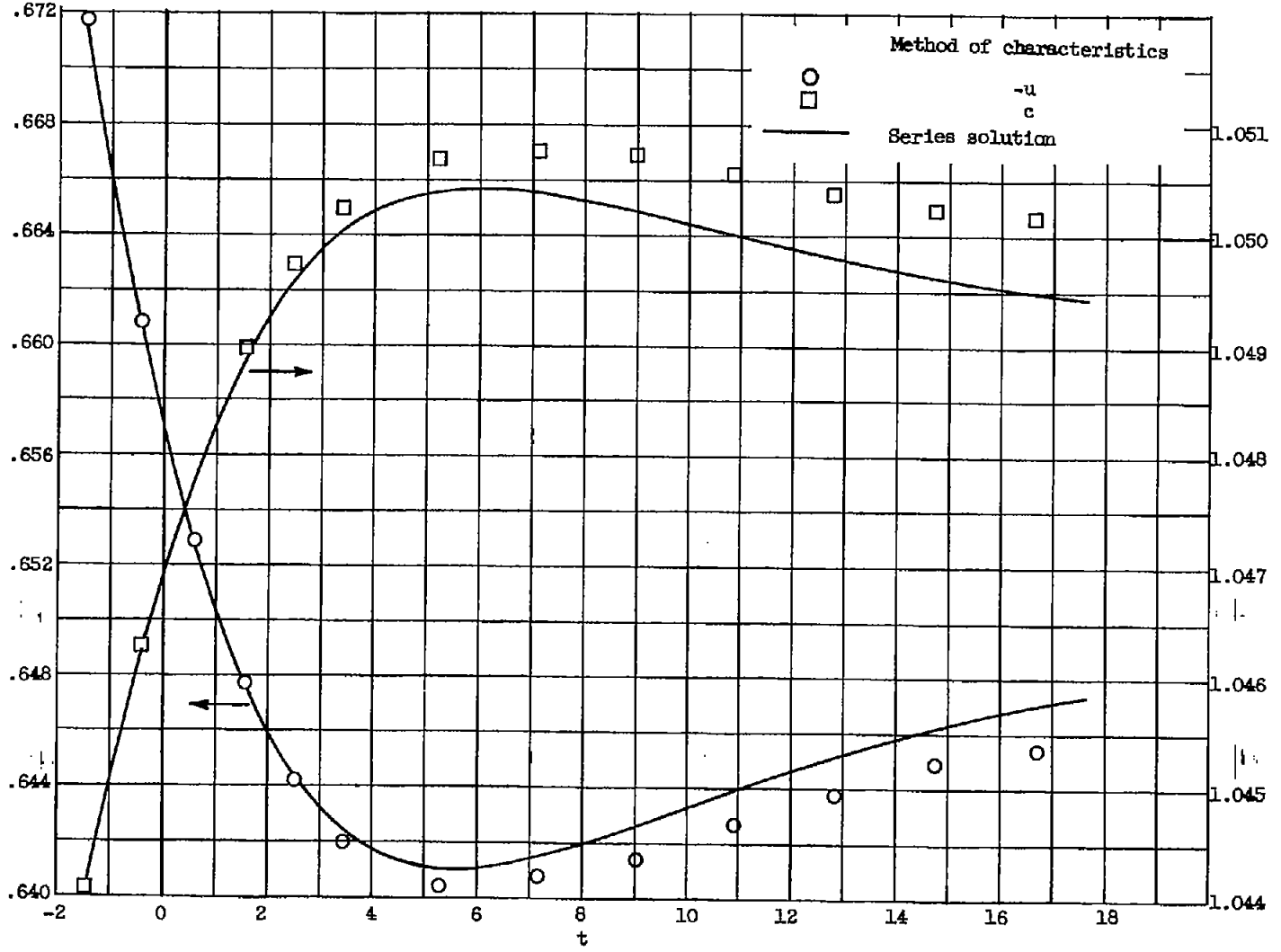

Figure 4.3. - Variation of flow variables at $x = -0.5$ for "exponential" shock path. Initial shock Mach number, 1.5; $B = 3.5$, $b = 0.2$, $\varepsilon = 0.1$.

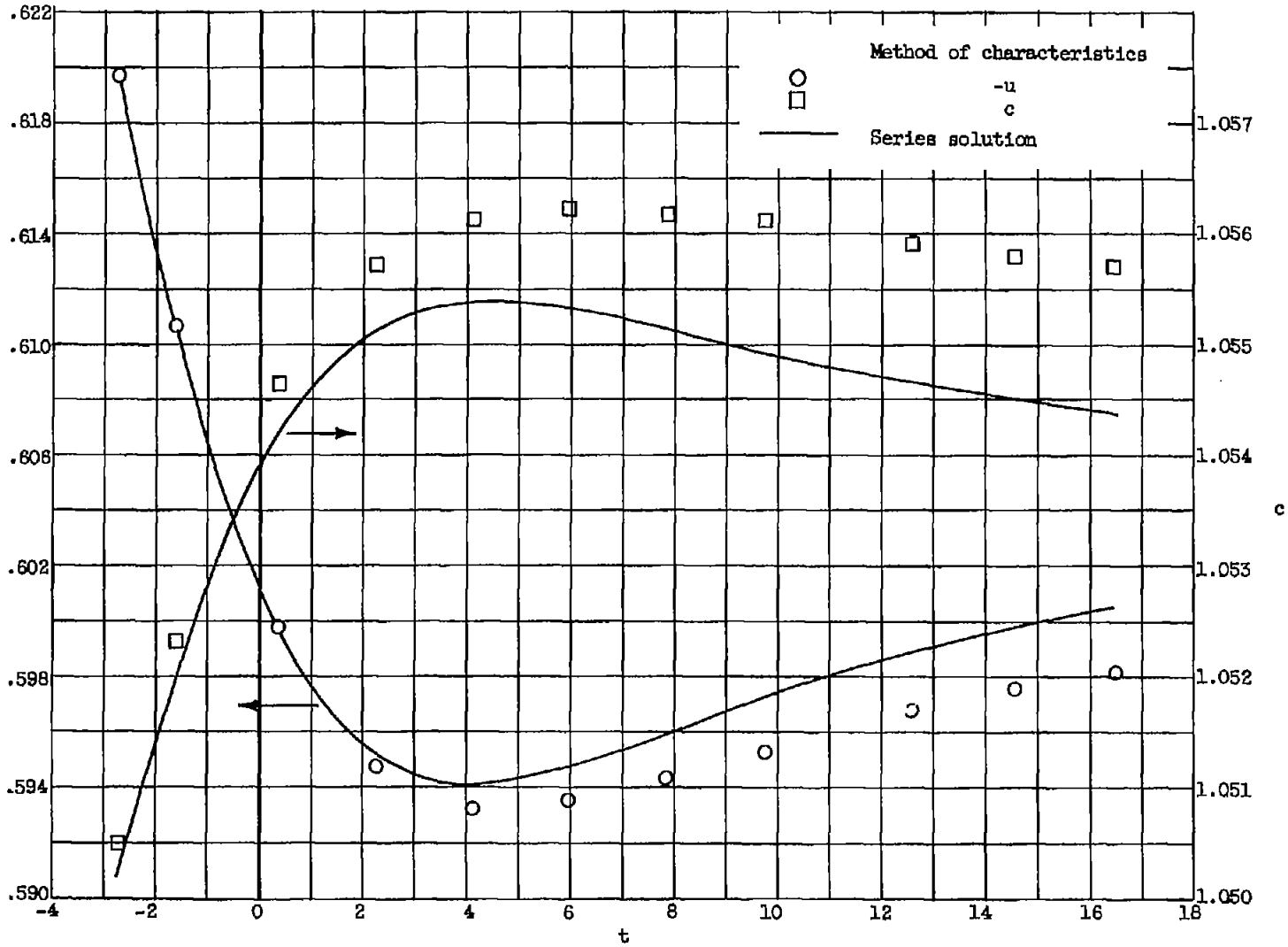

Figure 4.4. - Variation of flow variables at $x = -1.0$ for "exponential" shock path. Initial shock Mach number, 1.5; $B = 3.5$, $b = 0.2$, $\delta = 0.1$.

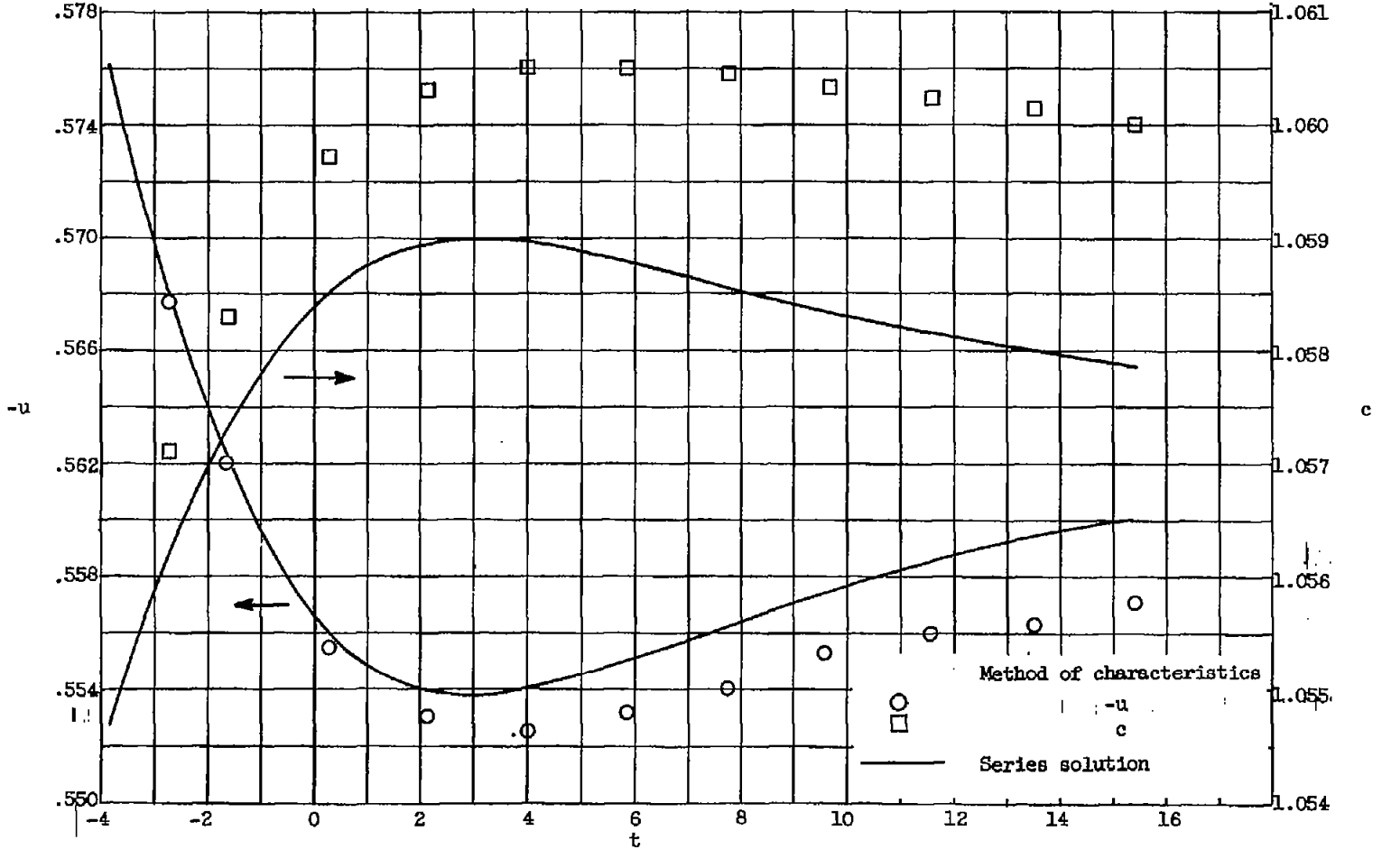

Figure 4.5. - Variation of flow variables at x = -1.5 for "exponential" shock path. Initial shock Mach number, 1.5; B = 3.5, b = 0.2, ε = 0.1.

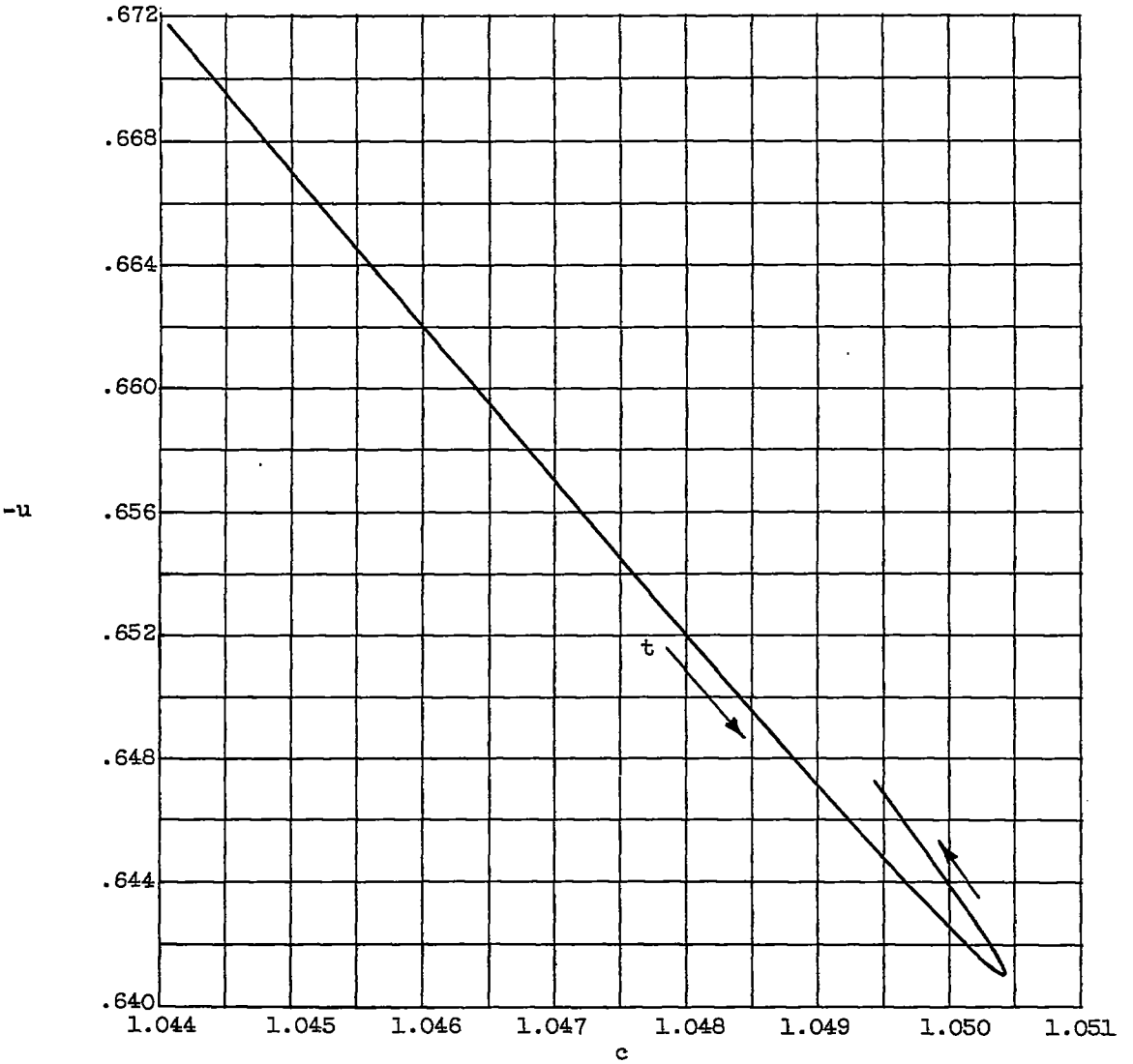

(a) x = -0.5.

Figure 4.6. - u,c-Relation at constant x for "exponential" shock path. Initial shock Mach number, 1.5; B = 3.5, b = 0.2, ε = 0.1.

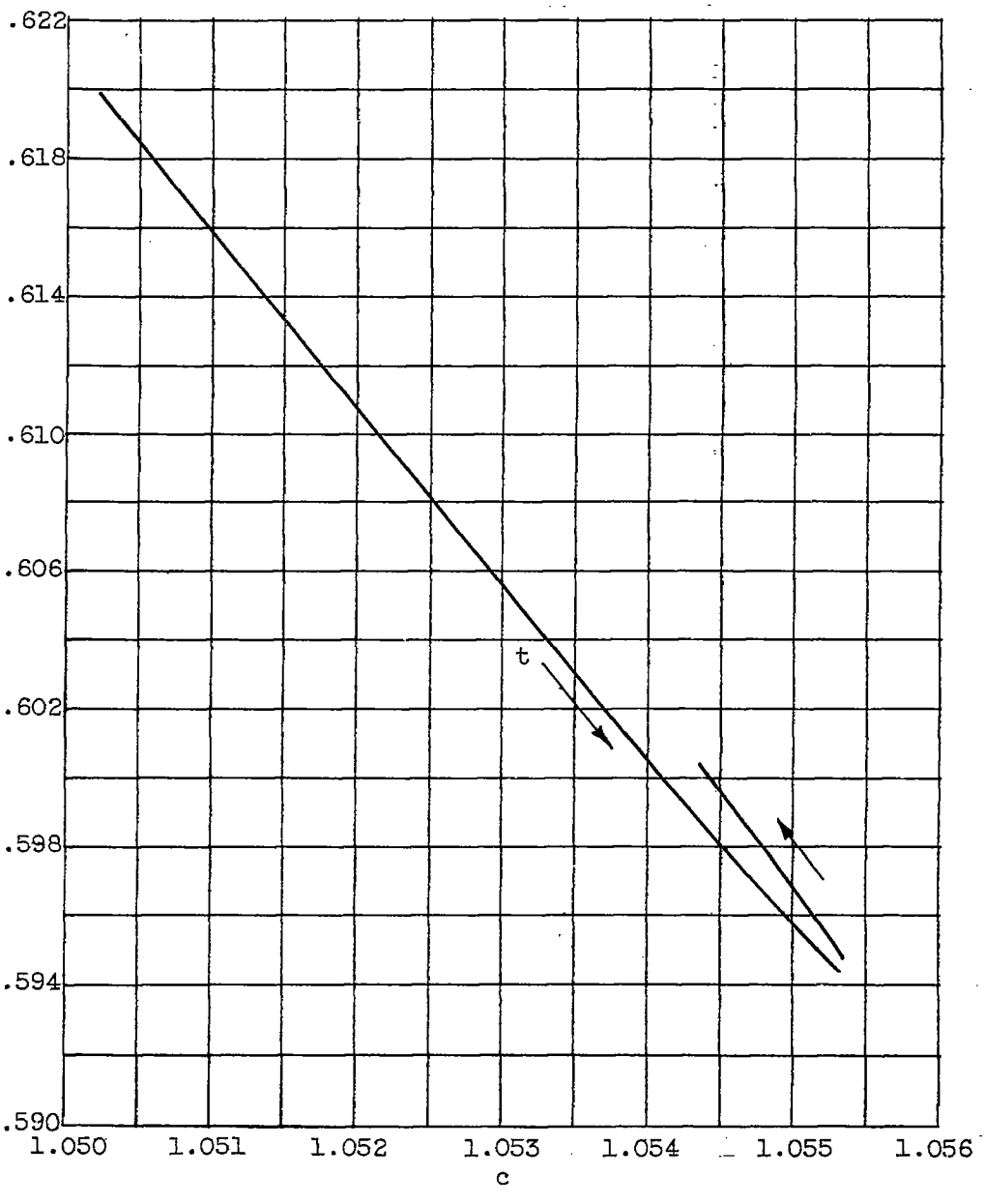

(b) x = -1.0.

Figure 4.6. - Continued. u,c-Relation at constant x for "exponential" shock path. Initial shock Mach number, 1.5; B = 3.5, b = 0.2, ε = 0.1.

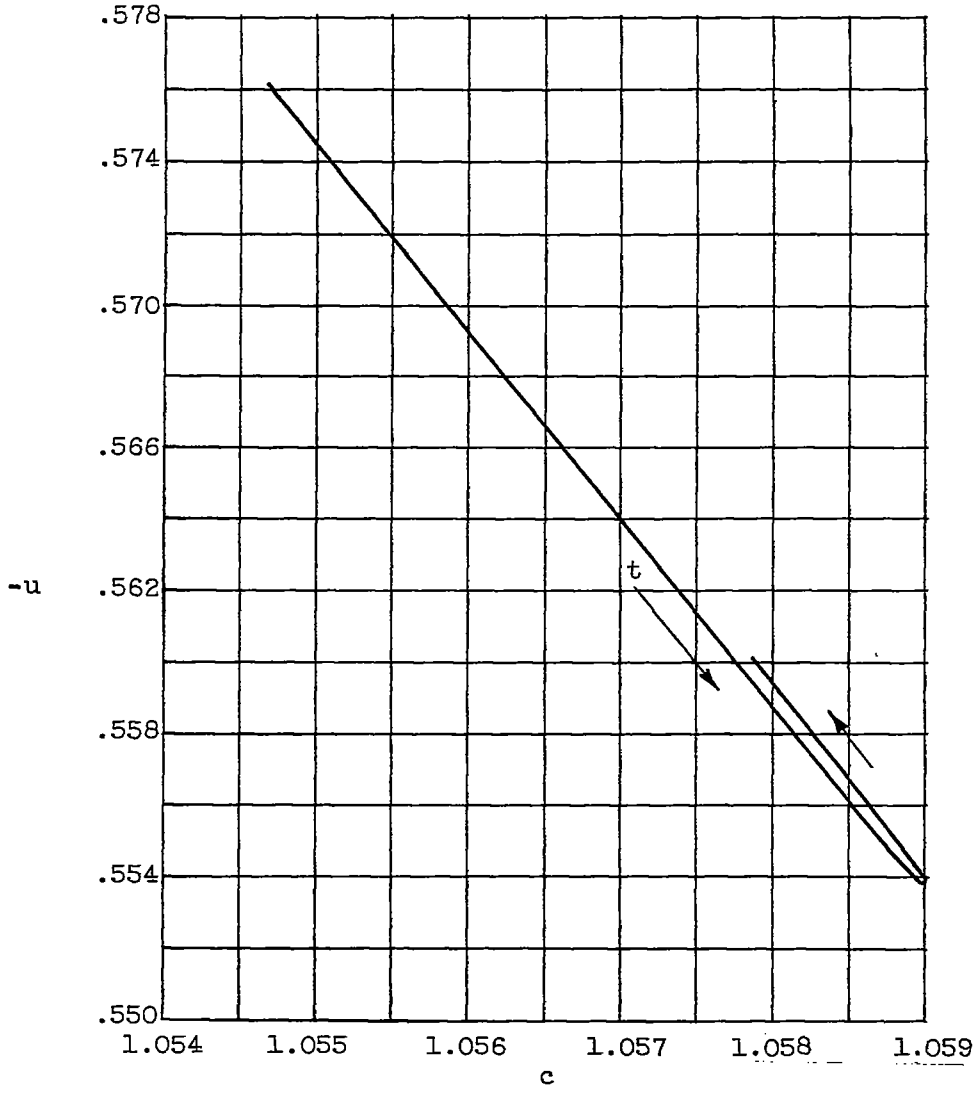

(c) x = -1.5.

Figure 4.6. - Concluded. u,c-Relation at constant x for "exponential" shock path. Initial shock Mach number, 1.5; B = 3.5, b = 0.2, ϵ = 0.1.

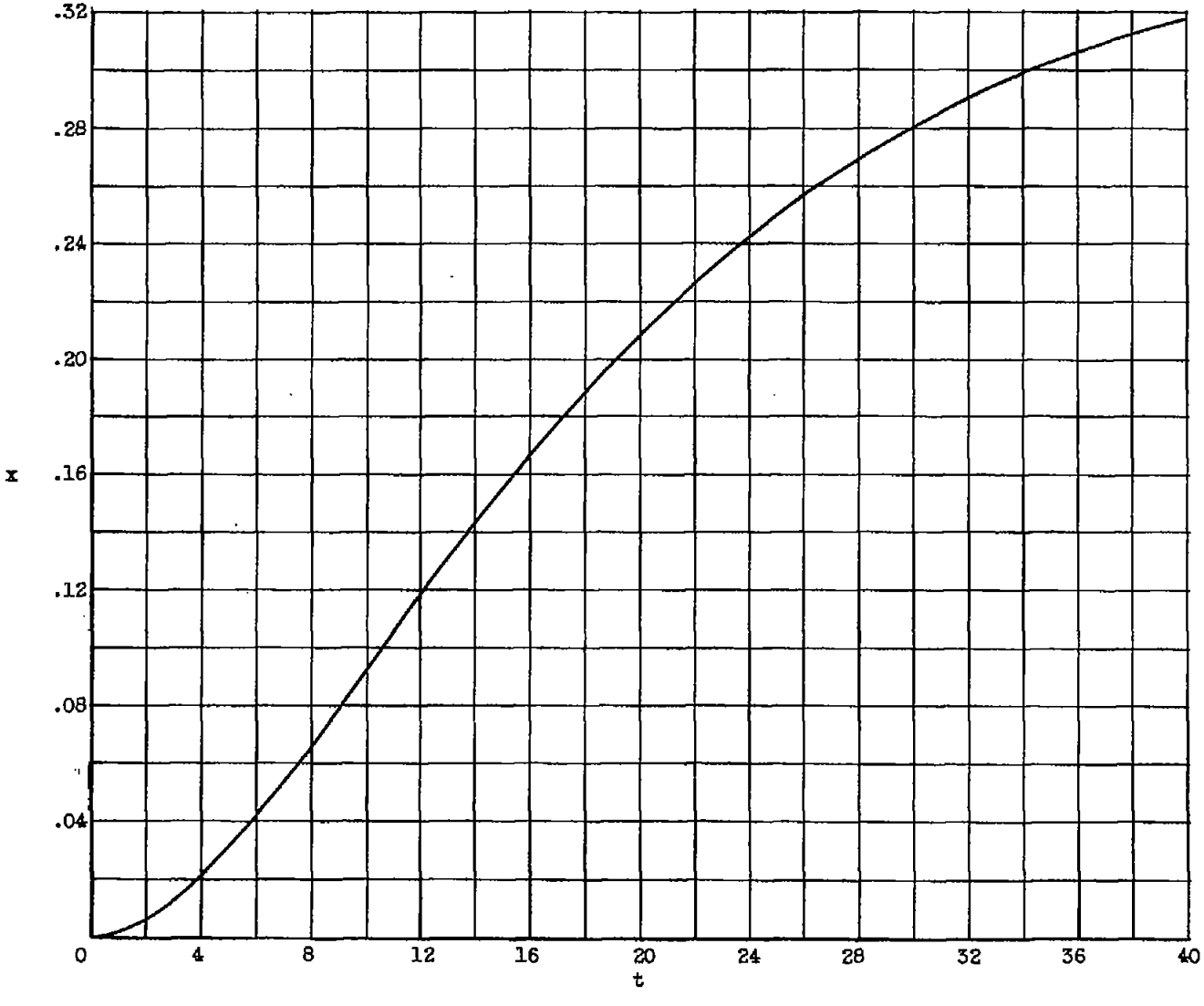

Figure 4.7. - Shock path for "exponential" function; B = 3.5, b = 0.1, ε = 0.1.

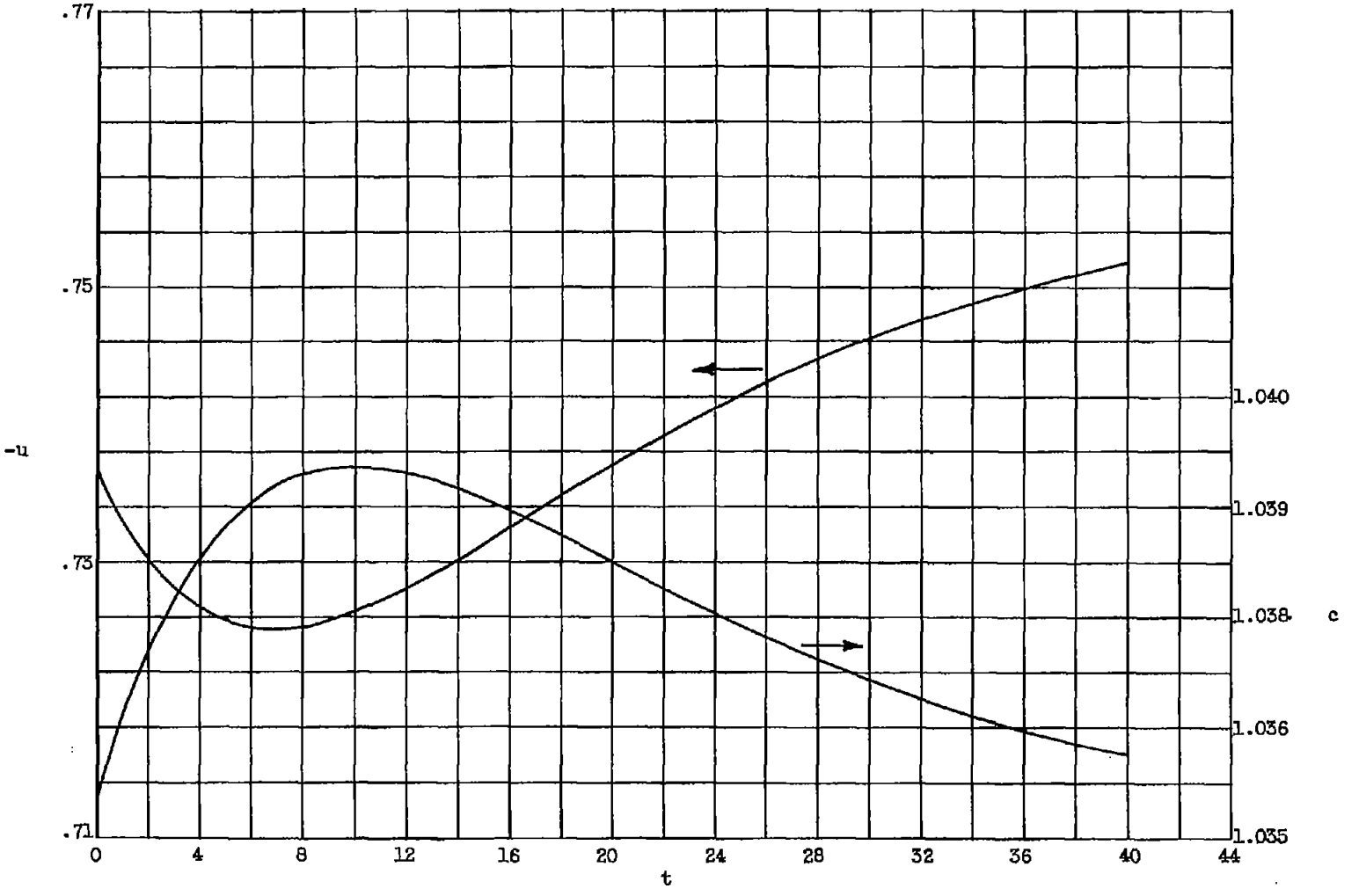

Figure 4.8. - Variation of downstream flow conditions along "exponential" shock path. Initial shock Mach number, 1.5; B = 3.5, b = 0.1, ϵ = 0.1.

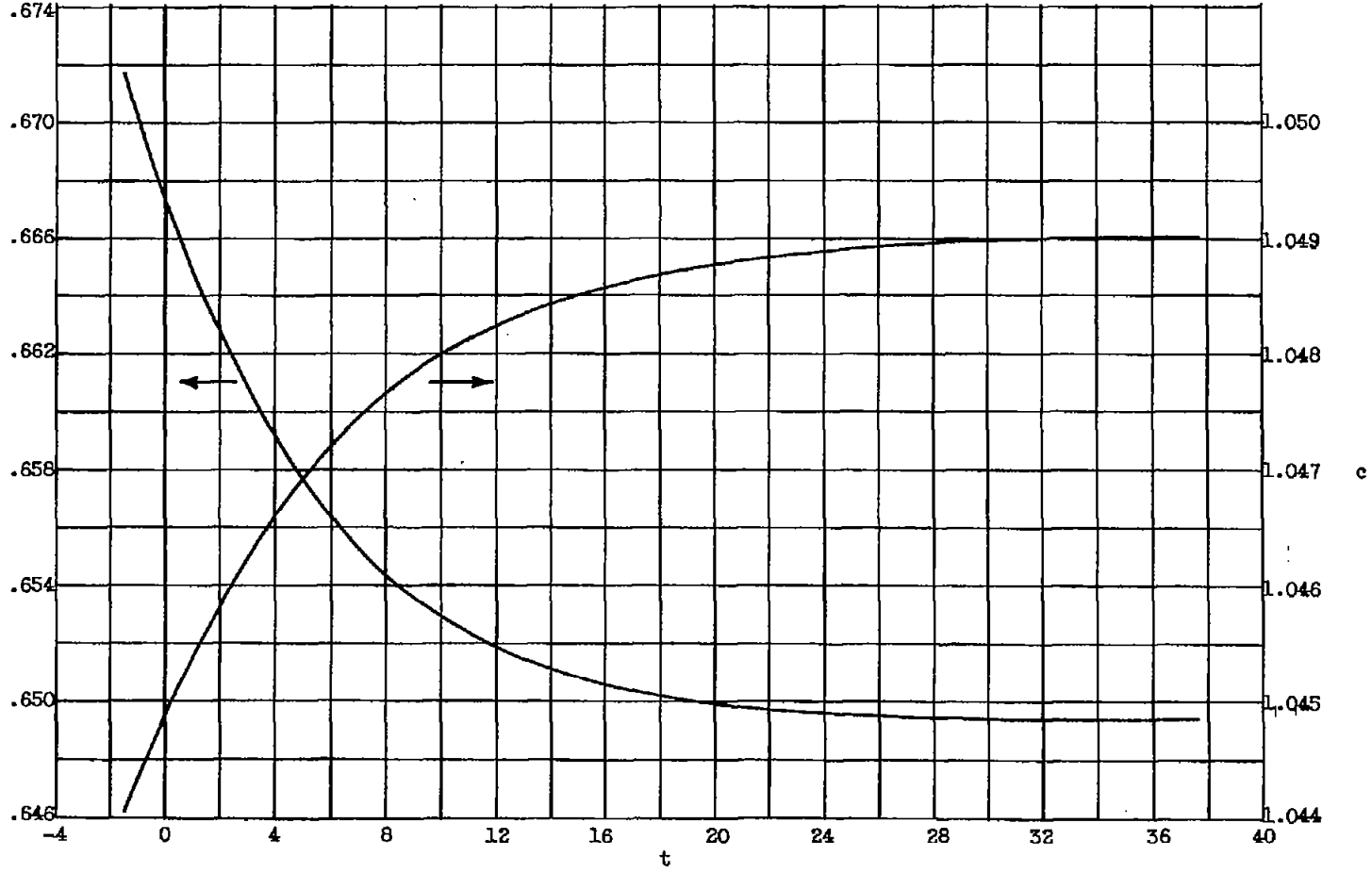

Figure 4.9. - Variation of flow variables at $x = -0.5$ for "exponential" shock path. Initial shock Mach number, 1.5; $B = 3.5$, $b = 0.1$, $\varepsilon = 0.1$.

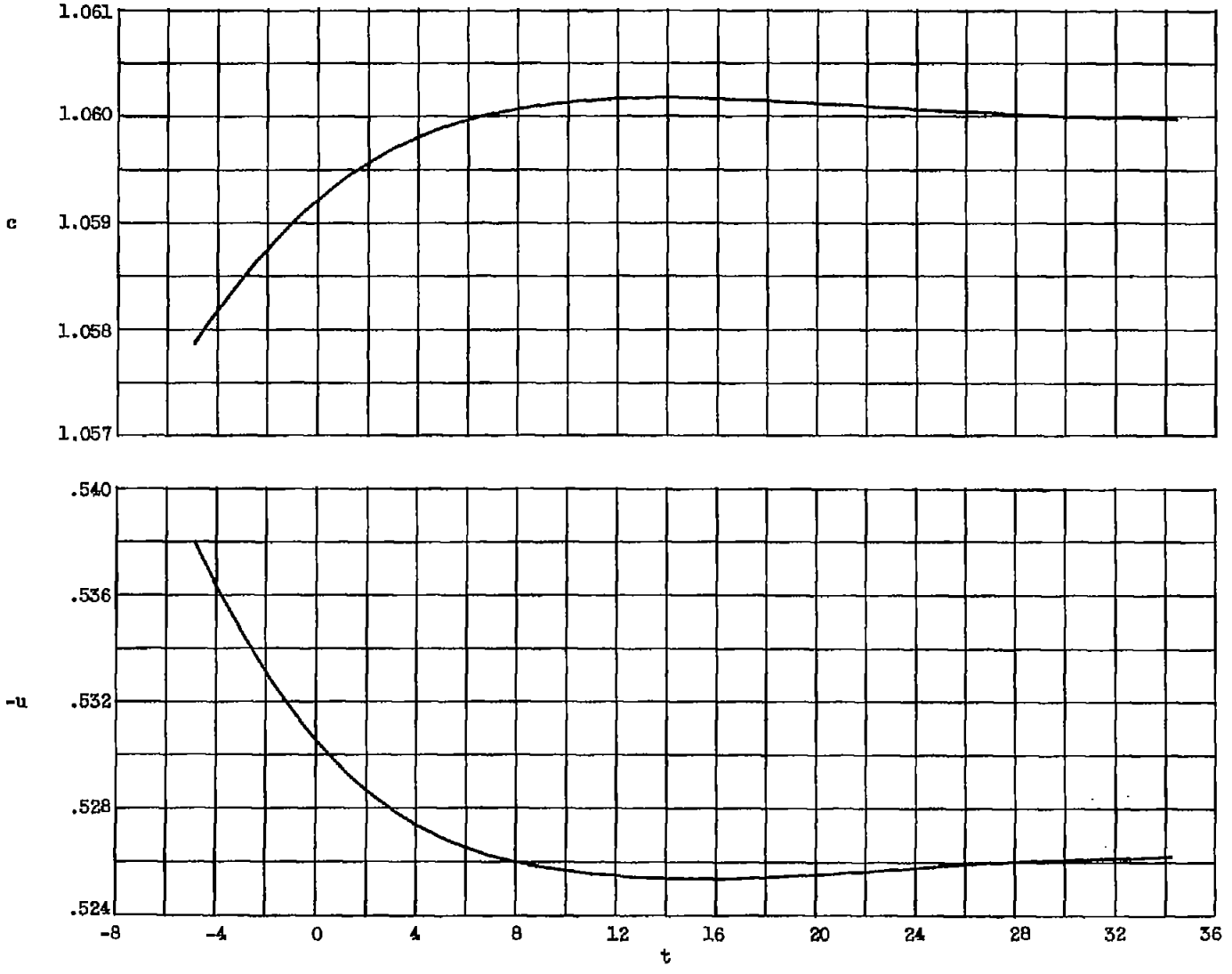

Figure 4.10. - Variation of flow variables at $x = -2.0$ for "exponential" shock path. Initial shock Mach number, 1.5; $B = 3.5$, $b = 0.1$, $\varepsilon = 0.1$.

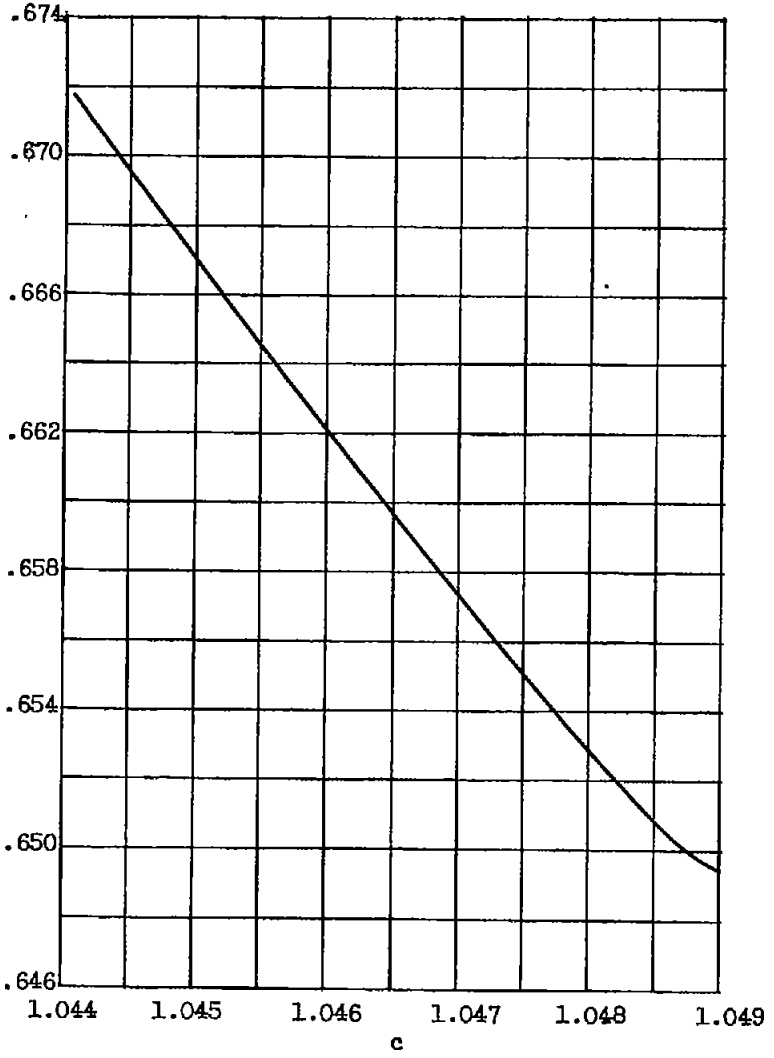

(a) x = -0.5.

Figure 4.11. - u,c-Relation at constant x for "exponential" shock path. Initial shock Mach number, 1.5; B = 3.5, b = 0.1, ε = 0.1.

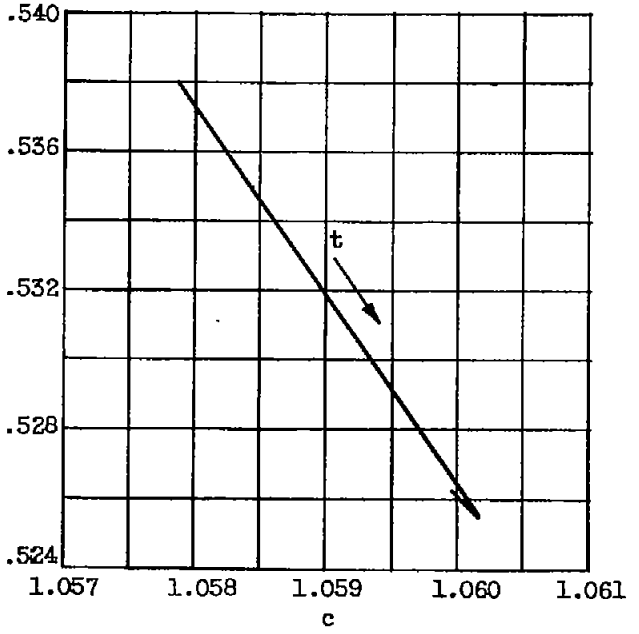

(b) x = -2.0.

Figure 4.11. - Concluded. u,c-Relation at constant x for "exponential" shock path. Initial shock Mach number, 1.5; B = 3.5, b = 0.1, ε = 0.1.

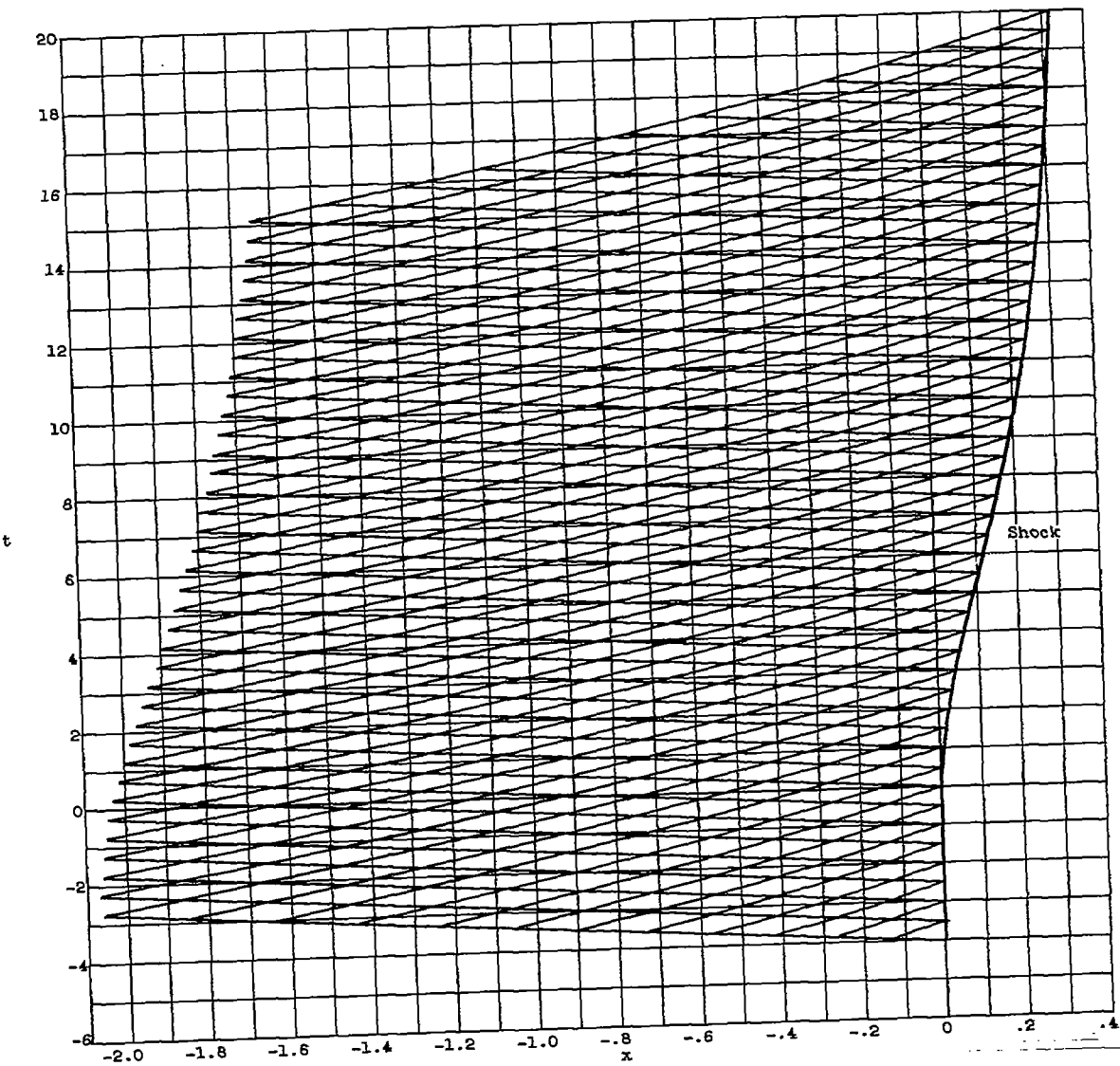

Figure 4.12. - Characteristics net for "exponential" shock path; B = 3.5, b = 0.2, ϵ = 0.1, σ = 5. Initial shock Mach number, 1.5.

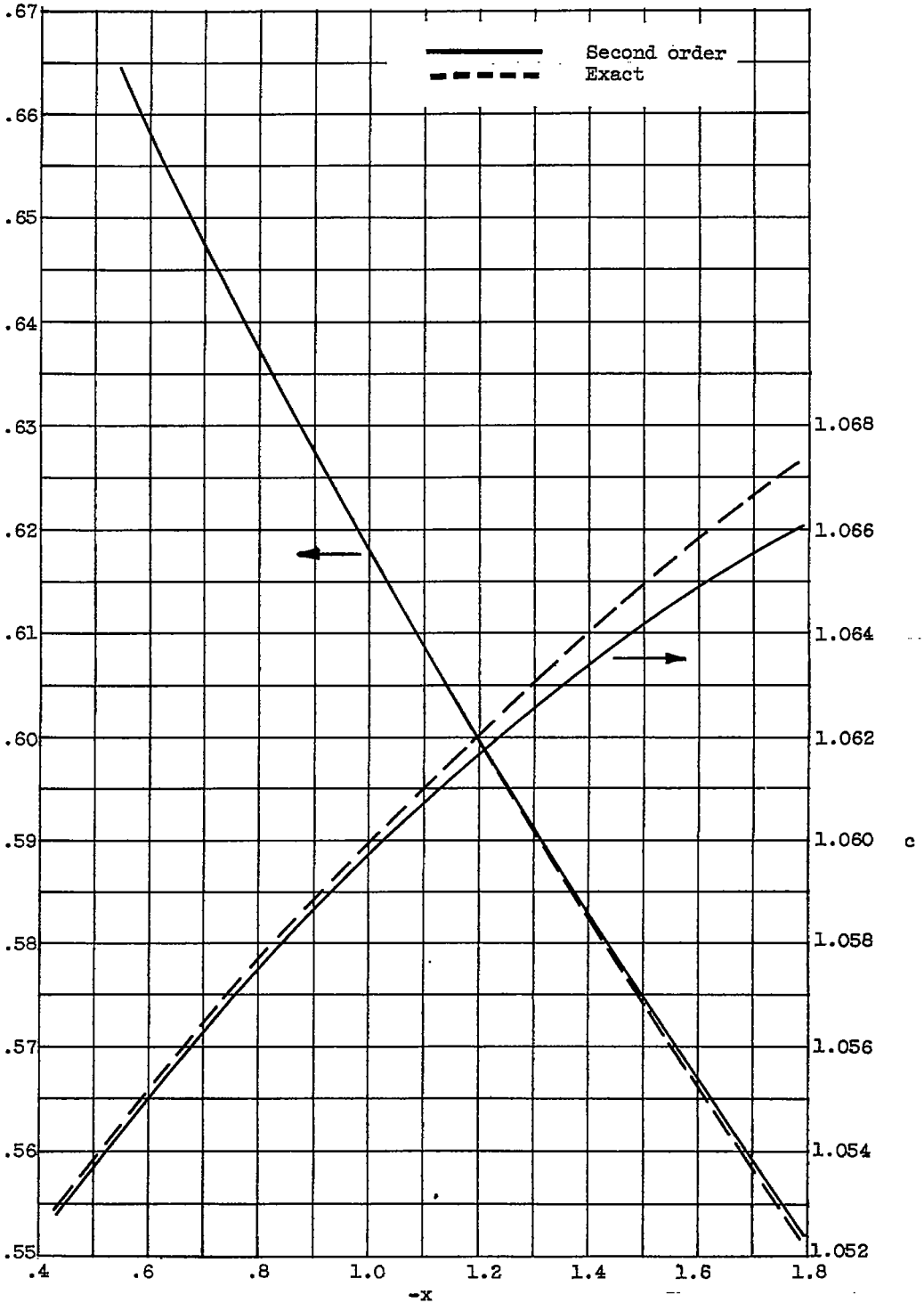

Figure 4.13. - Variation of flow variables with x for a subsonic steady flow specified at Mach 0.7 section; $\varepsilon = 0.1$, $\sigma = 5$.

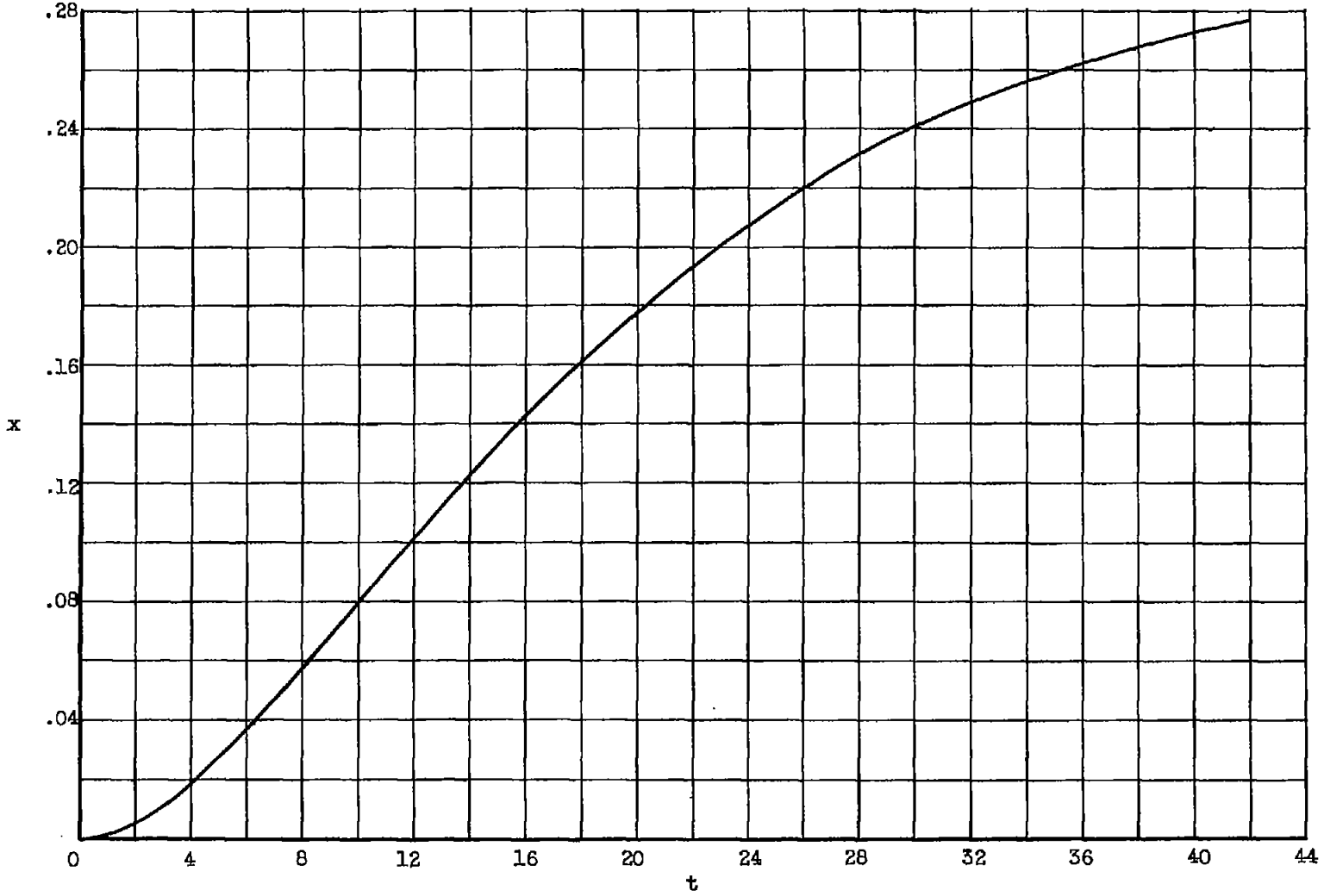

Figure 4.14. - Shock path for "exponential" function; B = 3.0, b = 0.1, ε = 0.1.

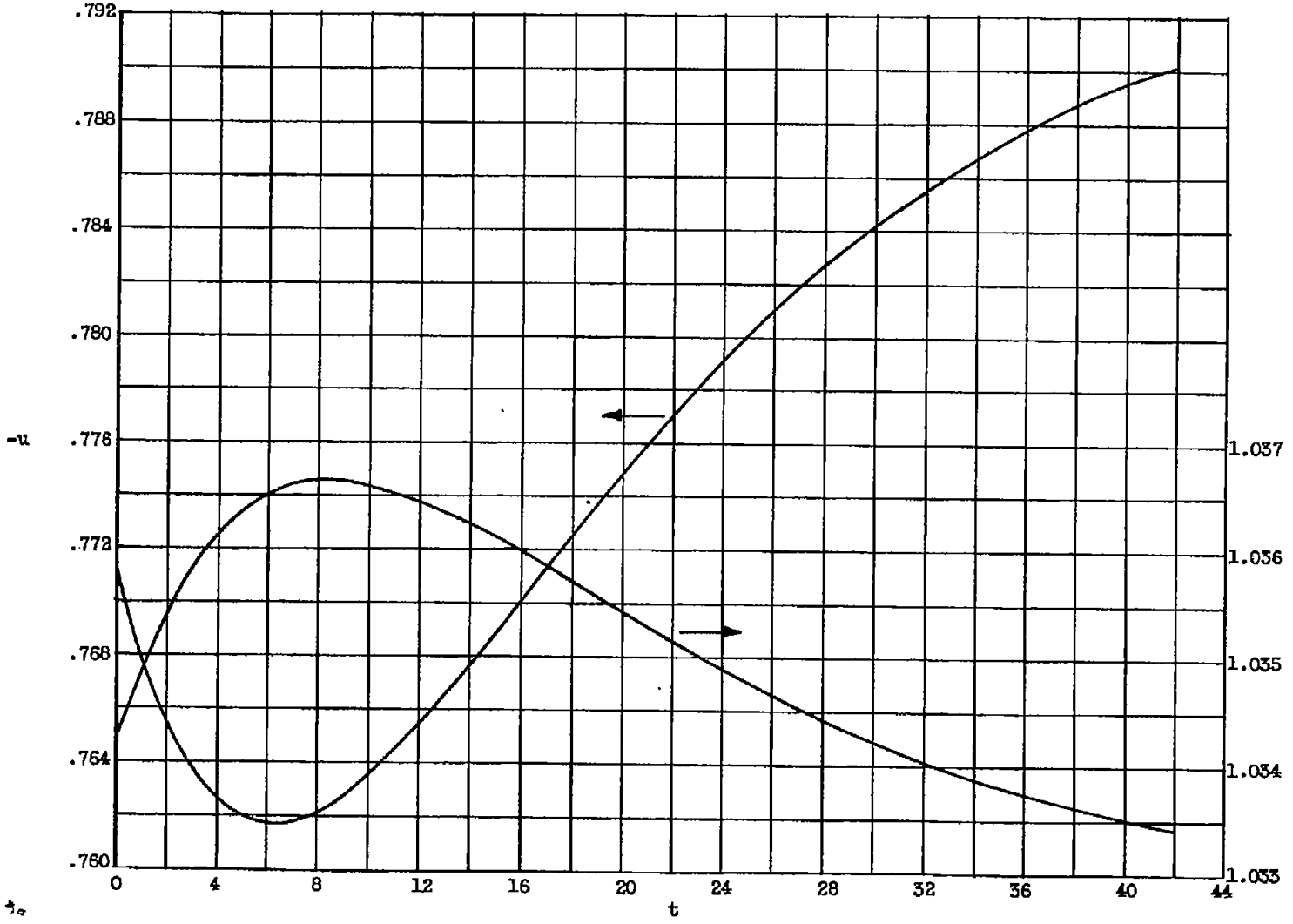

Figure 4.15. - Variation of downstream flow conditions along "exponential" shock path. Initial shock Mach number, 1.4; B = 3.0, b = 0.1, ε = 0.1.

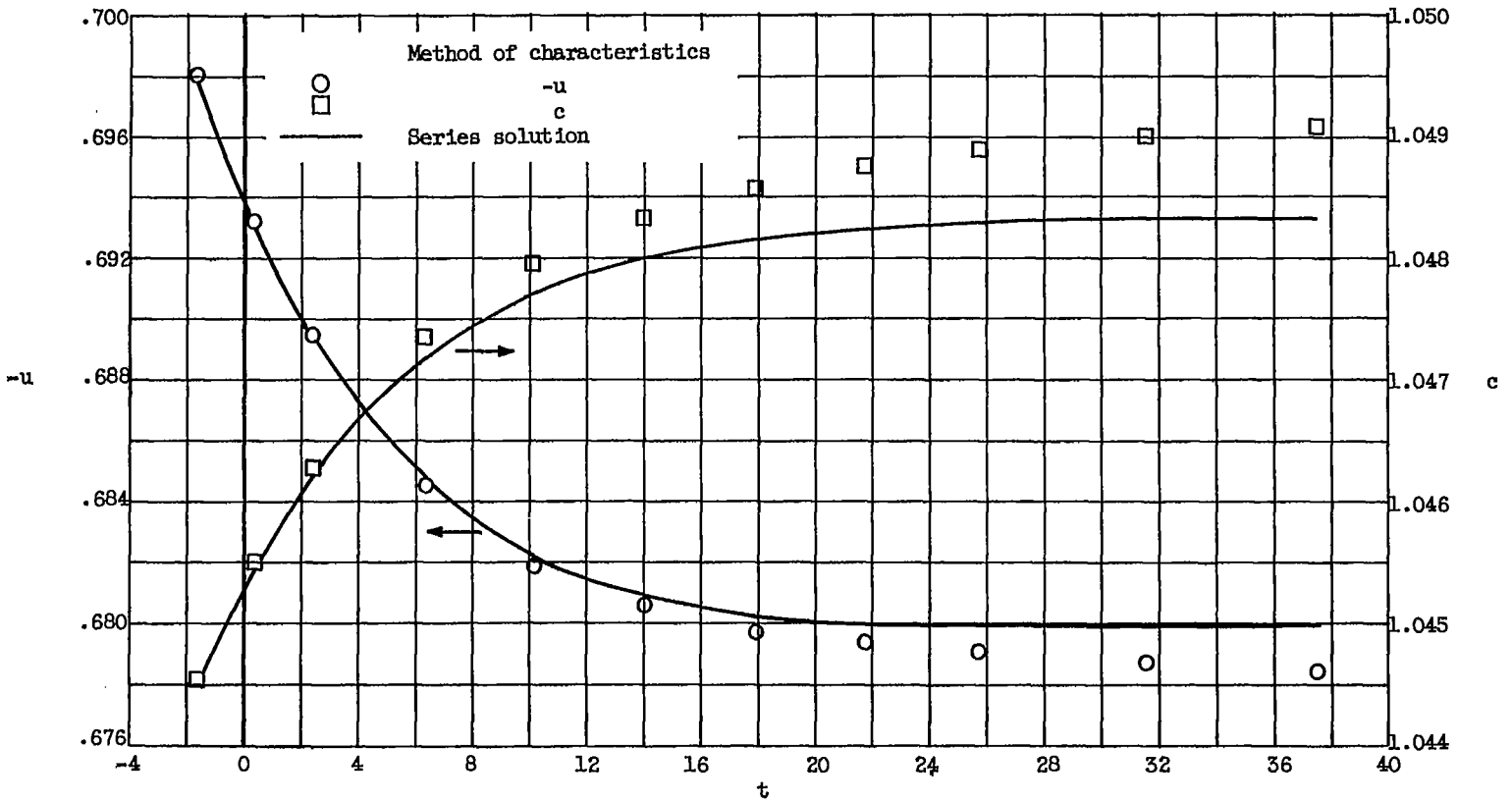

Figure 4.16. - Variation of flow variables at $x = -0.5$ for "exponential" shock path. Initial shock Mach number, 1.4; $B = 3.0$, $b = 0.1$, $\varepsilon = 0.1$.

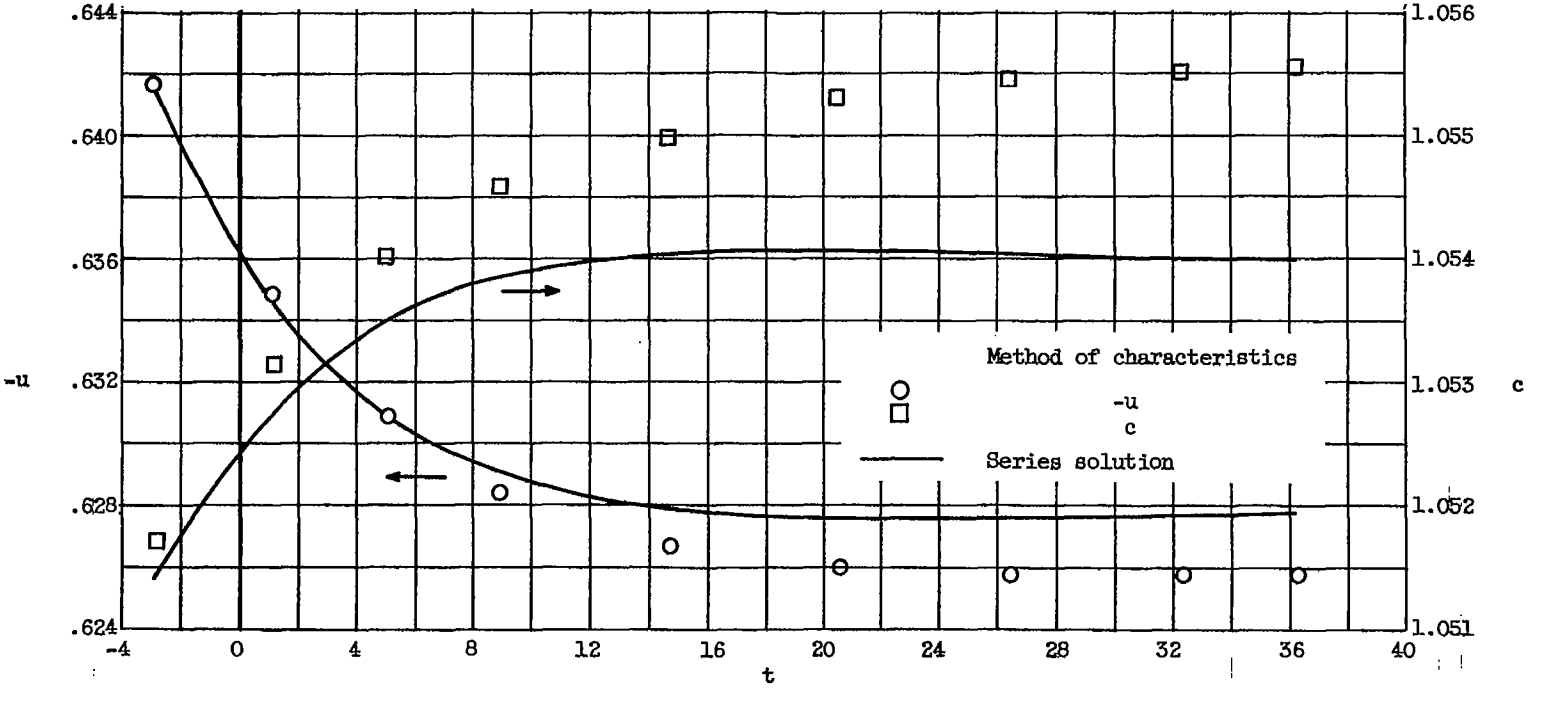

Figure 4.17. - Variation of flow variables at $x = -1.0$ for "exponential" shock path. Initial shock Mach number, 1.4; $B = 3.0$, $b = 0.1$, $\varepsilon = 0.1$.

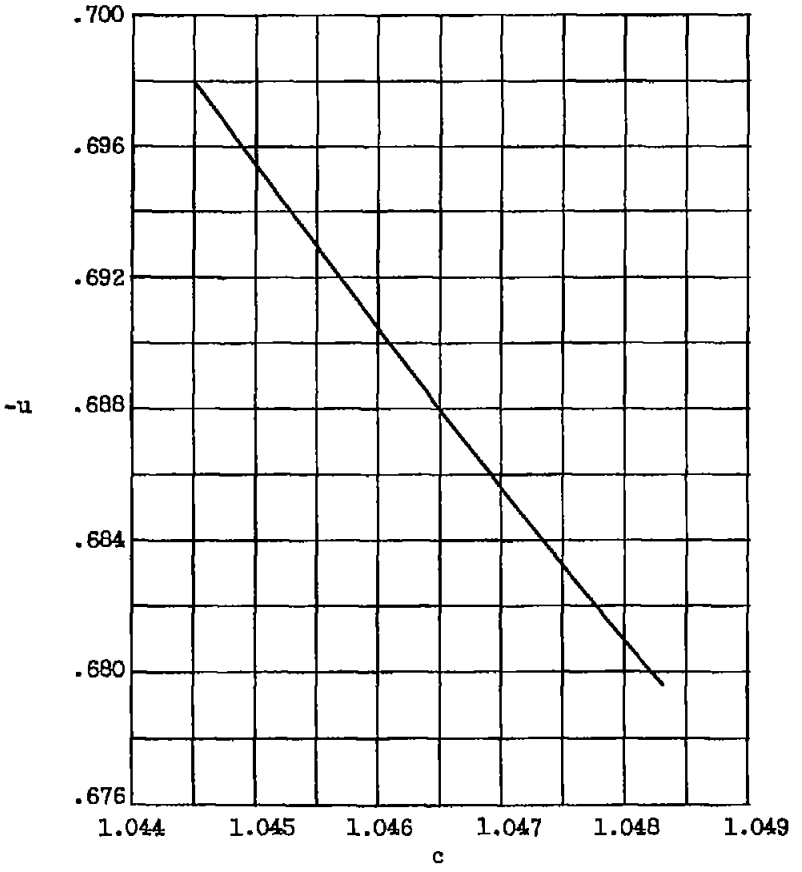

(a) x = -0.5.

Figure 4.18. - u,c-Relation at constant x for "exponential" shock path. Initial shock Mach number, 1.4; B = 3.0, b = 0.1, ε = 0.1.

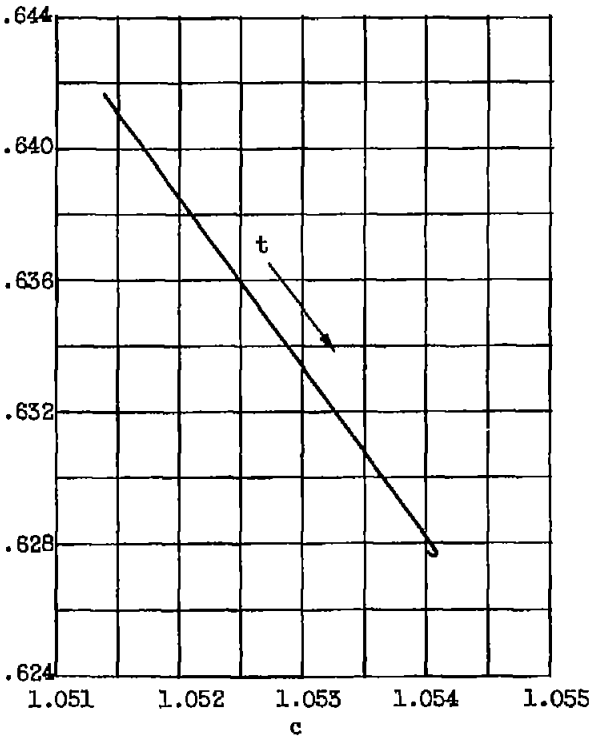

(b) x = -1.0.

Figure 4.18. - Concluded. u,c-Relation at constant x for "exponential" shock path. Initial shock Mach number, 1.4; B = 3.0, b = 0.1, ε = 0.1.

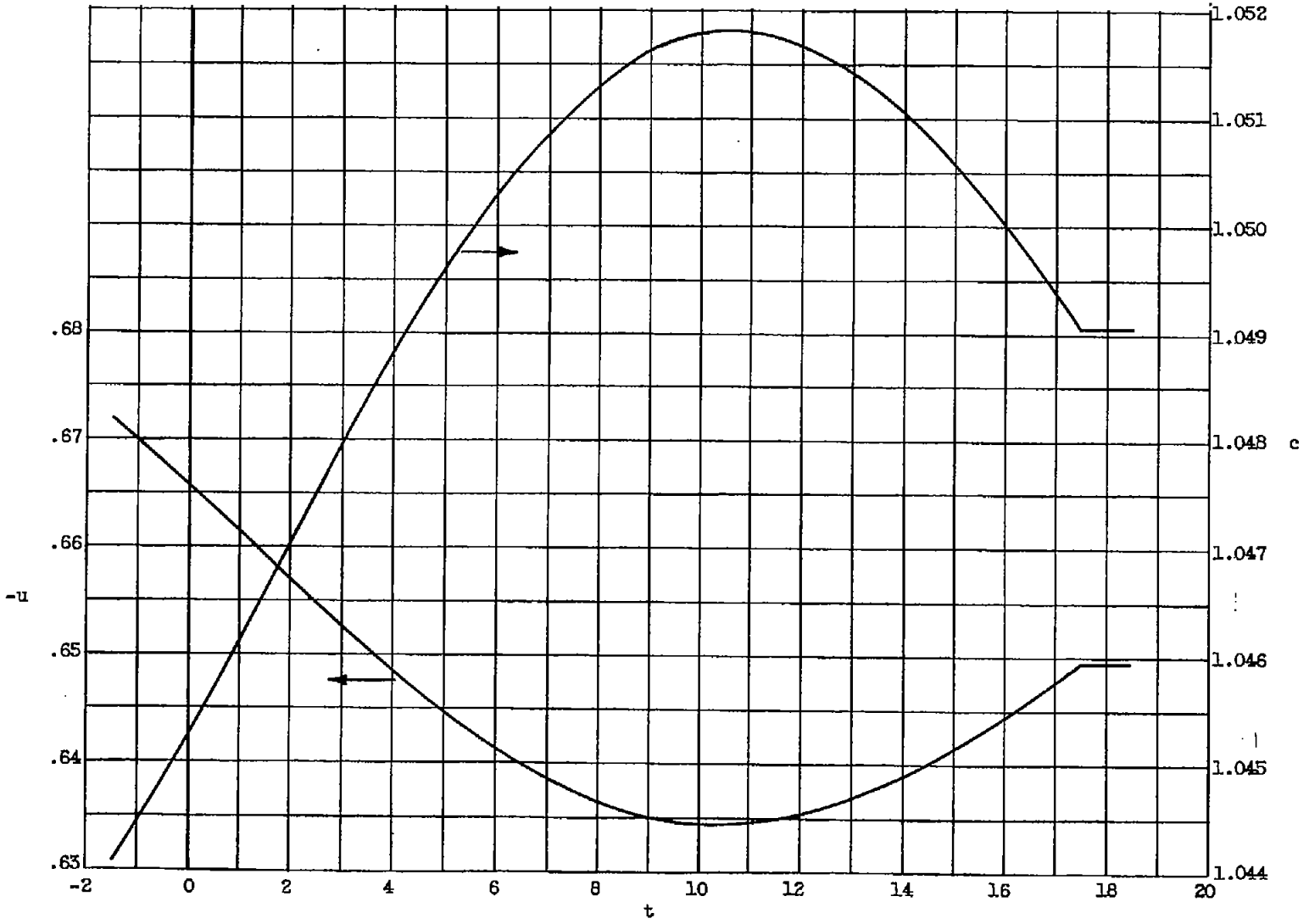

Figure 4.19. - Variation of flow variables at $x = -0.5$ for "cosine" shock path. Initial shock Mach number, 1.5; $B = 3.5$, $\omega = \pi/20$, $\epsilon = 0.1$.

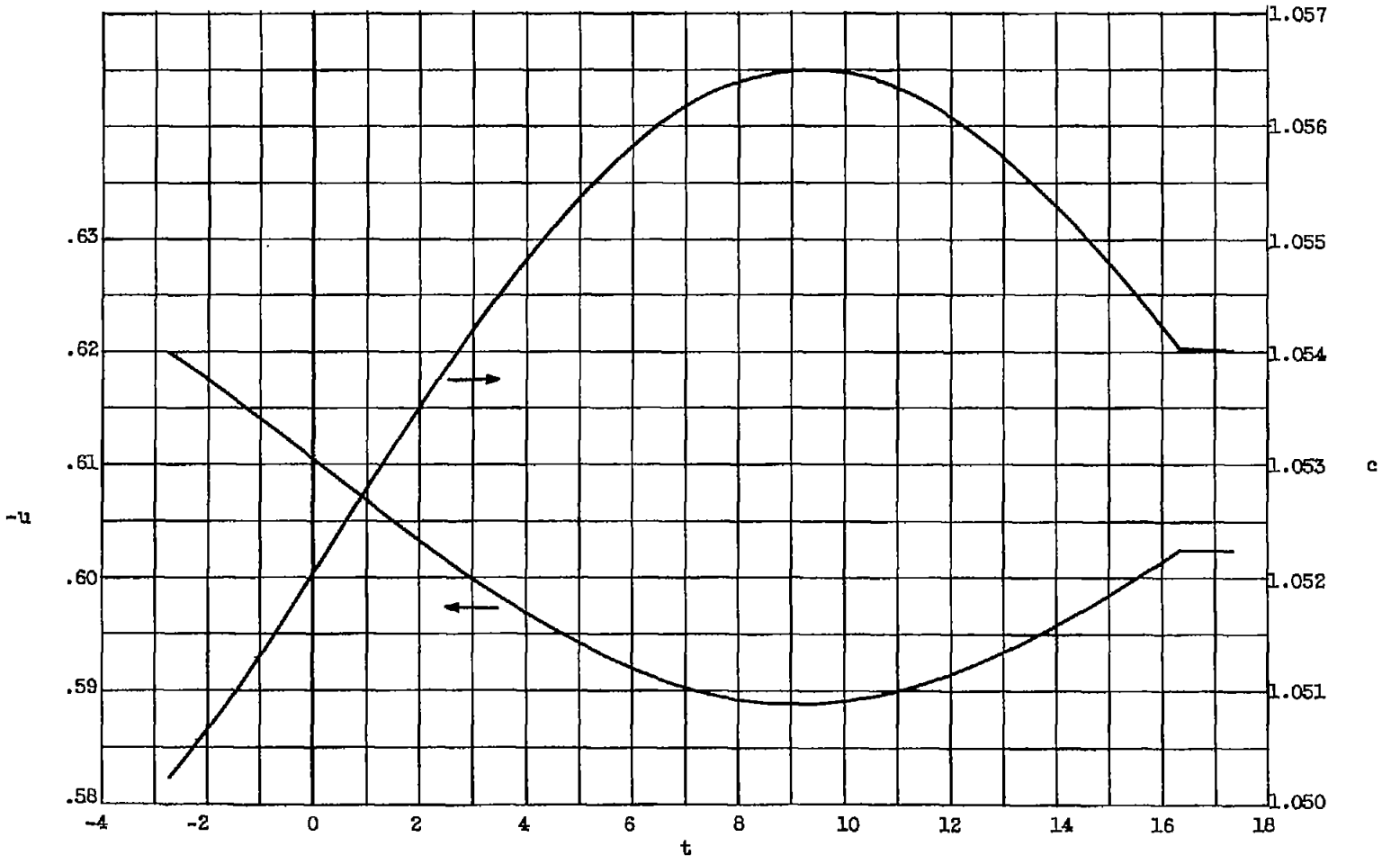

Figure 4.20. - Variation of flow variables at $x = -1.0$ for "cosine" shock path. Initial shock Mach number, 1.5; $B = 3.5$, $\omega = \pi/20$, $\epsilon = 0.1$.

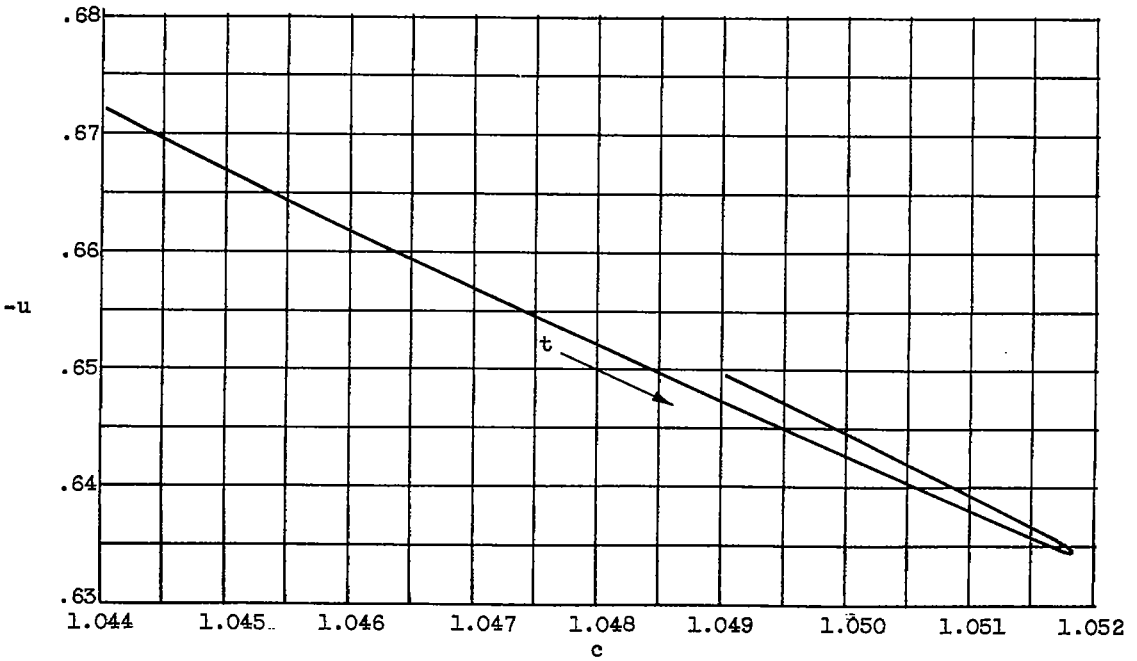

(a) x = -0.5.

Figure 4.21. - u,c-Relation at constant x for "cosine" shock path. Initial shock Mach number, 1.5; B = 3.5, $\omega = \pi/20$, $\varepsilon = 0.1$.

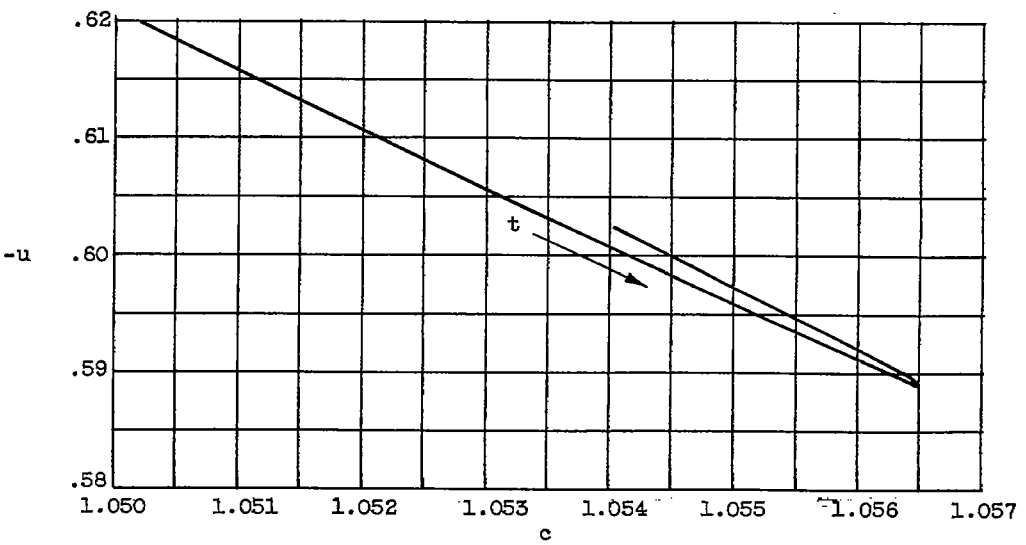

(b) x = -1.0.

Figure 4.21. - Concluded. u,c-Relation at constant x for "cosine" shock path. Initial shock Mach number, 1.5; B = 3.5, $\omega = \pi/20$, $\varepsilon = 0.1$.